

Field Guide to

Microscopy

Tomasz S. Tkaczyk

Field Guide to
Microscopy

Tomasz S.Tkaczyk

SPIE Field Guides
Volume FG13

John E. Greivenkamp, Series Editor

SPIE
PRESS

Bellingham, Washington USA

Library of Congress Cataloging-in-Publication Data

Tkaczyk, Tomasz S.

Field guide to microscopy / Tomasz S. Tkaczyk.

p. cm. -- (The field guide series)

Includes bibliographical references and index.

ISBN 978-0-8194-7246-5

1. Microscopy--Handbooks, manuals, etc. I. Title.

QH205.2.T53 2009

502.8'2--dc22

2009049648

Published by

SPIE

P.O. Box 10

Bellingham, Washington 98227-0010 USA

Phone: +1 360.676.3290

Fax: +1 360.647.1445

Email: spe@spie.org

Web: <http://spie.org>

Copyright © 2010 The Society of Photo-Optical Instrumentation Engineers (SPIE)

All rights reserved. No part of this publication may be reproduced or distributed in any form or by any means without written permission of the publisher.

The content of this book reflects the work and thought of the author. Every effort has been made to publish reliable and accurate information herein, but the publisher is not responsible for the validity of the information or for any outcomes resulting from reliance thereon.

Printed in the United States of America.



Introduction to the Series

Welcome to the *SPIE Field Guides*—a series of publications written directly for the practicing engineer or scientist. Many textbooks and professional reference books cover optical principles and techniques in depth. The aim of the *SPIE Field Guides* is to distill this information, providing readers with a handy desk or briefcase reference that provides basic, essential information about optical principles, techniques, or phenomena, including definitions and descriptions, key equations, illustrations, application examples, design considerations, and additional resources. A significant effort will be made to provide a consistent notation and style between volumes in the series.

Each *SPIE Field Guide* addresses a major field of optical science and technology. The concept of these *Field Guides* is a format-intensive presentation based on figures and equations supplemented by concise explanations. In most cases, this modular approach places a single topic on a page, and provides full coverage of that topic on that page. Highlights, insights, and rules of thumb are displayed in sidebars to the main text. The appendices at the end of each *Field Guide* provide additional information such as related material outside the main scope of the volume, key mathematical relationships, and alternative methods. While complete in their coverage, the concise presentation may not be appropriate for those new to the field.

The *SPIE Field Guides* are intended to be living documents. The modular page-based presentation format allows them to be easily updated and expanded. We are interested in your suggestions for new *Field Guide* topics as well as what material should be added to an individual volume to make these *Field Guides* more useful to you. Please contact us at fieldguides@SPIE.org.

John E. Greivenkamp, *Series Editor*
College of Optical Sciences
The University of Arizona

The Field Guide Series

Keep information at your fingertips with all of the titles in the *Field Guide* series:

Field Guide to Geometrical Optics, John E. Greivenkamp (FG01)

Field Guide to Atmospheric Optics, Larry C. Andrews (FG02)

Field Guide to Adaptive Optics, Robert K. Tyson & Benjamin W. Frazier (FG03)

Field Guide to Visual and Ophthalmic Optics, Jim Schwiegerling (FG04)

Field Guide to Polarization, Edward Collett (FG05)

Field Guide to Optical Lithography, Chris A. Mack (FG06)

Field Guide to Optical Thin Films, Ronald R. Willey (FG07)

Field Guide to Spectroscopy, David W. Ball (FG08)

Field Guide to Infrared Systems, Arnold Daniels (FG09)

Field Guide to Interferometric Optical Testing, Eric P. Goodwin & James C. Wyant (FG10)

Field Guide to Illumination, Angelo V. Arecchi; Tahar Messadi; R. John Koshel (FG11)

Field Guide to Lasers, Rüdiger Paschotta (FG12)

Field Guide to Microscopy, Tomasz Tkaczyk (FG13)

Field Guide to Laser Pulse Generation, Rüdiger Paschotta (FG14)

Field Guide to Infrared Systems, Detectors, and FPAs, Second Edition, Arnold Daniels (FG15)

Field Guide to Optical Fiber Technology, Rüdiger Paschotta (FG16)

Preface to the Field Guide to Microscopy

In the 17th century Robert Hooke developed a compound microscope, launching a wonderful journey. The impact of his invention was immediate; in the same century microscopy gave name to “cells” and imaged living bacteria. Since then microscopy has been the witness and subject of numerous scientific discoveries, serving as a constant companion in humans’ quest to understand life and the world at the small end of the universe’s scale.

Microscopy is one of the most exciting fields in optics, as its variety applies principles of interference, diffraction, and polarization. It persists in pushing the boundaries of imaging limits. For example, life sciences in need of nanometer resolution recently broke the diffraction limit. These new super-resolution techniques helped name microscopy the method of the year by *Nature Methods* in 2008.

Microscopy will critically change over the next few decades. Historically, microscopy was designed for visual imaging; however, enormous recent progress (in detectors, light sources, actuators, etc.) allows the easing of visual constraints, providing new opportunities. I am excited to witness microscopy’s path toward both integrated, digital systems and nanoscopy.

This Field Guide has three major aims: (1) to give a brief overview of concepts used in microscopy; (2) to present major microscopy principles and implementations; and (3) to point to some recent microscopy trends. While many presented topics deserve a much broader description, the hope is that this Field Guide will be a useful reference in everyday microscopy work and a starting point for further study.

I would like to express my special thanks to my colleague here at Rice University, Mark Pierce, for his crucial advice throughout the writing process and his tremendous help in acquiring microscopy images.

This Field Guide is dedicated to my family: my wife, Dorota, and my daughters, Antonina and Karolina.

Tomasz Tkaczyk
Rice University

Table of Contents

Glossary of Symbols	xi
Basics Concepts	1
Nature of Light	1
The Spectrum of Microscopy	2
Wave Equations	3
Wavefront Propagation	4
Optical Path Length (OPL)	5
Laws of Reflection and Refraction	6
Total Internal Reflection	7
Evanescent Wave in Total Internal Reflection	8
Propagation of Light in Anisotropic Media	9
Polarization of Light and Polarization States	10
Coherence and Monochromatic Light	11
Interference	12
Contrast vs Spatial and Temporal Coherence	13
Contrast of Fringes (Polarization and Amplitude Ratio)	15
Multiple Wave Interference	16
Interferometers	17
Diffraction	18
Diffraction Grating	19
Useful Definitions from Geometrical Optics	21
Image Formation	22
Magnification	23
Stops and Rays in an Optical System	24
Aberrations	25
Chromatic Aberrations	26
Spherical Aberration and Coma	27
Astigmatism, Field Curvature, and Distortion	28
Performance Metrics	29
Microscope Construction	31
The Compound Microscope	31
The Eye	32
Upright and Inverted Microscopes	33
The Finite Tube Length Microscope	34

Table of Contents

Infinity-Corrected Systems	35
Telecentricity of a Microscope	36
Magnification of a Microscope	37
Numerical Aperture	38
Resolution Limit	39
Useful Magnification	40
Depth of Field and Depth of Focus	41
Magnification and Frequency vs Depth of Field	42
Köhler Illumination	43
Alignment of Köhler Illumination	45
Critical Illumination	46
Stereo Microscopes	47
Eyepieces	48
Nomenclature and Marking of Objectives	50
Objective Designs	51
Special Objectives and Features	53
Special Lens Components	55
Cover Glass and Immersion	56
Common Light Sources for Microscopy	58
LED Light Sources	59
Filters	60
Polarizers and Polarization Prisms	61
Specialized Techniques	63
Amplitude and Phase Objects	63
The Selection of a Microscopy Technique	64
Image Comparison	65
Phase Contrast	66
Visibility in Phase Contrast	69
The Phase Contrast Microscope	70
Characteristic Features of Phase Contrast	71
Amplitude Contrast	72
Oblique Illumination	73
Modulation Contrast	74
Hoffman Contrast	75
Dark Field Microscopy	76
Optical Staining: Rheinberg Illumination	77

Table of Contents

Optical Staining: Dispersion Staining	78
Shearing Interferometry: The Basis for DIC	79
DIC Microscope Design	80
Appearance of DIC Images	81
Reflectance DIC	82
Polarization Microscopy	83
Images Obtained with Polarization Microscopes	84
Compensators	85
Confocal Microscopy	86
Scanning Approaches	87
Images from a Confocal Microscope	89
Fluorescence	90
Configuration of a Fluorescence Microscope	91
Images from Fluorescence Microscopy	93
Properties of Fluorophores	94
Single vs Multi-Photon Excitation	95
Light Sources for Scanning Microscopy	96
Practical Considerations in LSM	97
Interference Microscopy	98
Optical Coherence Tomography/Microscopy	99
Optical Profiling Techniques	100
Optical Profilometry: System Design	101
Phase-Shifting Algorithms	102
Resolution Enhancement Techniques	103
Structured Illumination: Axial Sectioning	103
Structured Illumination: Resolution	
Enhancement	104
TIRF Microscopy	105
Solid Immersion	106
Stimulated Emission Depletion	107
STORM	108
4Pi Microscopy	109
The Limits of Light Microscopy	110
Other Special Techniques	111
Raman and CARS Microscopy	111
SPIM	112

Table of Contents

Array Microscopy	113
Digital Microscopy and CCD Detectors	114
Digital Microscopy	114
Principles of CCD Operation	115
CCD Architectures	116
CCD Noise	118
Signal-to-Noise Ratio and the Digitization of CCD	119
CCD Sampling	120
Equation Summary	122
Bibliography	128
Index	133

Glossary of Symbols

$a(x, y)$, $b(x, y)$	Background and fringe amplitude
AO	Vector of light passing through amplitude object
A_R , A_S	Amplitudes of reference and sample beams
b	Fringe period
c	Velocity of light
C	Contrast, visibility
C_{ac}	Visibility of amplitude contrast
C_{ph}	Visibility of phase contrast
C_{ph-min}	Minimum detectable visibility of phase contrast
d	Airy disk dimension
d	Decay distance of evanescent wave
d	Diameter of the diffractive object
d	Grating constant
d	Resolution limit
D	Diopters
D	Number of pixels in the x and y directions (N_x and N_y , respectively)
DA	Vector of light diffracted at the amplitude object
DOF	Depth of focus
DP	Vector of light diffracted at phase object
$D_{pinhole}$	Pinhole diameter
d_{xy} , d_z	Spatial and axial resolution of confocal microscope
E	Electric field
E	Energy gap
E_x and E_y	Components of electric field
F	Coefficient of finesse
F	Fluorescent emission
f	Focal length
f_C , f_F	Focal length for lines C and F
f_e	Effective focal length
FOV	Field of view
FWHM	Full width at half maximum
h	Planck's constant
h, h'	Object and image height
H	Magnetic field
I	Intensity of light
i, j	Pixel coordinates
I_o	Intensity of incident light

Glossary of Symbols (cont.)

I_{\max}, I_{\min}	Maximum and minimum intensity in the image
I, I_t, I_r	Irradiances of incident, transmitted, and reflected light
$I_1, I_2, I_3 \dots$	Intensity of successive images
$I_0, I_{2\pi/3}, I_{4\pi/3}$	Intensities for the image point and three consecutive grid positions
k	Number of events
k	Wave number
L	Distance
l_c	Coherence length
m	Diffraction order
M	Magnification
M_{\min}	Minimum microscope magnification
MP	Magnifying power
MTF	Modulation transfer function
M_u	Angular magnification
n	Refractive index of the dielectric media
n	Step number
N	Expected value
N	Intensity decrease coefficient
N	Total number of grating lines
n_a	Probability of two-photon excitation
NA	Numerical aperture
n_e	Refractive index for propagation velocity of extraordinary wave
n_m, n_r	Refractive indices of the media surrounding the phase ring and the ring itself
n_o	Refractive index for propagation velocity of ordinary wave
n_1	Refractive index of media 1
n_2	Refractive index of media 2
o, e	Ordinary and extraordinary beams
OD	Optical density
OPD	Optical path difference
OPL	Optical path length
OTF	Optical transfer function
OTL	Optical tube length
P	Probability
P_{avg}	Average power
PO	Vector of light passing through phase object

Glossary of Symbols (cont.)

PSF	Point spread function
Q	Fluorophore quantum yield
r	Radius
r	Reflection coefficients
r , m, and o	Relative, media, or vacuum
r_{AS}	Radius of aperture stop
r_{PR}	Radius of phase ring
r_λ	Radius of filter for wavelength λ
s, s'	Shear between wavefront object and image space
S	Pinhole/slit separation
s_\perp	Lateral shift in TIR perpendicular component of electromagnetic vector
s_\parallel	Lateral shift in TIR for parallel component of electromagnetic vector
S_{FD}	Factor depending on specific Fraunhofer approximation
SM	Vector of light passing through surrounding media
SNR	Signal-to-noise ratio
SR	Strehl ratio
t	Lens separation
t	Thickness
t	Time
t	Transmission coefficient
T	Time required to pass the distance between wave oscillations
T	Throughput of a confocal microscope
t_c	Coherence time
u, u'	Object, image aperture angle
V_d, V_e	Abbe number as defined for lines d, F, C or e, F', C'
V_m	Velocity of light in media
w	Width of the slit
x, y	Coordinates
z	Distance along the direction of propagation
z	Fraunhofer diffraction distance
z, z'	Object and image distances
z_m, z_0	Imaged sample depth, length of reference path

Glossary of Symbols (cont.)

α	Angle between vectors of interfering waves
α	Birefringent prism angle
α	Grating incidence angle in plane perpendicular to grating plane
α_s	Visual stereo resolving power
β	Grating diffraction angle in plane perpendicular to grating plane
γ	Angle of fringe localization plane
γ	Convergence angle of a stereo microscope
γ	Incidence / diffraction angle from the plane perpendicular to grating plane
Γ	Retardation
δ	Birefringence
δ	Excitation cross section of dye
δz	Depth perception
Δ_b	Axial phase delay
Δf	Variation in focal length
$\Delta \mathbf{k}$	Phase mismatch
$\Delta z, \Delta z'$	Object and image separations
$\Delta \lambda$	Wavelength bandwidth
Δv	Frequency bandwidth
$\Delta \phi$	Phase delay
$\Delta \phi$	Phase difference
$\Delta \phi$	Phase shift
$\Delta \phi_{\min}$	Minimum perceived phase difference
ε	Angle between interfering beams
ε	Dielectric constant, i.e., medium permittivity
η	Quantum efficiency
θ'	Refraction angle
θ_{cr}	Critical angle
θ_i	Incidence angle
θ_r	Reflection angle
λ	Wavelength of light
λ_p	Peak wavelength for the m^{th} interference order
μ	Magnetic permeability
ν	Frequency of light
ν	Repetition frequency
ξ	Propagation direction
ρ	Spatial frequency
σ	Molecular absorption cross section

Glossary of Symbols (cont.)

σ_{dark}	Dark noise
σ_{photon}	Photon noise
σ_{read}	Read noise
τ	Integration time
τ	Length of a pulse
τ	Transmittance
ϕ	Incident photon flux
ϕ	Optical power
ϕ	Phase difference generated by a thin film
ϕ_0	Initial phase
ϕ_o	Phase delay through the object
ϕ_p	Phase delay in a phase plate
ϕ_{TF}	Phase difference generated by a thin film
ω	Angular frequency
ω	Bandgap frequency
\perp and \parallel	Perpendicular and parallel components of the light vector

Nature of Light

Optics uses two approaches, termed the **particle** and **wave models**, to describe the nature of light. The former arises from atomic structure, where the transitions between energy levels are quantized. Electrons can be excited into higher energy levels via external processes with the release of a discrete quantum of energy (a photon) upon their decay to a lower level.

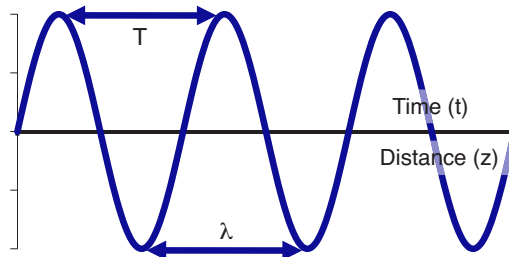
The wave model complements this corpuscular theory and explains optical effects involving diffraction and interference. The wave and particle models can be related through the frequency of oscillations, with the relationship between quanta of energy and frequency given by

$$E = h\nu \text{ [in eV or J],}$$

where $h = 4.135667 \times 10^{-15} \text{ [eV}\cdot\text{s]} = 6.626068 \times 10^{-34} \text{ [J}\cdot\text{s]}$ is **Planck's constant**, and ν is the **frequency of light** [Hz]. The frequency ν of a wave is the reciprocal of its period T [s]:

$$\nu = \frac{1}{T}.$$

The period T [s] corresponds to one cycle of a wave or, if defined in terms of the distance required to perform one



full oscillation, describes the **wavelength of light** λ [m]. The **velocity of light** in free space is $2.99792 \times 10^8 \text{ m/s}$ and is defined as the distance traveled in one period (λ) divided by the time taken (T):

$$c = \frac{\lambda}{T}.$$

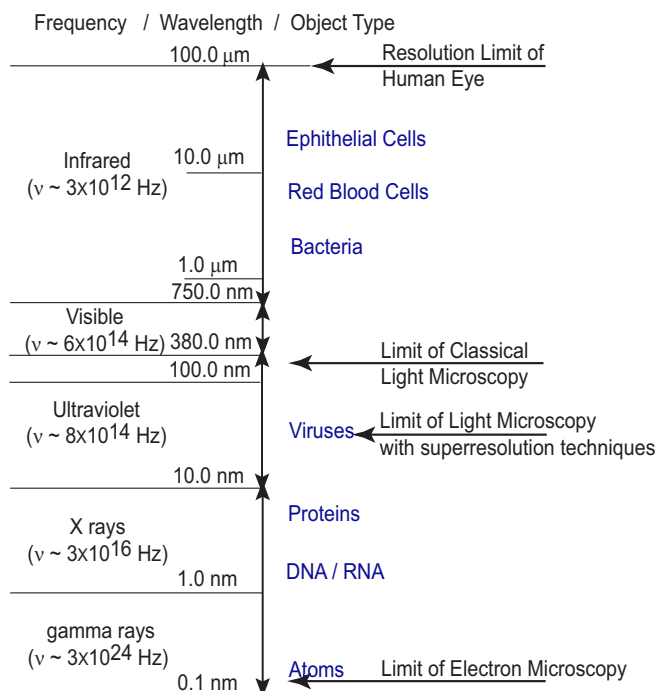
Note that wavelength is often measured indirectly as time T required to pass the distance between wave oscillations.

The relationship for the velocity of light c can be rewritten in terms of wavelength and frequency as

$$c = \lambda\nu.$$

The Spectrum of Microscopy

The range of electromagnetic radiation is called the **electromagnetic spectrum**. Various microscopy techniques employ wavelengths spanning from **x-ray radiation** and **ultraviolet radiation** (UV) through the **visible spectrum** (VIS) to **infrared radiation** (IR). The wavelength in combination with the microscope parameters determines the resolution limit of the microscope ($0.61\lambda/NA$). The smallest feature resolved using light microscopy and determined by diffraction is approximately 200 nm for UV light with a high numerical aperture (for more details, see *Resolution Limit* on page 39). However, recently emerging super-resolution techniques overcome this barrier, and features are observable in the 20–50 nm range.



Wave Equations

Maxwell's equations describe the propagation of an electromagnetic wave. For homogenous and isotropic media, magnetic (H) and electric (E) components of an electromagnetic field can be described by the wave equations derived from Maxwell's equations:

$$\nabla^2 \vec{E} - \epsilon_m \mu_m \frac{\partial^2 \vec{E}}{\partial t^2} = 0$$

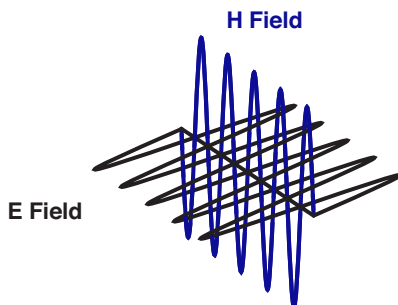
$$\nabla^2 \vec{H} - \epsilon_m \mu_m \frac{\partial^2 \vec{H}}{\partial t^2} = 0,$$

where ϵ is a **dielectric constant**, i.e., **medium permittivity** while μ is a **magnetic permeability**:

$$\epsilon_m = \epsilon_o \epsilon_r \quad \mu_m = \mu_o \mu_r$$

Indices r, m, and o stand for relative, media, or vacuum, respectively.

The above equations indicate that the time variation of the electric field and the current density creates a time-varying magnetic field. Variations in the magnetic field induce a time-varying electric field. Both fields depend on each other and compose an electromagnetic wave. Magnetic and electric components can be separated.



The electric component of an electromagnetic wave has primary significance for the phenomenon of light. This is because the magnetic component cannot be measured with optical detectors. Therefore, the magnetic component is most often neglected, and the electric vector \vec{E} is called a light vector.

Wavefront Propagation

Light propagating through isotropic media conforms to the equation

$$E = A \sin(\omega t - kz + \phi_0),$$

where t is time, z is distance along the direction of propagation, and ω is an **angular frequency** given by

$$\omega = \frac{2\pi}{T} = \frac{2\pi V_m}{\lambda}.$$

The term kz is called the **phase of light**, while ϕ_0 is an initial phase. In addition, k represents the **wave number** (equal to $2\pi/\lambda$) and V_m is the velocity of light in media:

$$kz = \frac{2\pi}{\lambda} nz$$

The above propagation equation pertains to the special case when the electric field vector varies only in one plane.

The **refractive index** of the dielectric media n describes the relationship between the speed of light in a vacuum and in media. It is

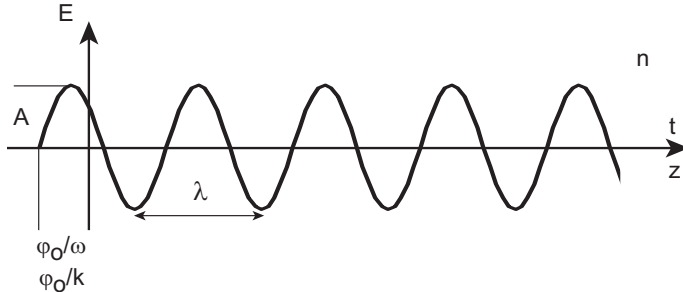
$$n = \frac{c}{V_m},$$

where c is the speed of light in vacuum.

An alternative way to describe the propagation of an electric field is with an exponential (complex) representation:

$$E = A \exp[-i(\omega t - kz + \phi_0)].$$

This form allows the easy separation of phase components of an electromagnetic wave.



Optical Path Length (OPL)

Fermat's principle states that “The path traveled by a light wave from a point to another point is stationary with respect to variations of this path.” In practical terms, this means that light travels along the minimum time path.

Optical path length (OPL) is related to the time required for light to travel from point P₁ to point P₂. It accounts for the media density through the refractive index:

$$t = \frac{1}{c} \int_{P_1}^{P_2} n ds$$

or

$$OPL = \int_{P_1}^{P_2} n ds ,$$

where

$$ds^2 = dx^2 + dy^2 + dz^2 .$$

Optical path length can also be discussed in the context of the number of periods required to propagate a certain distance L. In a medium with refractive index n, light slows down and more wave cycles are needed. Therefore, OPL is an equivalent path for light traveling with the same number of periods in a vacuum:

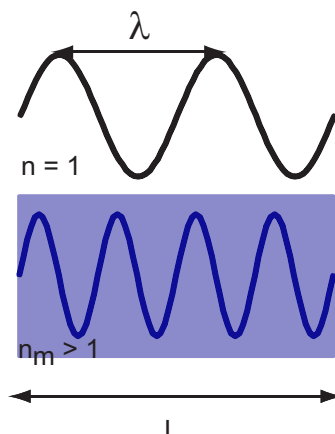
$$OPL = nL .$$

Optical path difference (OPD) is the difference between optical path lengths traversed by two light waves:

$$OPD = n_1 L_1 - n_2 L_2 .$$

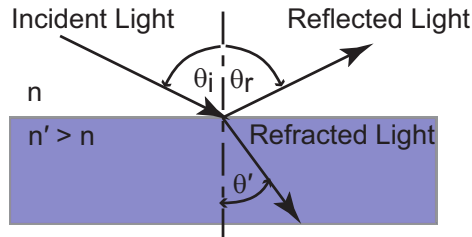
OPD can also be expressed as a phase difference:

$$\Delta\phi = 2\pi \frac{OPD}{\lambda} .$$



Laws of Reflection and Refraction

Light rays incident on an interface between different dielectric media experience reflection and refraction as shown.



Reflection Law: Angles of **incidence** and **reflection** are related by

$$\theta_i = -\theta_r .$$

Refraction Law (Snell's Law): Incident and refracted angles are related to each other and to the refractive indices of the two media by Snell's Law:

$$n \sin \theta_i = n' \sin \theta' .$$

Fresnel reflection: The division of light at a dielectric boundary into transmitted and reflected rays is described for nonlossy, nonmagnetic media by the Fresnel equations:

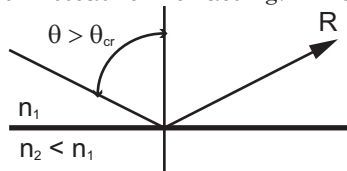
Reflectance coefficients	Transmission Coefficients
$r_{\perp} = \frac{I_{r\perp}}{I_{\perp}} = \frac{\sin^2(\theta_i - \theta')}{\sin^2(\theta_i + \theta')}$	$t_{\perp} = \frac{I_{t\perp}}{I_{\perp}} = \frac{4 \sin^2 \theta' \cos^2 \theta_i}{\sin^2(\theta_i + \theta')}$
$r_{\parallel} = \frac{I_{r\parallel}}{I_{\parallel}} = \frac{\tan^2(\theta_i - \theta')}{\tan^2(\theta_i + \theta')}$	$t_{\parallel} = \frac{I_{t\parallel}}{I_{\parallel}} = \frac{4 \sin^2 \theta' \cos^2 \theta_i}{\sin^2(\theta_i + \theta') \cos^2(\theta_i - \theta')}$

t and r are transmission and reflection coefficients, respectively. I , I_t , and I_r are the irradiances of incident, transmitted, and reflected light, respectively. \perp and \parallel denote perpendicular and parallel components of the light vector with respect to the plane of incidence. θ_i and θ' in the table are the angles of incidence and reflection/refraction, respectively. At a normal incidence ($\theta' = \theta_i = 0$ deg), the Fresnel equations reduce to

$$r = r_{\perp} = r_{\parallel} = \frac{(n' - n)^2}{(n' + n)^2} \quad \text{and} \quad t = t_{\perp} = t_{\parallel} = \frac{4nn'}{(n' + n)^2} .$$

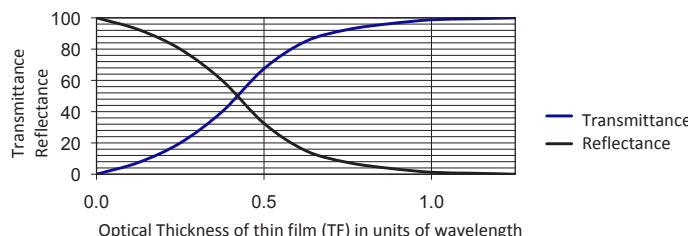
Total Internal Reflection

When light passes from one medium to a medium with a higher refractive index, the angle of the light in the medium bends toward the normal, according to Snell's Law. Conversely, when light passes from one medium to a medium with a lower refractive index, the angle of the light in the second medium bends away from the normal. If the angle of refraction is greater than 90 deg, the light cannot escape the denser medium, and it reflects instead of refracting. This effect is known as **total internal reflection** (TIR). TIR occurs only for illumination with an angle larger than the **critical angle**, defined as



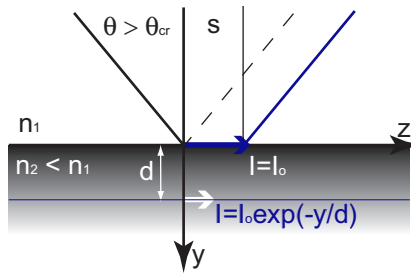
$$\theta_{\text{cr}} = \arcsin\left(\frac{n_1}{n_2}\right).$$

It appears, however, that light can propagate through (at a limited range) to the lower-density material as an **evanescent wave** (a nearly standing wave occurring at the material boundary), even if illuminated under an angle larger than θ_{cr} . Such a phenomenon is called **frustrated total internal reflection**. Frustrated TIR is used, for example, with thin films (TF) to build beam splitters. The proper selection of the film thickness provides the desired beam ratio (see the figure below for various split ratios). Note that the maximum film thickness must be approximately a single wavelength or less, otherwise light decays entirely. The effect of an evanescent wave propagating in the lower-density material under TIR conditions is also used in total internal reflection fluorescence (**TIRF**) microscopy.



Evanescent Wave in Total Internal Reflection

A beam reflected at the dielectric interface during **total internal reflection** is subject to a small lateral shift, also known as the **Goos-Hänchen effect**. The shift is different for the parallel and perpendicular components of the electromagnetic vector.



	Lateral shift in TIR
Parallel* component of e/m vector	$s_{\parallel} = \frac{\lambda n_1}{\pi n_2^2} \frac{\tan \theta}{\sqrt{\sin^2 \theta - \sin^2 \theta_c}}$
Perpendicular* component of e/m vector	$s_{\perp} = \frac{\lambda}{\pi n_1} \frac{\tan \theta}{\sqrt{\sin^2 \theta - \sin^2 \theta_c}}$

* to the plane of incidence

The intensity of the illuminating beam decays exponentially with distance y in the direction perpendicular to the material boundary:

$$I = I_o \exp(-y/d).$$

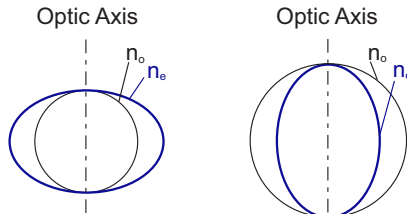
Note that d denotes the distance at which the intensity of the illuminating light I_o drops by e . The decay distance is smaller than a wavelength. It is also inversely proportional to the illumination angle.

Decay distance (d) of evanescent wave	
Decay distance as a function of incidence and critical angles	$d = \frac{\lambda}{4\pi n_1} \frac{1}{\sqrt{\sin^2 \theta - \sin^2 \theta_c}}$
Decay distance as a function of incidence angle and refractive indices of media	$d = \frac{\lambda}{4\pi} \frac{1}{\sqrt{n_1^2 \sin^2 \theta - n_2^2}}$

Propagation of Light in Anisotropic Media

In anisotropic media the velocity of light depends on the direction of propagation. Common anisotropic and optically transparent materials include **uniaxial crystals**. Such crystals exhibit one direction of travel with a single propagation velocity. The single velocity direction is called the **optic axis** of the crystal. For any other direction, there are two velocities of propagation.

The wave in birefringent crystals can be divided into two components: ordinary and extraordinary. An **ordinary wave** has a uniform velocity in all directions, while the velocity of an **extraordinary wave** varies with orientation. The extreme value of an extraordinary wave's velocity is perpendicular to the optic axis. Both waves are linearly polarized, which means that the electric vector oscillates in one plane. The vibration planes of extraordinary and ordinary vectors are perpendicular. Refractive indices corresponding to the direction of the optic axis and perpendicular to the optic axis are $n_o = c/V_o$ and $n_e = c/V_e$ respectively.



Uniaxial crystals Positive Birefringence Negative Birefringence can be positive or negative (see table). The **refractive index** $n(\xi)$ for velocities between the two extreme (n_o and n_e) values is

$$\frac{1}{n^2(\xi)} = \frac{\cos^2 \xi}{n_o^2} + \frac{\sin^2 \xi}{n_e^2}.$$

	Positive Birefringence	$V_e \leq V_o$
	Negative Birefringence	$V_e \geq V_o$

Note that the propagation direction ξ (with regard to the optic axis) is slightly off from the ray direction, which is defined by the Poynting (energy) vector.

Uniaxial Crystal	Refractive index	Abbe Number	Wavelength Range [μm]
Quartz	$n_o = 1.54424$ $n_e = 1.55335$	70 69	0.18–4.0
Calcite	$n_o = 1.65835$ $n_e = 1.48640$	50 68	0.2–2.0

The refractive index is given for the *D* spectral line (589.2 nm).

(Adapted from Pluta, 1988)

Polarization of Light and Polarization States

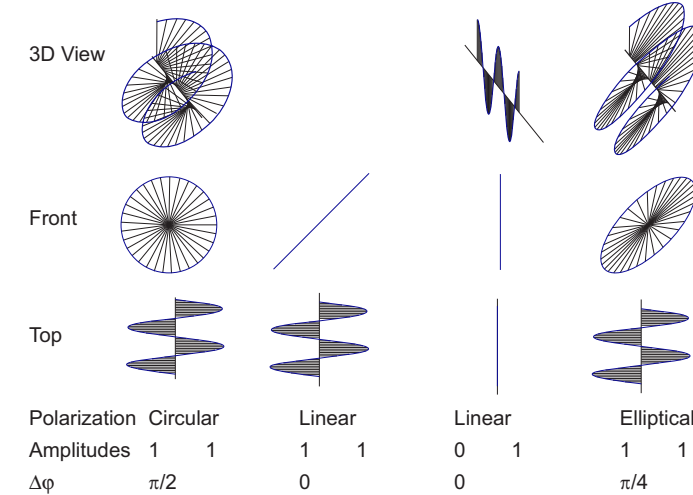
The orientation characteristic of a light vector vibrating in time and space is called the **polarization of light**. For example, if the vector of an electric wave vibrates in one plane, the state of polarization is linear. A vector vibrating with a random orientation represents unpolarized light.

The wave vector E consists of two components E_x and E_y .

$$\begin{aligned} E(z,t) &= E_x + E_y \\ E_x &= A_x \exp[-i(\omega t - kz + \varphi_x)] \\ E_y &= A_y \exp[-i(\omega t - kz + \varphi_y)]. \end{aligned}$$

The **electric vector** rotates periodically (the periodicity corresponds to wavelength λ) in the plane perpendicular to the propagation axis (z) and generally forms an elliptical shape. The specific shape depends on the A_x and A_y ratios and the phase delay between the E_x and E_y components, defined as $\Delta\varphi = \varphi_x - \varphi_y$.

Linearly polarized light is obtained when one of the components E_x or E_y is zero, or when $\Delta\varphi$ is zero or π . **Circularly polarized light** is obtained when $E_x = E_y$ and $\Delta\varphi = \pm\pi/2$. The light is called right circularly polarized (RCP) if it rotates in a clockwise direction or left circularly polarized (LCP) if it rotates counterclockwise when looking at the oncoming beam.



Coherence and Monochromatic Light

An ideal light wave that extends in space at any instance to $\pm\infty$ and has only one wavelength λ (or frequency v) is said to be **monochromatic**. If the range of wavelengths λ or frequencies v is very small (around λ_0 or v_0 , respectively), the wave is **quasi-monochromatic**. Such a wave packet is usually called a **wave group**.

Note that for monochromatic and quasi-monochromatic waves, no phase relationship is required, and the intensity of light can be calculated as a simple summation of intensities from different waves; phase changes are very fast and random, so only the average intensity can be recorded.

If multiple waves have a common phase relation dependence, they are **coherent** or **partially coherent**. These cases correspond to full- and partial-phase correlation respectively. A common source of a coherent wave is a laser where waves must be in resonance and therefore in phase. The average length of the wave packet (group) is called the **coherence length**, while the time required to pass this length is called **coherence time**. Both values are linked by the equations

$$\Delta v = \frac{1}{t_c} = \frac{V}{l_c}$$

where coherence length is

$$l_c = \frac{\lambda^2}{\Delta\lambda}.$$

The coherence length l_c and **temporal coherence** t_c are inversely proportional to the bandwidth $\Delta\lambda$ of the light source.

Spatial coherence is a term related to the coherence of light with regard to the extent of the light source. The fringe contrast varies for interference of any two spatially different source points. Light is **partially coherent** if its coherence is limited by the source bandwidth, dimension, temperature, or other effects.

Interference

Interference is a process of superposition of two coherent (correlated) or partially coherent waves. Waves interact with each other, and the resulting intensity is described by summing the **complex amplitudes (electric fields)** E_1 and E_2 of both wavefronts:

$$E_1 = A_1 \exp[-i(\omega t - kz + \varphi_1)]$$

and

$$E_2 = A_2 \exp[-i(\omega t - kz + \varphi_2)].$$

The resultant field is

$$E = E_1 + E_2.$$

Therefore, the **interference** of the two beams can be written as

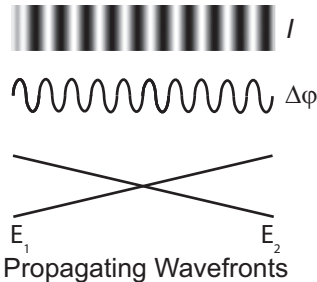
$$I = EE^*,$$

$$I = A_1^2 + A_2^2 + 2A_1A_2 \cos(\Delta\varphi),$$

$$I = I_1 + I_2 + 2\sqrt{I_1I_2} \cos(\Delta\varphi),$$

$$I_1 = E_1E_1^*, \quad I_2 = E_2E_2^*, \text{ and}$$

$$\Delta\varphi = \varphi_2 - \varphi_1,$$



where * denotes a conjugate function, I is the **intensity of light**, A is an amplitude of an electric field, and $\Delta\varphi$ is the phase difference between the two interfering beams. **Contrast** C (called also **visibility**) of the interference fringes can be expressed as

$$C = \frac{I_{\max} - I_{\min}}{I_{\max} + I_{\min}}.$$

The fringe existence and visibility depends on several conditions. To obtain the interference effect,

- Interfering beams must originate from the same light source and be temporally and spatially coherent;
- The polarization of interfering beams must be aligned;
- To maximize the contrast, interfering beams should have equal or similar amplitudes.

Conversely, if two noncorrelated, random waves are in the same region of space, the sum of intensities (irradiances) of these waves gives a total intensity in that region: $I = I_1 + I_2$.

Contrast vs Spatial and Temporal Coherence

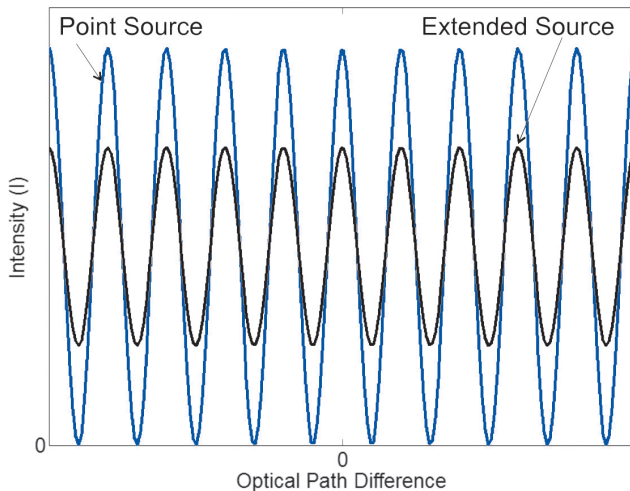
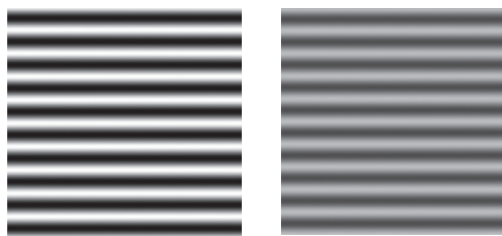
The result of interference is a periodic intensity change in space, which creates fringes when incident on a screen or detector. **Spatial coherence** relates to the contrast of these fringes depending on the extent of the source and is not a function of the phase difference (or OPD) between beams. The intensity of interfering fringes is given by

$$I = I_1 + I_2 + 2C(\text{Source Extent})\sqrt{I_1 I_2} \cos(\Delta\phi),$$

where C is a constant, depending on the extent of the source.

$$C = 1$$

$$C = 0.5$$

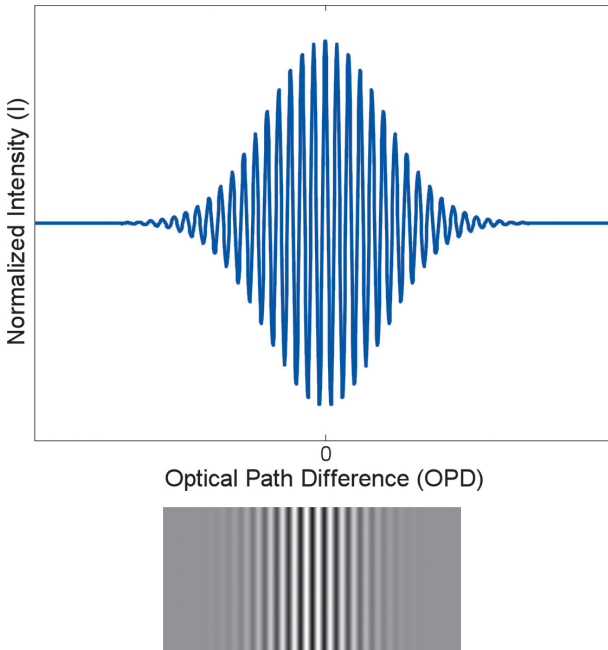


The spatial coherence can be improved through spatial filtering. For example, light can be focused on the pinhole (or coupled into the fiber) by using a microscope objective. In microscopy, spatial coherence can be adjusted by changing the diaphragm size in the conjugate plane of the light source.

Contrast vs Spatial and Temporal Coherence (cont.)

The intensity of the fringes depends on the OPD and the **temporal coherence** of the source. The fringe contrast trends toward zero as the OPD increases beyond the coherence length:

$$I = I_1 + I_2 + 2\sqrt{I_1 I_2} C(OPD) \cos(\Delta\phi).$$

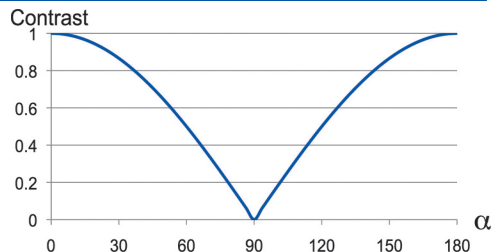


The spatial width of a fringe pattern envelope decreases with shorter temporal coherence. The location of the envelope's peak (with respect to the reference) and narrow width can be efficiently used as a gating mechanism in both imaging and metrology. For example, it is used in interference microscopy for optical profiling (white light interferometry) and for imaging using optical coherence tomography. Examples of short coherence sources include white light sources, luminescent diodes, and broadband lasers.

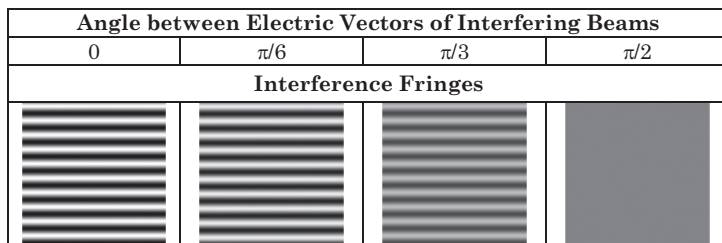
Long coherence length is beneficial in applications that do not naturally provide near-zero OPD, e.g., in surface measurements with a Fizeau interferometer.

Contrast of Fringes (Polarization and Amplitude Ratio)

The contrast of fringes depends on the polarization orientation of the electric vectors. For linearly polarized beams,



it can be described as $C = |\cos \alpha|$, where α represents the angle between polarization states.



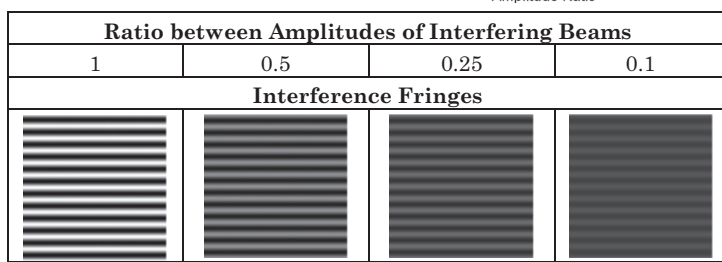
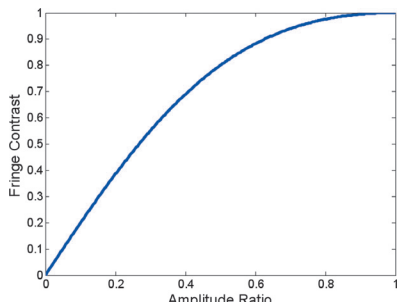
Fringe contrast also depends on the interfering beams' amplitude ratio. The intensity of the fringes is simply calculated by using the main interference equation. The contrast is maximum for equal beam intensities and for the interference pattern,

defined as

$$I = I_1 + I_2 + 2\sqrt{I_1 I_2} \cos(\Delta\phi),$$

it is

$$C = \frac{2\sqrt{I_1 I_2}}{I_1 + I_2}.$$



Multiple Wave Interference

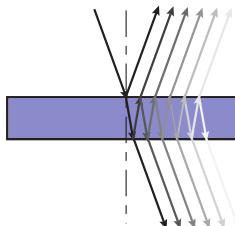
If light reflects inside a thin film, its intensity gradually decreases and **multiple beam interference** occurs.

The intensity of reflected light is

$$I_r = I_i \frac{F \sin^2(\varphi/2)}{1 + F \sin^2(\varphi/2)},$$

and for transmitted light is

$$I_t = I_i \frac{1}{1 + F \sin^2(\varphi/2)}.$$



The coefficient of finesse F of such a resonator is

$$F = \frac{4r}{(1-r)^2}.$$

Because phase depends on the wavelength, it is possible to design selective **interference filters**. In this case, a dielectric thin film is coated with metallic layers. The peak wavelength for the m^{th} interference order of the filter can be defined as

$$\lambda_p = \frac{2nt \cos \theta'}{m - \left(\frac{\varphi_{TF}}{2\pi}\right)},$$

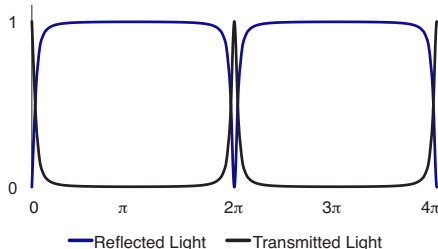
where φ_{TF} is the phase difference generated by a thin film of thickness t and a specific incidence angle. The **interference order** relates to the phase difference in multiples of 2π .

Interference filters usually operate for illumination with flat wavefronts at a normal incidence angle. Therefore, the equation simplifies as

$$\lambda_p = \frac{2nt}{m}.$$

The **half bandwidth** (HBW) of the filter for normal incidence is

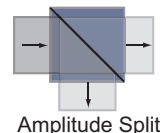
$$HBW = \frac{1-r}{m\pi} \lambda_p [\text{m}].$$



The peak intensity transmission is usually at 20% to 50%, or up to 90% of the incident light for metal-dielectric or multi-dielectric filters respectively.

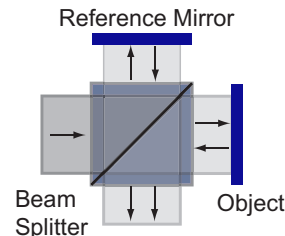
Interferometers

Due to the high frequency of light, it is not possible to detect the phase of the light wave directly. To acquire the phase, interferometry techniques may be used. There are two major classes of interferometers, based on **amplitude splitting** and **wavefront splitting**.

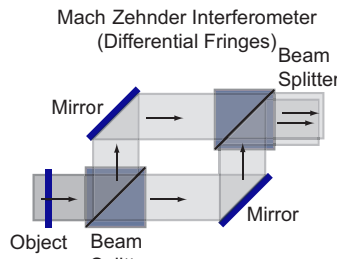
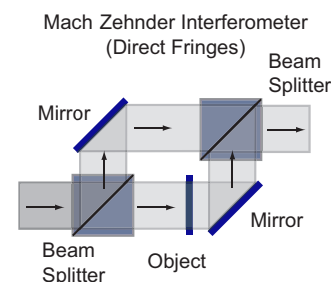
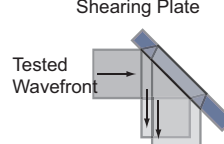


From the point of view of fringe pattern interpretation, interferometers can also be divided into those that deliver fringes, which directly correspond to the phase distribution, and those providing a derivative of the phase map (also called shearing interferometers). The first type is realized by obtaining the interference between the test beam and a reference beam. An example of such a system is the **Michelson interferometer**. **Shearing interferometers** provide the interference of two shifted object wavefronts.

Michelson Interferometer

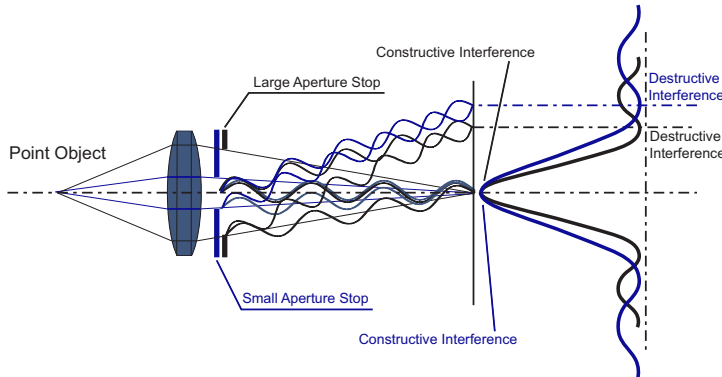


There are numerous ways of introducing shear (linear, radial, etc.). Examples of shearing interferometers include the parallel or wedge plate, the grating interferometer, the **Sagnac**, and polarization interferometers (commonly used in microscopy). The **Mach-Zehnder interferometer** can be configured for direct and differential fringes, depending on the position of the sample.



Diffraction

The bending of waves by apertures and objects is called **diffraction of light**. Waves diffracted inside the optical system interfere (for path differences within the coherence length of the source) with each other and create diffraction patterns in the image of an object.



There are two common approximations of diffraction phenomena: **Fresnel diffraction** (near-field) and **Fraunhofer diffraction** (far-field). Both diffraction types complement each other but are not sharply divided due to various definitions of their regions. Fraunhofer diffraction occurs when one can assume that propagating wavefronts are flat (collimated), while the Fresnel diffraction is the near-field case. Thus, Fraunhofer diffraction (distance z) for a free-space case is infinity, but in practice it can be defined for a region

$$z > S_{FD} \frac{d^2}{\lambda},$$

where d is the diameter of the diffractive object, and S_{FD} is a factor depending on approximation. A conservative definition of the Fraunhofer region is $S_{FD} = 1$, while for most practical cases it can be assumed to be 10 times smaller ($S_{FD} = 0.1$).

Diffraction effects influence the resolution of an imaging system and are a reason for fringes (ring patterns) in the image of a point. Specifically, Fraunhofer fringes appear in the conjugate image plane. This is due to the fact that the image is located in the Fraunhofer diffracting region of an optical system's aperture stop.

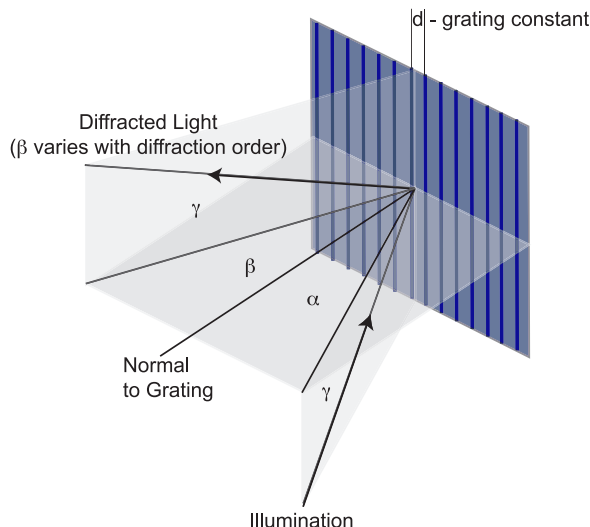
Diffraction Grating

Diffraction gratings are optical components consisting of periodic linear structures that provide “organized” diffraction of light. In practical terms, this means that for specific angles (depending on illumination and grating parameters), it is possible to obtain constructive (2π phase difference) and destructive (π phase difference) interference at specific directions. The angles of constructive interference are defined by the diffraction grating equation and called **diffraction orders** (m).

Gratings can be classified as transmission or reflection (mode of operation), amplitude (periodic amplitude changes) or phase (periodic phase changes), or ruled or holographic (method of fabrication). Ruled gratings are mechanically cut and usually have a triangular profile (each facet can thereby promote select diffraction angles). Holographic gratings are made using interference (sinusoidal profiles).

Diffraction angles depend on the ratio between the grating constant and wavelength so various wavelengths can be separated. This makes them applicable for spectroscopic detection or spectral imaging. The **grating equation** is

$$m\lambda = d \cos \gamma (\sin \beta \pm \sin \alpha)$$

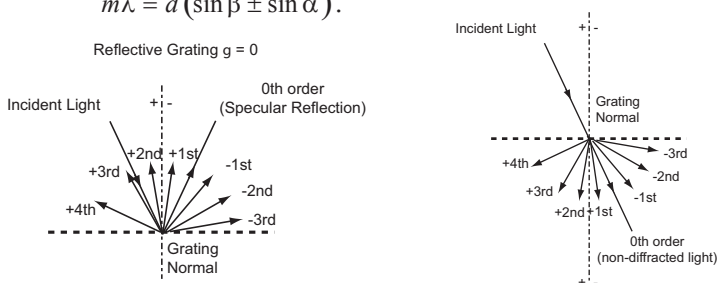


Diffraction Grating (cont.)

The sign in the diffraction grating equation defines the type of grating: A **transmission grating** is identified with a minus sign (-), and a **reflective grating** is identified with a plus sign (+).

For a grating illuminated in the plane perpendicular to the grating, its equation simplifies and is

$$m\lambda = d(\sin \beta \pm \sin \alpha).$$



For normal illumination, the grating equation becomes

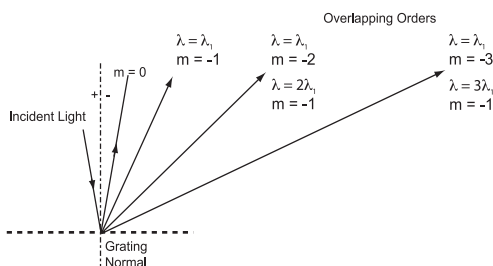
$$m\lambda = d \sin \beta.$$

The **chromatic resolving power** of a grating depends on its size (total number of lines N). If the grating has more lines, the diffraction orders are narrower, and the resolving power increases:

$$\frac{\lambda}{\Delta\lambda} = mN.$$

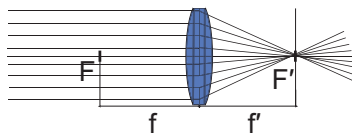
The **free spectral range** $\Delta\lambda$ of the grating is the bandwidth in the m^{th} order without overlapping other orders. It defines useful bandwidth for spectroscopic detection as

$$\Delta\lambda = \frac{m+1}{m} \lambda_1 - \lambda_1 = \frac{\lambda_1}{m}.$$



Useful Definitions from Geometrical Optics

All optical systems consist of refractive or reflective interfaces (surfaces) changing the propagation angles of **optical rays**.



Rays define the propagation trajectory and always travel perpendicular to the wavefronts. They are used to describe imaging in the regime of geometrical optics and to perform optical design.

There are two **optical spaces** corresponding to each optical system: **object space** and **image space**. Both spaces extend from $-\infty$ to $+\infty$ and are divided into real and virtual parts. Ability to access the image or object defines the real part of the optical space.

Paraxial optics is an approximation assuming small ray angles and is used to determine first-order parameters of the optical system (image location, magnification etc.).

Thin lenses are optical components reduced to zero thickness and are used to perform first-order optical designs (see next page).

The **focal point** of an optical system is a location that collimated beams converge to or diverge from. Planes perpendicular to the optical axis at the focal points are called **focal planes**. **Focal length** is the distance between the lens (specifically, its principal plane) and the focal plane. For thin lenses, principal planes overlap with the lens.

Sign Convention: The common sign convention assigns positive values to distances traced from left to right (the direction of propagation) and to the top. Angles are positive if they are measured counterclockwise from normal to the surface or optical axis. If light travels from right to left, the refractive index is negative. The surface radius is measured from its vertex to its center of curvature.

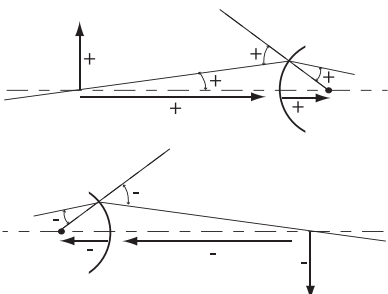
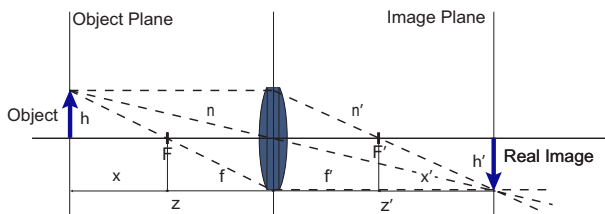


Image Formation

A simple model describing imaging through an optical system is based on thin lens relationships. A **real image** is formed at the point where rays converge.



A **virtual image** is formed at the point from which rays appear to diverge.

For a lens made of glass, surrounded on both sides by air ($n = n' = 1$), the imaging relationship is described by the **Newtonian equation**

$$xx' = ff' \quad \text{or} \quad xx' = -f'^2.$$

Note that Newtonian equations refer to the distance from the focal planes so, in practice, they are used with thin lenses.

Imaging can also be described by the **Gaussian imaging equation**

$$\frac{f}{z} + \frac{f'}{z'} = 1.$$

The **effective focal length** of the system is

$$f_e = \frac{1}{\varphi} = -\frac{f}{n} = \frac{f'}{n'},$$

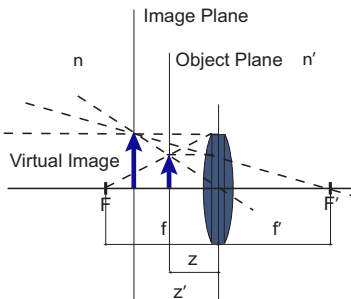
where φ is the **optical power** expressed in diopters $D [m^{-1}]$.

Therefore,

$$\frac{n'}{z'} = \frac{n}{z} + \frac{1}{f_e}.$$

For air, when n and n' are equal to 1, the imaging relation is

$$\frac{1}{z'} = \frac{1}{z} + \frac{1}{f_e}.$$



Magnification

Transverse magnification (also called **lateral magnification**) of an optical system is defined as the ratio of the image and object size measured in the direction perpendicular to the optical axis:

$$M = \frac{h'}{h} = -\frac{x'}{f'} = -\frac{f}{x} = \frac{z'}{z} = \frac{-f}{z-f} = \frac{-(z'-f')}{f'}.$$

Longitudinal magnification defines the ratio of distances for a pair of conjugate planes:

$$\frac{\Delta z'}{\Delta z} = \left(-\frac{f'}{f} \right) M_1 M_2,$$

where

$$\Delta z = z_2 - z_1$$

$$\Delta z' = z'_2 - z'_1$$

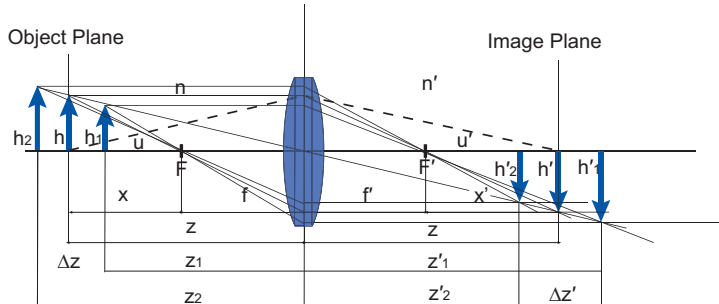
and

$$M_1 = \frac{h'_1}{h_1}$$

$$M_2 = \frac{h'_2}{h_2}.$$

Angular magnification is the ratio of angular image size to angular object size and can be calculated with

$$M_u = \frac{u'}{u} = \frac{z}{z'}.$$



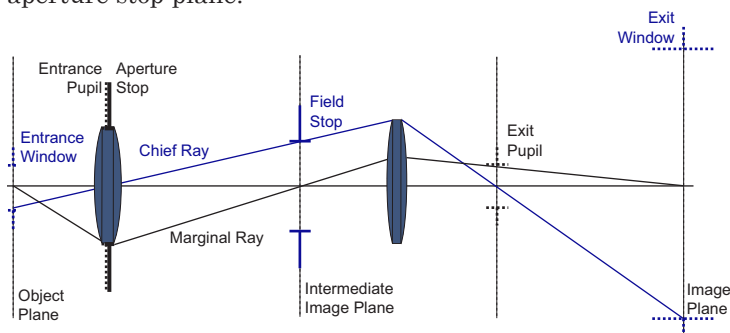
Stops and Rays in an Optical System

The primary stops in any optical system are the **aperture stop** (which limits light) and **field stop** (which limits the extent of the imaged object or the field of view). The aperture stop also defines the resolution of the optical system. To determine the aperture stop, all system diaphragms including the lens mounts should be imaged to either the image or the object space of the system. The aperture stop is determined as the smallest diaphragm or diaphragm image (in terms of angle) as seen from the on-axis object/image point in the same optical space.

Note that there are two important conjugates of the aperture stop in object and image space. They are called the **entrance pupil** and **exit pupil**, respectively.

The physical stop limiting the extent of the field is called the **field stop**. To find a field stop, all of the diaphragms should be imaged to the object or image space, with the smallest diaphragm defining the actual field stop, as seen from the entrance/exit pupil. Conjugates of the field stop in the object and image space are called the **entrance window** and **exit window**, respectively.

Two major rays that pass through the system are the **marginal ray** and the **chief ray**. The marginal ray crosses the optical axis at the conjugate of the field stop (and object) and the edge of the aperture stop. The chief ray goes through the edge of the field and crosses the optical axis at the aperture stop plane.



Aberrations

Individual spherical lenses cannot deliver perfect imaging because they exhibit errors called aberrations. All aberrations can be considered either **chromatic** or **monochromatic**. To correct for aberrations, optical systems use multiple elements, aspherical surfaces, and a variety of optical materials.

Chromatic aberrations are a consequence of the **dispersion** of optical materials, which is a change in the refractive index as a function of wavelength. The parameter characterizing dispersion of any material is called the **Abbe number** and is defined as

$$V_d = \frac{n_d - 1}{n_F - n_C}.$$

Alternatively, the following equation might be used for other wavelengths:

$$V_e = \frac{n_e - 1}{n_{F'} - n_{C'}}.$$

λ [nm]	Symbol	Spectral Line
656	C	red hydrogen
644	C'	red cadmium
588	d	yellow helium
546	e	green mercury
486	F	blue hydrogen
480	F'	blue cadmium

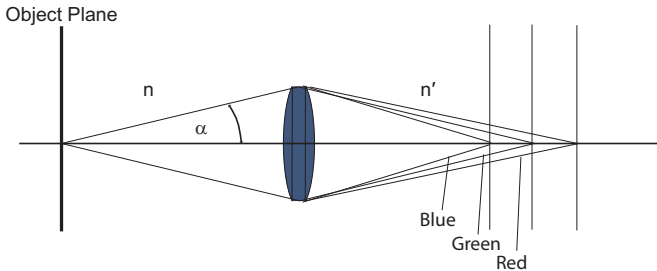
In general, V can be defined by using refractive indices at any three wavelengths, which should be specified for material characteristics. Indices in the equations denote spectral lines. If V does not have an index, V_d is assumed.

Geometrical aberrations occur when optical rays do not meet at a single point. There are longitudinal and transverse ray aberrations describing the axial and lateral deviations from the paraxial image of a point (along the axis and perpendicular to the axis in the image plane), respectively.

Wave aberrations describe a deviation of the wavefront from a perfect sphere. They are defined as a distance (the optical path difference) between the wavefront and the reference sphere along the optical ray.

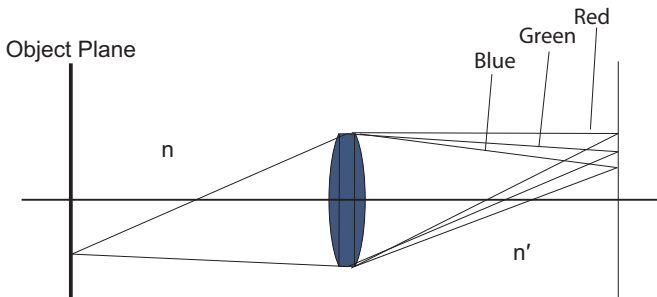
Chromatic Aberrations

Chromatic aberrations occur due to the dispersion of optical materials used for lens fabrication. This means that the refractive index is different for different wavelengths; consequently, various wavelengths are refracted differently.



Chromatic aberrations include axial (longitudinal) or transverse (lateral) aberrations. **Axial chromatic aberration** arises from the fact that various wavelengths are focused at different distances behind the optical system. It is described as a variation in focal length:

$$\frac{\Delta f}{f} = \frac{f_F - f_C}{f} = \frac{1}{V}.$$



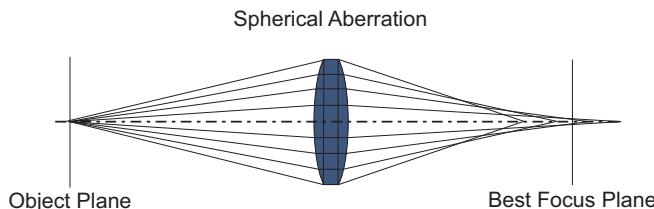
Transverse chromatic aberration is an off-axis imaging of colors at different locations on the image plane.

To compensate for chromatic aberrations, materials with low and high Abbe numbers are used (such as flint and crown glass). Correcting chromatic aberrations is crucial for most microscopy applications, but it is especially important for multi-photon microscopy. Obtaining multi-photon excitation requires high laser power and is most effective using short pulse lasers. Such a light source has a broad spectrum, and chromatic aberrations may cause pulse broadening.

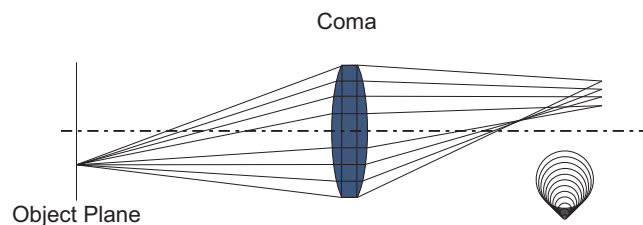
Spherical Aberration and Coma

The most important wave aberrations are spherical, coma, astigmatism, field curvature, and distortion.

Spherical aberration (on-axis) is a consequence of building an optical system with components with spherical surfaces. It occurs when rays from different heights in the pupil are focused at different planes along the optical axis. This results in an axial blur. The most common approach for correcting spherical aberration uses a combination of negative and positive lenses. Systems that correct spherical aberration heavily depend on imaging conditions. For example, in microscopy a cover glass must be of an appropriate thickness and refractive index in order to work with an objective. Also, the media between the objective and the sample (such as air, oil, or water) must be taken into account.

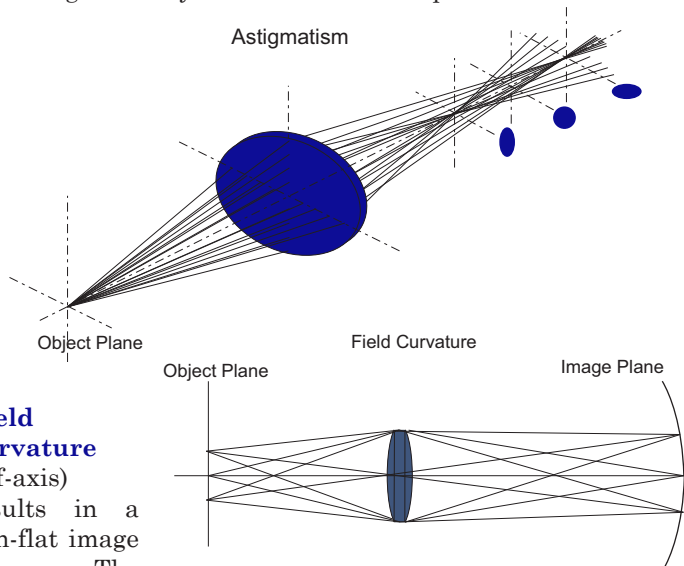


Coma (off-axis) can be defined as a variation of magnification with aperture location. This means that rays passing through a different azimuth of the lens are magnified differently. The name “coma” was inspired by the aberration’s appearance, because it resembles a comet’s tail as it emanates from the focus spot. It is usually stronger for lenses with a larger field, and its correction requires accommodation of the field diameter.



Astigmatism, Field Curvature, and Distortion

Astigmatism (off-axis) is responsible for different magnifications along orthogonal meridians in an optical system. It manifests as elliptical, elongated spots for the horizontal and vertical directions on opposite sides of the best focal plane. It is more pronounced for an object farther from the axis and is a direct consequence of improper lens mounting or an asymmetric fabrication process.



Field curvature (off-axis) results in a non-flat image plane. The image plane created is a concave surface as seen from the objective; therefore, various zones of the image can be seen in focus after moving the object along the optical axis. This aberration is corrected by an objective design combined with a tube lens or eyepiece.

Barrel Distortion and **Pincushion Distortion** are types of **Distortion**. **Distortion** is a radial variation of magnification that will image a square as a pincushion or barrel. It is corrected in the same manner as field curvature. If preceded with system calibration, it can also be corrected numerically after image acquisition.

Performance Metrics

The major metrics describing the performance of an optical system are the **modulation transfer function** (MTF), the **point spread function** (PSF), and the **Strehl ratio** (SR).

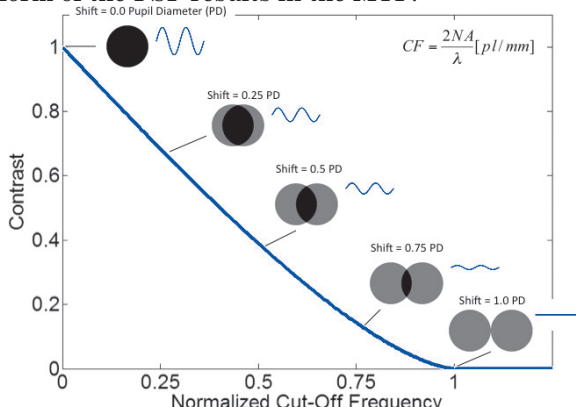
The MTF is the modulus of the **optical transfer function** described by

$$OTF(\rho) = MTF(\rho) \exp[i\phi(\rho)],$$

where the complex term in the equation relates to the phase transfer function. The MTF is a contrast distribution in the image in relation to contrast in the object as a function of spatial frequency ρ (for sinusoidal object harmonics) and can be defined as

$$MTF(\rho) = \frac{C(\rho)_{\text{image}}}{C(\rho)_{\text{object}}}.$$

The PSF is the intensity distribution at the image of a point object. This means that the PSF is a metric directly related to the image, while the MTF corresponds to spatial frequency distributions in the pupil. The MTF and PSF are closely related and comprehensively describe the quality of the optical system. In fact, the amplitude of the Fourier transform of the PSF results in the MTF.



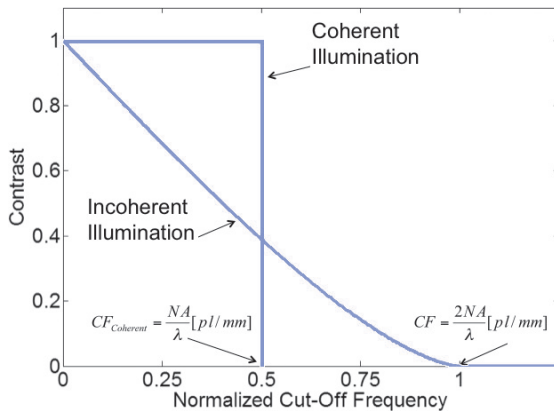
The MTF can be calculated as the autocorrelation of the **pupil function**. The pupil function describes the field distribution of an optical wave in the pupil plane of the optical system. In the case of a uniform pupil's transmission, it directly relates to the field overlap of two mutually shifted pupils where the shift corresponds to spatial frequency.

Performance Metrics (cont.)

The **modulation transfer function** has different results for coherent and incoherent illumination. For incoherent illumination, the phase component of the field is neglected since it is an average of random fields propagating under random angles.

For coherent illumination, the contrast of transferring harmonics of the field is constant and equal to 1 until the location of the spatial frequency in the pupil reaches its edge. For higher frequencies, the contrast sharply drops to zero since they cannot pass the optical system. Note that contrast for the coherent case is equal to 1 for the entire MTF range.

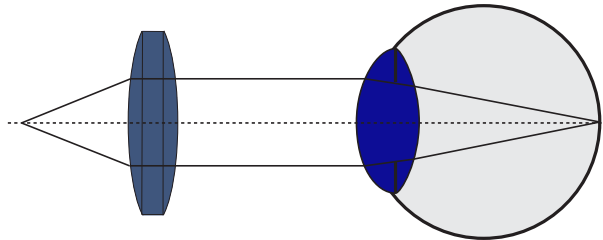
The **cutoff frequency** for an incoherent system is two times the cutoff frequency of the equivalent aperture coherent system and defines the **Sparrow resolution limit**.



The **Strehl ratio** is a parametric measurement that defines the quality of the optical system in a single number. It is defined as the ratio of irradiance within the theoretical dimension of a diffraction-limited spot to the entire irradiance in the image of the point. One simple method to estimate the Strehl ratio is to divide the field below the MTF curve of a tested system by the field of the diffraction-limited system of the same numerical aperture. For practical optical design consideration it is usually assumed that the system is diffraction limited if the Strehl ratio is equal to or larger than 0.8.

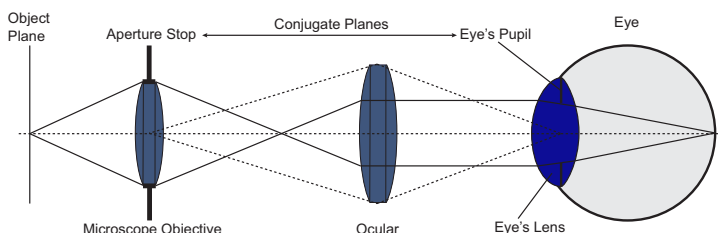
The Compound Microscope

The primary goal of microscopy is to provide the ability to resolve the small details of an object. Historically, microscopy was developed for visual observation and, therefore, was set up to work in conjunction with the human eye. An effective high-resolution optical system must have resolving ability and be able to deliver proper magnification for the detector. In the case of visual observations, the detectors are the cones and rods of the retina.

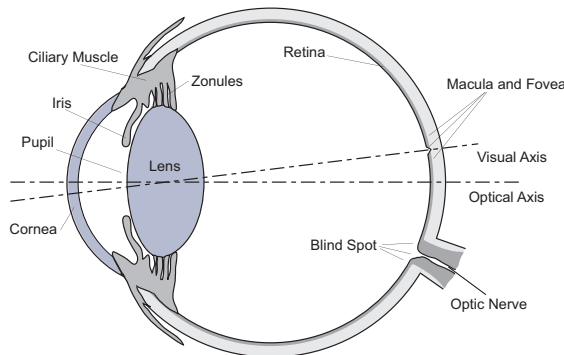


A basic microscope can be built with a single-element, short-focal-length lens (**magnifier**). The object is located in the focal plane of the lens and is imaged to infinity. The eye creates a final image of the object on the retina. The system stop is the eye's pupil.

To obtain higher resolution for visual observation, the **compound microscope** was first built in the 17th century by Robert Hooke. It consists of two major components: the **objective** and the **eyepiece**. The short-focal-length lens (objective) is placed close to the object under examination and creates a real image of an object at the focal plane of the second lens. The eyepiece (similar to the magnifier) throws an image to infinity, and the human eye creates the final image. An important function of the eyepiece is to match the eye's pupil with the system stop, which is located in the back focal plane of the microscope objective.



The Eye



The **eye** was the first—and for a long time, the only—real-time detector used in microscopy. Therefore, the design of the microscope had to incorporate parameters responding to the needs of visual observation.

Cornea—the transparent portion of the sclera (the white portion of the human eye), which is a rigid tissue that gives the eyeball its shape. The cornea is responsible for two thirds of the eye's refractive power.

Lens—the lens is responsible for one third of the eye's power. Ciliary muscles can change the lens's power (accommodation) within the range of 15–30 diopters.

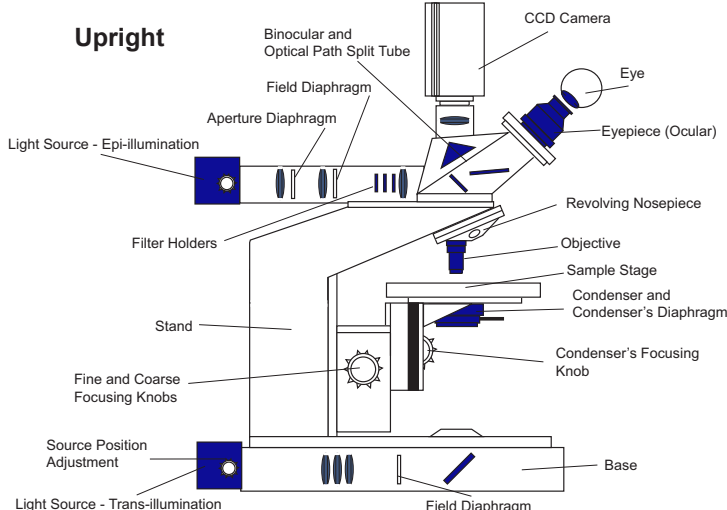
Iris—controls the diameter of the pupil (1.5–8 mm).

Retina—a layer with two types of photoreceptors: rods and cones. **Cones** (about 7 million) are in the area of the **macula** (~3 mm in diameter) and **fovea** (~1.5 mm in diameter, with the highest cone density), and they are designed for bright vision and color detection. There are three types of cones (red, green, and blue sensitive), and the spectral range of the eye is approximately 400–750 nm. **Rods** are responsible for night/low-light vision, and there are about 130 million located outside the fovea region.

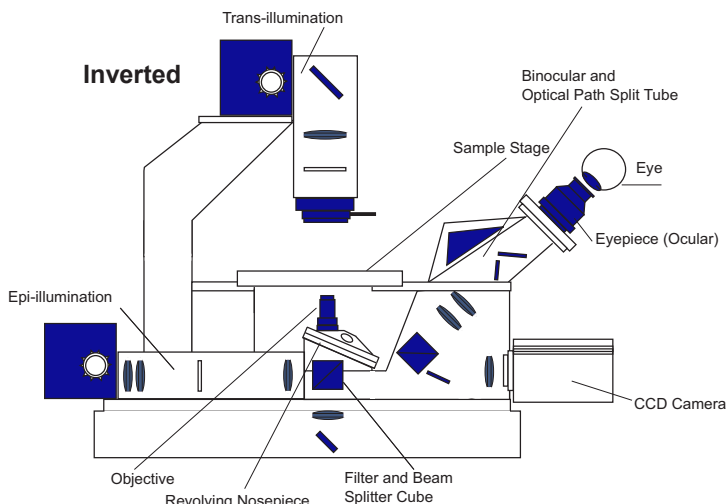
It is arbitrarily assumed that the eye can provide sharp images for objects between 250 mm and infinity. A 250-mm distance is called the **minimum focus distance** or **near point**. The maximum eye resolution for bright illumination is 1 arc minute.

Upright and Inverted Microscopes

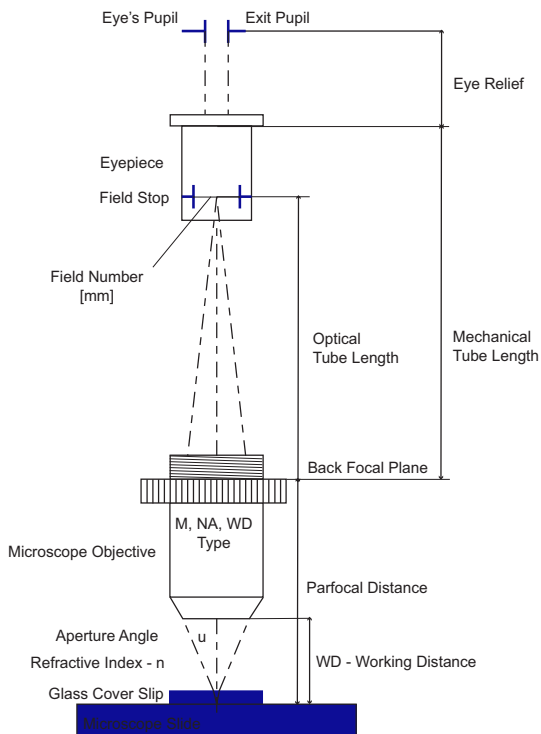
The two major microscope geometries are **upright** and **inverted**. Both systems can operate in reflectance and transmittance modes.



The inverted microscope is primarily designed to work with samples in cell culture dishes and to provide space (with a long-working distance condenser) for sample manipulation (for example, with patch pipettes in electrophysiology).



The Finite Tube Length Microscope



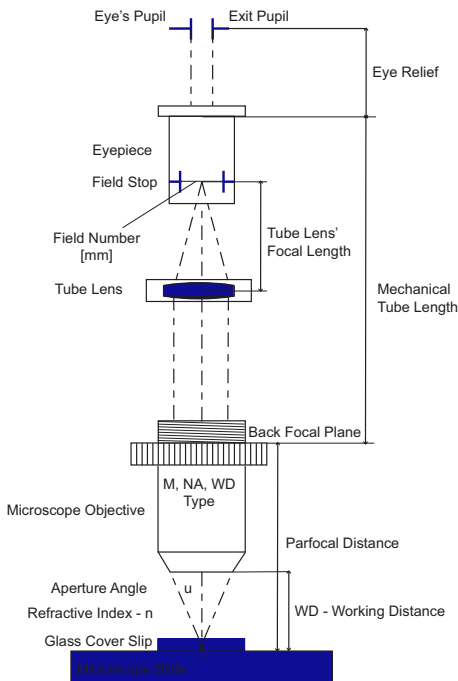
Historically, microscopes were built with a **finite tube length**. With this geometry, the microscope objective images the object into the tube end. This intermediate image is then relayed to the observer by an eyepiece. Depending on the manufacturer, different **optical tube lengths** are possible (for example, the standard tube length for Zeiss is 160 mm). The use of a standard tube length by each manufacturer unifies the optomechanical design of the microscope.

A constant **parfocal distance** for microscope objectives enables switching between different magnifications without defocusing. The **field number**, corresponding to the physical dimension (in millimeters) of the **field stop** inside the eyepiece, allows the microscope's field of view (FOV) to be determined according to

$$FOV = \frac{FieldNumber}{M_{\text{objective}}} [\text{mm}].$$

Infinity-Corrected Systems

Microscope objectives can be corrected for a conjugate located at infinity, which means that the microscope objective images an object into infinity. An infinite conjugate is useful for introducing beam splitters or filters that should work with small incidence angles. Also, an infinity-corrected system accommodates additional components like DIC prisms,



polarizers, etc. The collimated beam is focused to create an intermediate image with additional optics, called a **tube lens**. The tube lens either creates an image directly onto a CCD chip or an intermediate image, which is further reimaged with an eyepiece. Additionally, the tube lens might be used for system correction. For example, Zeiss corrects aberrations in its microscopes with a combination objective-tube lens.

In the case of an **infinity-corrected objective**, the transverse magnification can only be defined in the presence of a tube lens that will form a real image. It is given by the ratio between the tube lens's focal length and

the focal length of the microscope objective.

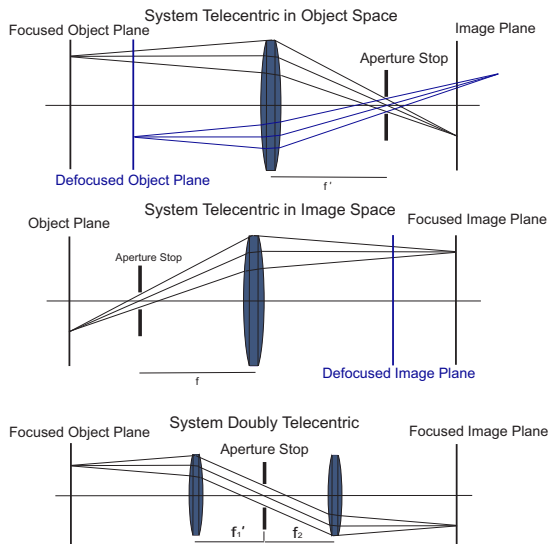
Manufacturer	Focal Length of Tube Lens
Zeiss	164.5 mm
Olympus	180.0 mm
Nikon	200.0 mm
Leica	200.0 mm

Telecentricity of a Microscope

Telecentricity is a feature of an optical system where the principal ray in object, image, or both spaces is parallel to the optical axis. This means that the object or image does not shift laterally, even with defocus; the distance between two object or image points is constant along the optical axis.

An optical system can be **telecentric** in

- Object space, where the entrance pupil is at infinity, and the aperture stop is in the back focal plane;
- Image space, where the exit pupil is at infinity, and the aperture stop is in the front focal plane; or
- Both (doubly telecentric), where the entrance and exit pupils are at infinity, and the aperture stop is at the center of the system, in the back focal plane of the element before the stop and front focal length of the element after the stop (afocal system).

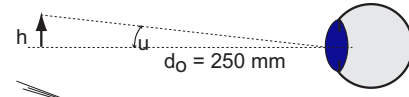


The aperture stop in a microscope is located at the back focal plane of the microscope objective. This makes the microscope objective telecentric in object space. Therefore, in microscopy, the object is observed with constant magnification, even for defocused object planes. This feature of microscopy systems significantly simplifies their operation and increases the reliability of image analysis.

Magnification of a Microscope

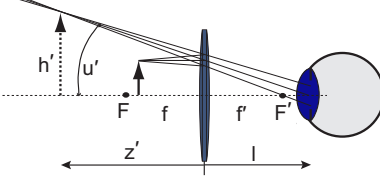
Magnifying power (MP) is defined as the ratio between the angles subtended by an object with and without magnification. The magnifying power (as defined for a single lens) creates an enlarged virtual image of an object. The angle of an object observed with magnification is

$$u' = \frac{h'}{z' - l} = \frac{h(f - z')}{f(z' - l)}.$$



Therefore,

$$MP = \frac{u'}{u} = \frac{d_o(f - z')}{f(z' - l)}.$$



The angle for an unaided eye is defined for the **minimum focus distance** (d_o) of 10 inches or 250 mm, which is the distance that the object (real or virtual) may be examined without discomfort for the average population. A distance l between the lens and the eye is often small and can be assumed to equal zero:

$$MP \approx \frac{250\text{mm}}{f} - \frac{250\text{mm}}{z'}.$$

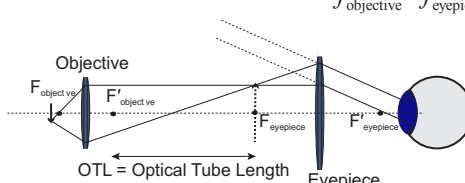
If the virtual image is at infinity (observed with a relaxed eye), $z' = -\infty$, and

$$MP \approx \frac{250\text{mm}}{f}.$$

The total magnifying power of the microscope results from the magnification of the microscope objective and the magnifying power of the eyepiece (usually 10 \times):

$$M_{\text{objective}} = \frac{OTL}{f_{\text{objective}}}$$

$$MP_{\text{microscope}} = M_{\text{objective}} MP_{\text{eyepiece}} = -\frac{OTL}{f_{\text{objective}}} \frac{250\text{mm}}{f_{\text{eyepiece}}}.$$



Numerical Aperture

The aperture diaphragm of the optical system determines the angle at which rays emerge from the axial object point and, after refraction, pass through the optical system. This acceptance angle is called the object space aperture angle. The parameter describing system throughput and this acceptance angle is called the **numerical aperture** (NA):

$$NA = n \sin u.$$

As seen from the equation, throughput of the optical system may be increased by using media with a high refractive index n , e.g., oil or water. This effectively decreases the refraction angles at the interfaces.

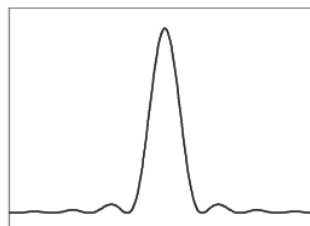
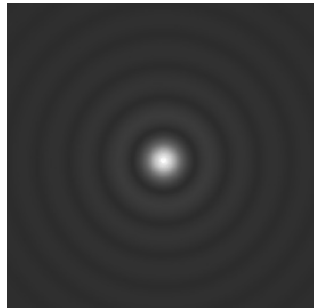
The dependence between the numerical aperture in the object space NA and the numerical aperture in the image space between the objective and the eyepiece NA' is calculated using the objective magnification:

$$NA = NA' M_{\text{objective}}.$$

As a result of diffraction at the aperture of the optical system, self-luminous points of the object are not imaged as points but as so-called Airy disks. An **Airy disk** is a bright disk surrounded by concentric rings with gradually decreasing intensities. The disk diameter (where the intensity reaches the first zero) is

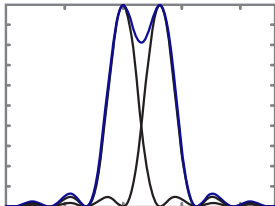
$$d = \frac{1.22\lambda}{n \sin u} = \frac{1.22\lambda}{NA}.$$

Note that the refractive index in the equation is for media between the object and the optical system.



Media	Refractive Index
Air	1
Water	1.33
Oil	1.45–1.6 (1.515 is typical)

Resolution Limit



The lateral resolution of an optical system can be defined in terms of its ability to resolve images of two adjacent, self-luminous points. When two **Airy disks** are too close, they form a continuous intensity distribution and cannot be distinguished. The **Rayleigh resolution limit** is defined as occurring when the peak of the Airy pattern arising from one point coincides with the first minimum of the Airy pattern arising from a second point object. Such a distribution gives an intensity dip of 26%. The distance between the two points in this case is

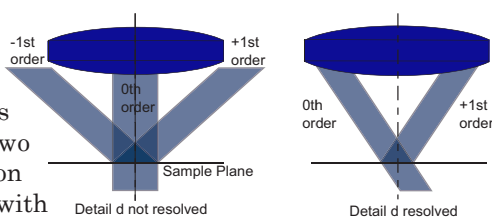
$$d = \frac{0.61\lambda}{n \sin u} = \frac{0.61\lambda}{NA}.$$

The equation indicates that the resolution of an optical system improves with an increase in NA and decreases with increasing wavelength λ . For example, for $\lambda = 450$ nm (blue) and oil immersion $NA = 1.4$, the microscope objective can optically resolve points separated by less than 200 nm.

The situation in which the intensity dip between two adjacent self-luminous points becomes zero defines the **Sparrow resolution limit**. In this case $d = 0.5\lambda/NA$.

The **Abbe resolution limit** considers both the diffraction caused by the object and the NA of the optical system. It assumes that if at least two adjacent diffraction orders for points with spacing d are accepted by the objective, these two points can be resolved. Therefore, the resolution depends on both imaging and illumination apertures and is

$$d = \frac{\lambda}{NA_{\text{objective}} + NA_{\text{condenser}}}.$$



Useful Magnification

For visual observation, the **angular resolving power** can be defined as 1.5 arc minutes. For unmagnified objects at a distance of 250 mm (the eye's minimum focus distance), 1.5 arc minutes converts to $d_{\text{eye}} = 0.1 \text{ mm}$. Since microscope objectives by themselves do not usually provide sufficient magnification, they are combined with oculars or eyepieces. The resolving power of the microscope is then

$$d_{\text{mic}} = \frac{d_{\text{eye}}}{M_{\text{min}}} = \frac{d_{\text{eye}}}{M_{\text{obj}} M_{\text{eyepiece}}}.$$

In the Sparrow resolution limit, the minimum microscope magnification is

$$M_{\text{min}} = 2d_{\text{eye}} NA / \lambda.$$

Therefore, a total minimum magnification M_{min} can be defined as approximately 250–500 NA (depending on wavelength). For lower magnification the image will appear brighter, but imaging is performed below the overall resolution limit of the microscope. For larger magnification, the contrast decreases and resolution does not improve. While a theoretically higher magnification should not provide additional information, it is useful to increase it to approximately 1000 NA to provide comfortable sampling of the object. Therefore, it is assumed that the **useful magnification** of a microscope is between 500 NA and 1000 NA. Usually, any magnification above 1000 NA is called **empty magnification**. The image size in such cases is enlarged, but no additional useful information is provided. The highest useful magnification of a microscope is approximately 1500 for an oil-immersion microscope objective with $NA = 1.5$.

Similar analysis can be performed for digital microscopy, which uses CCD or CMOS cameras as image sensors. Camera pixels are usually small (between 2 and 30 microns), and useful magnification must be estimated for a particular image sensor rather than the eye. Therefore, digital microscopy can work at lower magnification, and magnification of the microscope objective alone is usually sufficient.

Depth of Field and Depth of Focus

Two important terms are used to define axial resolution: **depth of field** and **depth of focus**. Depth of field refers to the object thickness for which an image is in focus, while

depth of focus is the corresponding thickness of the image plane. In the case of a diffraction-limited optical system, the depth of focus is determined for an intensity drop along the optical axis to 80%, defined as

$$DOF = 2\Delta z' = \frac{n'\lambda}{NA'^2}.$$

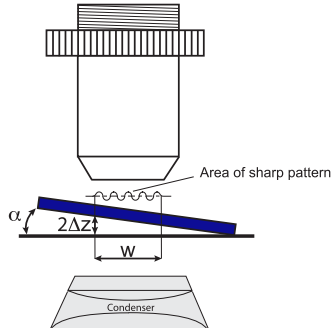
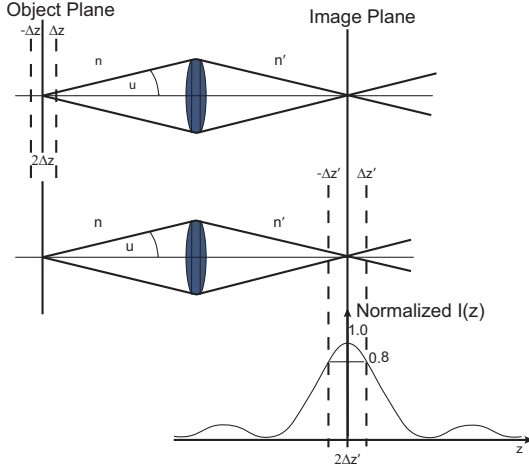
The relation between depth of field ($2\Delta z$) and depth of focus ($2\Delta z'$) incorporates the objective magnification:

$$2\Delta z' = M_{\text{objective}}^2 2\Delta z \frac{n'}{n},$$

where n' and n are medium refractive indexes in the object and image space, respectively.

To quickly measure the depth of field for a particular microscope objective, the grid amplitude structure can be placed on the microscope stage and tilted with the known angle α . The depth of field is determined after measuring the grid zone w while in focus:

$$2\Delta z = nw \tan \alpha .$$

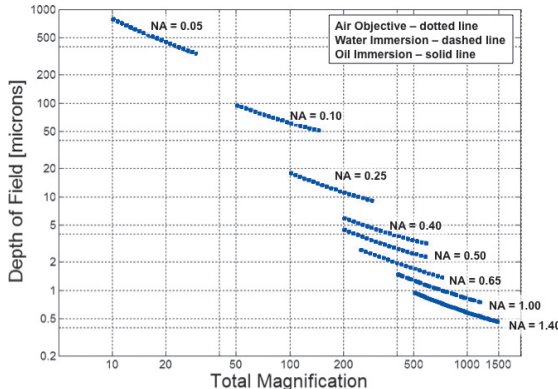


Magnification and Frequency vs Depth of Field

Depth of field for visual observation is a function of the total microscope magnification and the NA of the objective, approximated as

$$2\Delta z = n \frac{0.5\lambda}{NA^2} + n \frac{340}{M_{\text{microscope}} NA} .$$

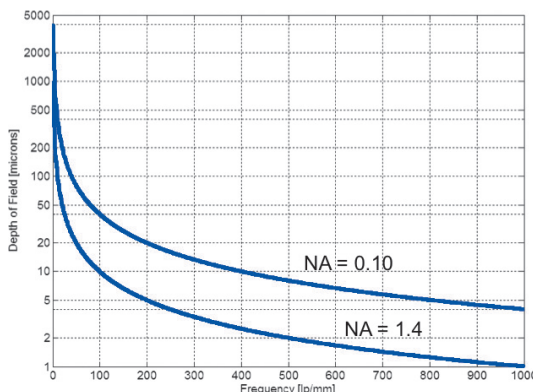
Note that estimated values do not include eye accommodation. The graph below presents depth of field for visual observation. Refractive index n of the object space was assumed to equal 1. For other media, values from the graph must be multiplied by an appropriate n .



Depth of field can also be defined for a specific frequency present in the object because imaging contrast changes for a particular object frequency, as described by the modulation transfer function. The approximated equation is

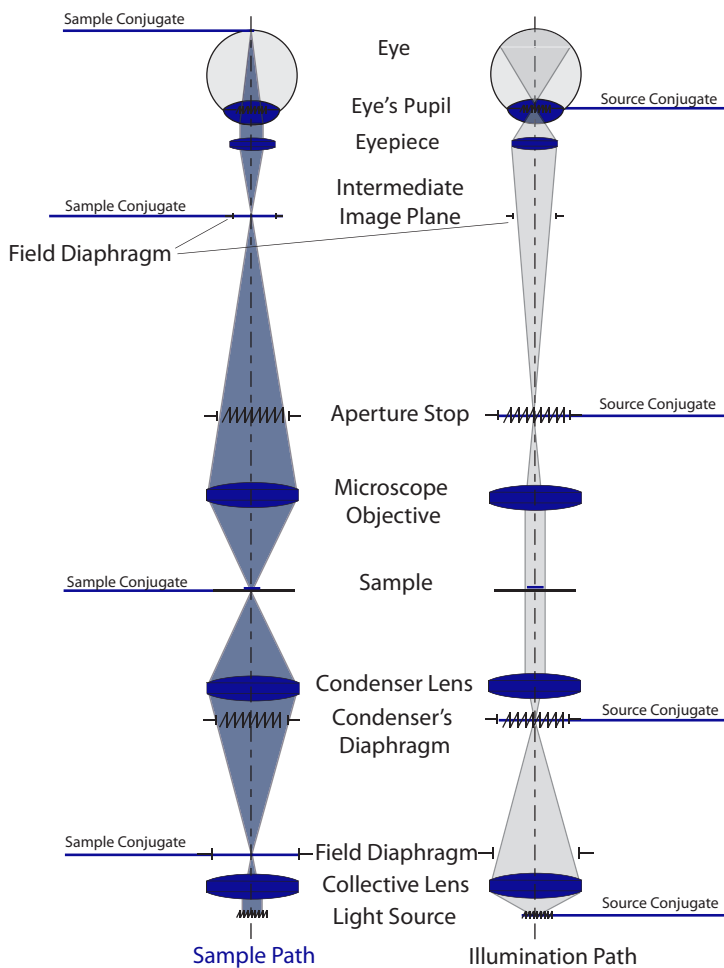
$$2\Delta z = \frac{0.4}{\rho NA} ,$$

where ρ is the frequency in cycles per millimeter.



Köhler Illumination

One of the most critical elements in efficient microscope operation is proper set up of the illumination system. To assist with this, August Köhler introduced a solution that provides uniform and bright illumination over the field of view, even for light sources that are not uniform (e.g., a lamp filament). This system consists of a light source, a field-stop diaphragm, a condenser aperture, and collective and condenser lenses. This solution is now called **Köhler illumination** and is commonly used for a variety of imaging modes.



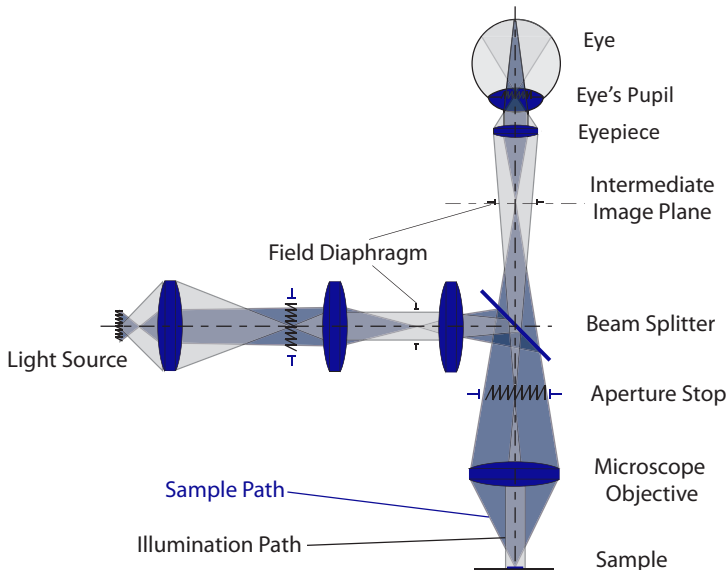
Köhler Illumination (cont.)

The illumination system is configured such that an image of the light source completely fills the condenser aperture.

Köhler illumination requires setting up the microscope system so that the field diaphragm, object plane, and intermediate image in the eyepiece's field stop, retina, or CCD are in conjugate planes. Similarly, the lamp filament, front aperture of the condenser, microscope objective's back focal plane (aperture stop), exit pupil of the eyepiece, and the eye's pupil are also at conjugate planes. Köhler illumination can be set up for both the transmission mode (also called **DIA**) and the reflectance mode (also called **EPI**).

The uniformity of the illumination is the result of having the light source at infinity with respect to the illuminated sample.

EPI illumination is especially useful for the biological and metallurgical imaging of thick or opaque samples.



Alignment of Köhler Illumination

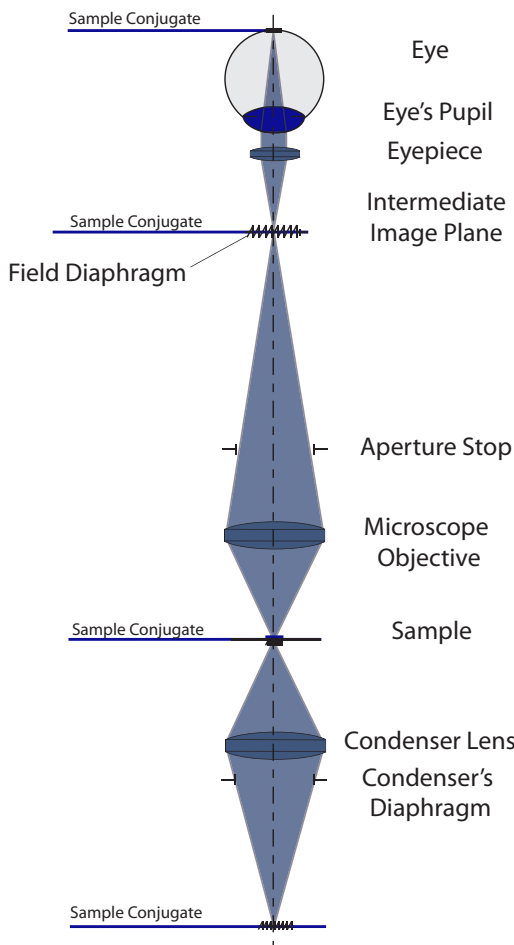
The procedure for **Köhler illumination** alignment consists of the following steps:

1. Place the sample on the microscope stage and move it so that the front surface of the condenser lens is 1–2 mm from the microscope slide. The condenser and collective diaphragms should be wide open.
2. Adjust the location of the source so illumination fills the condenser's diaphragm. The sharp image of the lamp filament should be visible at the condenser's diaphragm plane and at the back focal plane of the microscope objective. To see the filament at the back focal plane of the objective, a **Bertrand lens** can be applied (also see *Special Lens Components* on page 55). The filament should be centered in the aperture stop using the bulb's adjustment knobs on the illuminator.
3. For a low-power objective, bring the sample into focus. Since a microscope objective works at a parfocal distance, switching to a higher magnification later is easy and requires few adjustments.
4. Focus and center the condenser lens. Close down the field diaphragm, focus down the outline of the diaphragm, and adjust the condenser's position. After adjusting the x -, y -, and z -axis, open the field diaphragm so it accommodates the entire field of view.
5. Adjust the position of the condenser's diaphragm by observing the back focal objective plane through the Bertrand lens. When the edges of the aperture are sharply seen, the condenser's diaphragm should be closed to approximately three quarters of the objective's aperture.
6. Tune the brightness of the lamp. This adjustment should be performed by regulating the voltage of the lamp's power supply or, preferably, through the neutral density filters in the beam path. Do not adjust the brightness by closing the condenser's diaphragm because it affects the illumination setup and the overall microscope resolution.

Note that while three quarters of the aperture stop is recommended for initial illumination, adjusting the aperture of the illumination system affects the resolution of the microscope. Therefore, the final setting should be adjusted after examining the images.

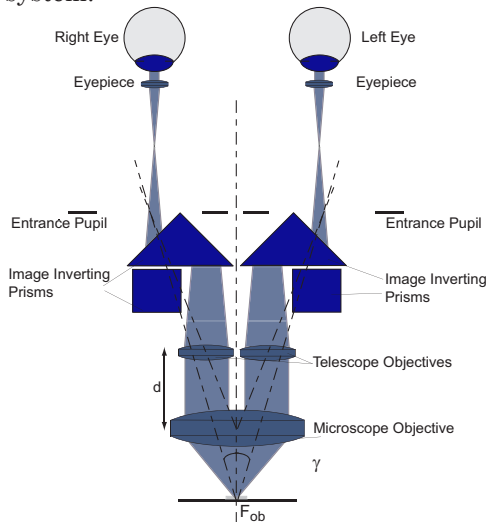
Critical Illumination

An alternative to Köhler illumination is **critical illumination**, which is based on imaging the light source directly onto the sample. This type of illumination requires a highly uniform light source. Any source non-uniformities will result in intensity variations across the image. Its major advantage is high efficiency, since it can collect a larger solid angle than Köhler illumination and therefore provides a higher energy density at the sample. For parabolic or elliptical reflective collectors, critical illumination can utilize up to 85% of the light emitted by the source.



Stereo Microscopes

Stereo microscopes are built to provide depth perception, which is important for applications like micro-assembly and biological and surgical imaging. Two primary stereo-microscope approaches involve building two separate tilted systems, or using a common objective combined with a binocular system.



In the latter, the angle of convergence γ of a stereo microscope depends on the focal length of a microscope objective and a distance d between the microscope objective and telescope objectives. The entrance pupils of the microscope are images of the stops (located at the plane of the telescope objectives) through the microscope objective.

Depth perception δz can be defined as

$$\delta z = \frac{250\alpha_s}{M_{\text{microscope}} \tan \gamma} [\text{mm}],$$

where α_s is a **visual stereo resolving power**, which for daylight vision is approximately 5–10 arc seconds.

Stereo microscopes have a convergence angle γ in the range of 10–15 deg. Note that γ is 15 deg for visual observation and 0 for a standard microscope. For example, depth perception for the human eye is approximately 0.05 mm (at 250 mm), while for a stereo microscope of $M_{\text{microscope}} = 100$ and $\gamma = 15$ deg, it is $\delta z = 0.5 \mu\text{m}$.

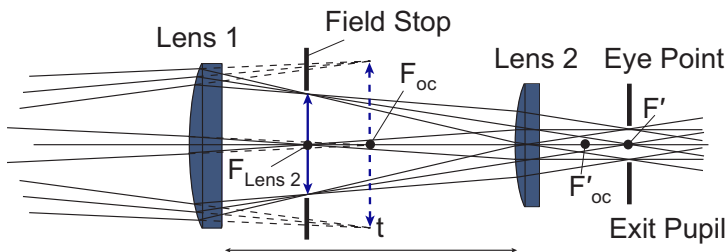
Eyepieces

The eyepiece relays an intermediate image into the eye, corrects for some remaining objective aberrations, and provides measurement capabilities. It also needs to relay an exit pupil of a microscope objective onto the entrance pupil of the eye. The location of the relayed exit pupil is called the **eye point** and needs to be in a comfortable observation distance behind the eyepiece. The clearance between the mechanical mounting of the eyepiece and the eye point is called **eye relief**. Typical eye relief is 7–12 mm.

An eyepiece usually consists of two lenses: one (closer to the eye) which magnifies the image, and a second working as a collective lens and also responsible for the location of the exit pupil of the microscope. An eyepiece contains a field stop that provides a sharp image edge.

Parameters like **magnifying power** of an eyepiece and **field number** (FN), i.e., field of view of an eyepiece, are engraved on an eyepiece's barrel: $M \times / FN$. Field number and magnification of a microscope objective allow quick calculation of the imaged area of a sample (see also *The Finite Tube Length Microscope* on p. 34). Field number varies with microscopy vendors and eyepiece magnification. For 10 \times or lower magnification eyepieces, it is usually 20–28 mm while for higher magnification, wide-angle oculars can get down to approximately 5 mm.

The majority of eyepieces are **Huygens**, **Ramsden**, or derivations of them. The Huygens eyepiece consists of two plano-convex lenses with convex surfaces facing the microscope objective:



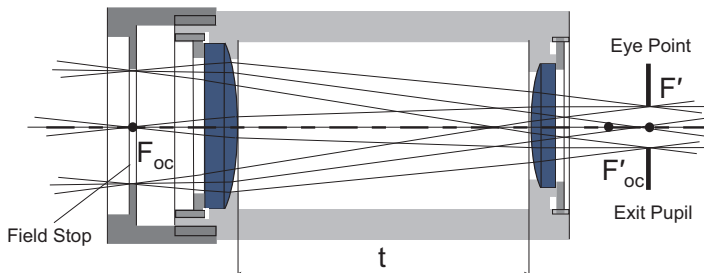
Eyepieces (cont.)

Both lenses are usually made with crown glass and allow for some correction of lateral color, coma, and astigmatism. To correct for color, the following conditions should be met:

$$f_1 \approx f_2 \quad \text{and} \quad t \approx 1.5f_2.$$

For higher magnifications, the exit pupil moves toward the ocular, making observation less convenient, and so this eyepiece is used only for low magnifications ($\leq 10\times$). In addition, Huygens oculars effectively correct for chromatic aberrations, and therefore can be more effectively used with lower-end microscope objectives (e.g., achromatic).

The Ramsden eyepiece consists of two plano-convex lenses with convex surfaces facing each other. Both focal lengths are very similar, and the distance between lenses is smaller than f_2 :



The field stop is placed in the front focal plane of the eyepiece. A collective lens does not participate in creating an intermediate image, so the Ramsden eyepiece works as a simple magnifier:

$$f_1 = f_2 \quad \text{and} \quad t < f_2.$$

Compensating eyepieces work in conjunction with microscope objectives to correct for lateral color (apoachromatic).

High-eye point oculars provide an extended distance between the last mechanical surface and the exit pupil of the eyepiece. They allow users with glasses to comfortably use a microscope. The convenient high eye-point location should be 20–25 mm behind the eyepiece.

Nomenclature and Marking of Objectives

Objective parameters include:

Objective correction—such as Achromat, Plan Achromat, Fluor, Plan Fluor, Apochromat (Apo), and Plan Apochromat.

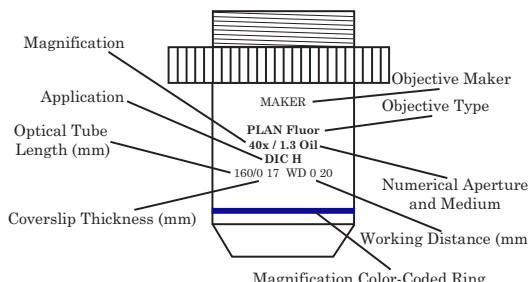
Magnification—the lens magnification for a finite tube length, or for a microscope objective in combination with a tube lens. In infinity-corrected systems, magnification depends on the ratio between the focal lengths of a tube lens and a microscope objective. A particular objective type should be used only in combination with the proper tube lens.

Magnification	Zeiss Code
1×, 1.25×	Black
2.5×	Khaki
4×, 5×	Red
6.3×	Orange
10×	Yellow
16×, 20×, 25×, 32×	Green
25×, 32×	Green
40×, 50×	Light Blue
63×	Dark Blue
> 100×	White

Application—specialized use or design of an objective, e.g., H (bright field), D (dark field), DIC (differential interference contrast), RL (reflected light), PH (phase contrast), or P (polarization).

Tube length—an infinity corrected (∞) or finite tube length in mm.

Cover slip—the thickness of the cover slip used (in mm). “0” or “–” means no cover glass or the cover slip is optional, respectively.



Numerical aperture (NA) and medium—defines system throughput and resolution. It depends on the media between the sample and objective. The most common media are air (no marking), oil (Oil), water (W), or Glycerine.

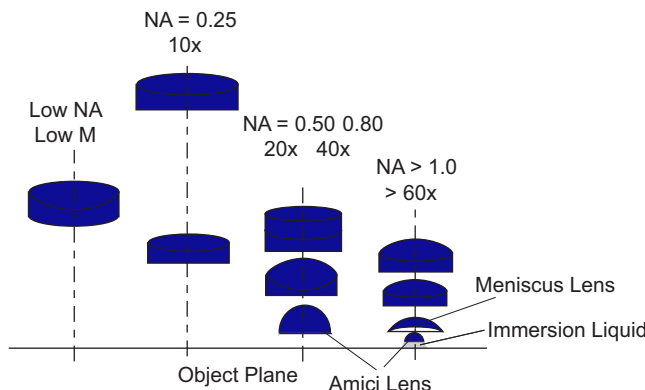
Working distance (WD)—the distance in millimeters between the surface of the front objective lens and the object.

Objective Designs

Achromatic objectives (also called **achromats**) are corrected at two wavelengths: 656 nm and 486 nm. Also, spherical aberration and coma are corrected for green (546 nm), while astigmatism is very low. Their major problems are a secondary spectrum and field curvature.

Achromatic objectives are usually built with a lower NA (below 0.5) and magnification (below 40 \times). They work well for white light illumination or single wavelength use. When corrected for field curvature, they are called plan-achromats.

Achromatic Objectives

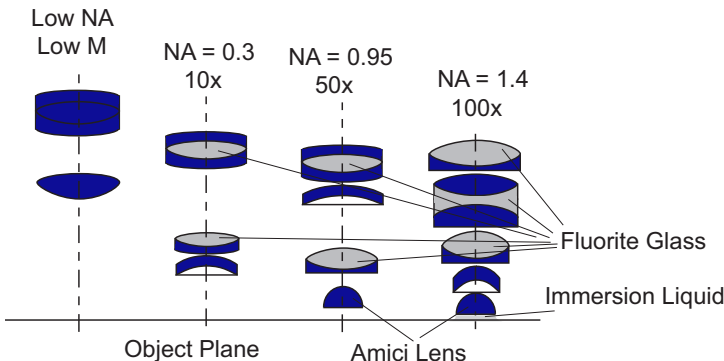


Fluorites or **semi-apochromats** have similar color correction as **achromats**; however, they correct for spherical aberration for two or three colors. The name “fluorites” was assigned to this type of objective due to the materials originally used to build this type of objective. They can be applied for higher NA (e.g., 1.3) and magnifications, and used for applications like immunofluorescence, polarization, or differential interference contrast microscopy.

The most advanced microscope objectives are **apochromats**, which are usually chromatically corrected for three colors, with spherical aberration correction for at least two colors. They are similar in construction to fluorites but with different thicknesses and surface figures. With the correction of field curvature, they are called plan-apochromats. They are used in fluorescence microscopy with multiple dyes and can provide very high NA (1.4). Therefore, they are suitable for low-light applications.

Objective Designs (cont.)

Apochromatic Objectives



Type	Number of wavelengths for spherical correction	Number of colors for chromatic correction
Achromat	1	2
Fluorite	2–3	2–3
Plan-Fluorite	2–4	2–4
Plan-Apochromat	2–4	3–5

(Adapted from Murphy, 2001 and <http://www.microscopyu.com/>)

Examples of typical objective parameters are shown in the table below:

M	Type	Medium	WD	NA	d	DOF
10	Achromat	Air	4.4	0.25	1.34	8.80
20	Achromat	Air	0.53	0.45	0.75	2.72
40	Fluorite	Air	0.50	0.75	0.45	0.98
40	Fluorite	Oil	0.20	1.30	0.26	0.49
60	Apochromat	Air	0.15	0.95	0.35	0.61
60	Apochromat	Oil	0.09	1.40	0.24	0.43
100	Apochromat	Oil	0.09	1.40	0.24	0.43

Refractive index of oil is $n = 1.515$

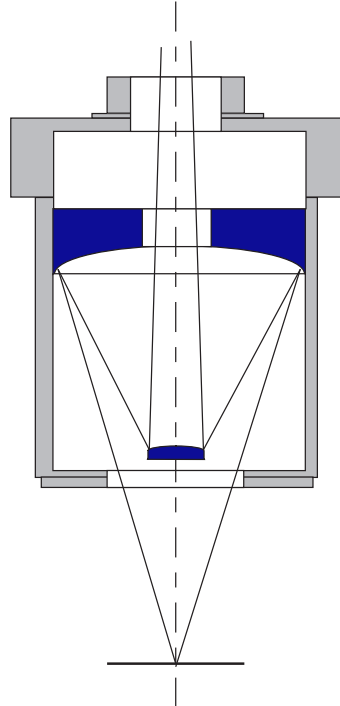
(Adapted from Murphy, 2001)

Special Objectives and Features

Special types of objectives include long working distance objectives, ultra-low-magnification objectives, water-immersion objectives, and UV lenses.

Long working distance objectives allow imaging through thick substrates like culture dishes. They are also developed for interferometric applications in Michelson and Mirau configurations. Alternatively, they can allow for the placement of instrumentation (e.g., micropipettes) between a sample and an objective. To provide a long working distance and high NA, a common solution is to use reflective objectives, or extend the working distance of a standard microscope objective by using a reflective attachment. While reflective objectives have the advantage of being free of chromatic aberrations, their serious drawback is a smaller field of view relative to refractive objectives. The central obscuration also decreases throughput by 15%–20%.

LWD Reflective Objective



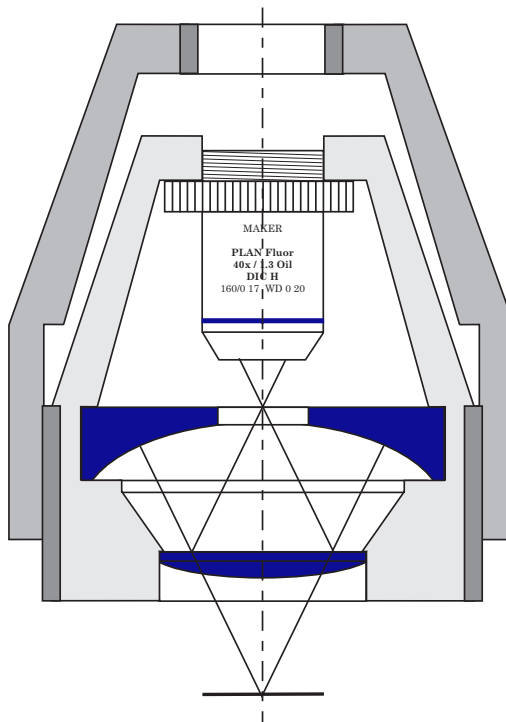
Special Objectives and Features (cont.)

Low magnification objectives can achieve magnifications as low as 0.5. However, in some cases they are not fully compatible with microscopy systems, and may not be telecentric in the image space. They also often require special tube lenses and special condensers to provide Köhler illumination.

Water immersion objectives are increasingly common, especially for biological imaging, because they provide a high NA and avoid toxic immersion oils. They usually work without a cover slip.

UV objectives are made using UV transparent, low-dispersion materials such as quartz. These objectives enable imaging at wavelengths from the near-UV through the visible spectrum, e.g., 240–700 nm. Reflective objectives can also be used for the IR bands.

Reflective Adapter to extend working distance WD

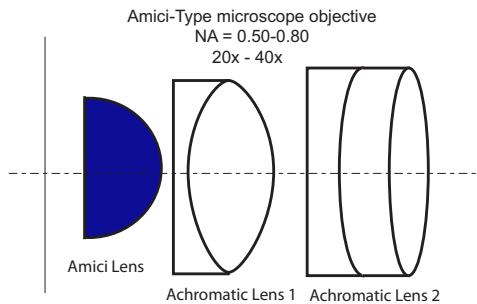


Special Lens Components

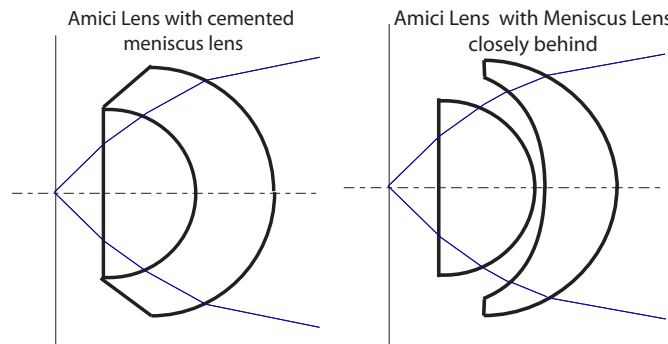
The **Bertrand lens** is a focusable eyepiece telescope that can be easily placed in the light path of the microscope. This lens is used to view the back aperture of the objective, which simplifies microscope alignment, specifically when setting up Köhler illumination.

To construct a high-numerical-aperture microscope objective with good correction, numerous optical designs implement the **Amici lens** as a first component of the objective. It is a thick lens placed in close proximity to the sample. An Amici lens usually has a plane (or nearly plane) first surface and a large-curvature spherical second surface. To ensure good chromatic aberration correction, an achromatic lens is located closely behind the Amici lens. In such configurations, microscope objectives usually reach an NA of 0.5–0.7.

To further increase the NA, an Amici lens is improved by either cementing a high-refractive-index meniscus lens to it or placing a meniscus lens



closely behind the Amici lens. This makes it possible to construct well-corrected high magnification ($100\times$) and high numerical aperture ($NA > 1.0$) oil-immersion objective lenses.

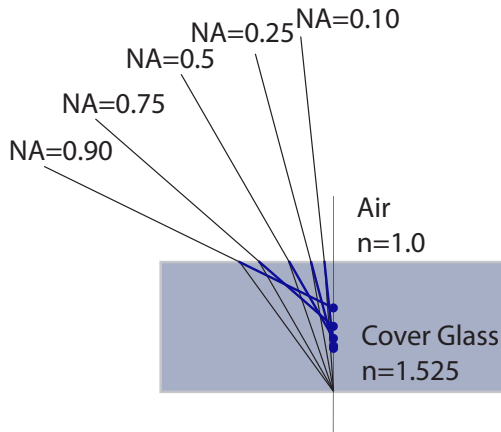


Cover Glass and Immersion

The **cover slip** is located between the object and the microscope objective. It protects the imaged sample and is an important element in the optical path of the microscope. Cover glass can reduce imaging performance and cause spherical aberration, while different imaging angles experience movement of the object point along the optical axis toward the microscope objective. The object point moves closer to the objective with an increase in angle.

The importance of the cover glass increases in proportion to the objective's NA, especially in high-NA dry lenses. For lenses with an NA smaller than 0.5, the type of cover glass may not be a critical parameter, but should always be properly used to optimize imaging quality. Cover glasses are likely to be encountered when imaging biological samples. Note that the presence of a standard-thickness cover glass is accounted for in the design of high-NA objectives. The important parameters that define a cover glass are its thickness, index of refraction, and Abbe number. The ISO standards for refractive index and Abbe number are $n = 1.5255 \pm 0.0015$ and $V = 56 \pm 2$, respectively.

Microscope objectives are available that can accommodate a range of cover-slip thicknesses. An adjustable collar allows the user to adjust for cover slip thickness in the range from 100 microns to over 200 microns.



Cover Glass Grade Number	Thickness (in microns)
0	83–130
1	130–160
1.5	160–190
2	190–250

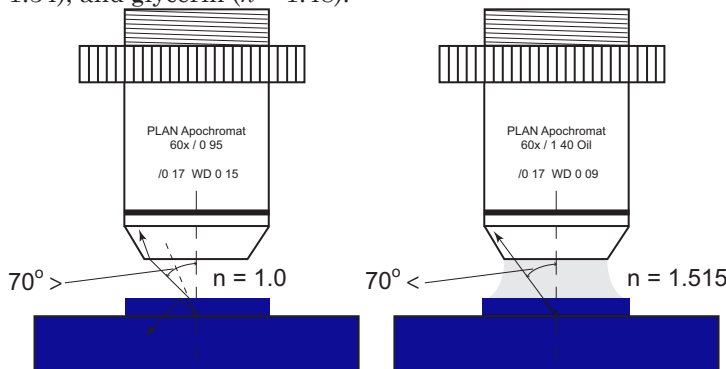
Cover Glass and Immersion (cont.)

The table below presents a summary of acceptable cover glass thickness deviations from 0.17 mm and the allowed thicknesses for Zeiss air objectives with different NAs.

NA of the Objective	Allowed Thickness Deviations (from 0.17 mm)	Allowed Thickness Range
<0.3	—	0.000–0.300
0.30–0.45	0.07	0.100–0.240
0.45–0.55	0.05	0.120–0.220
0.55–0.65	0.03	0.140–0.200
0.65–0.75	0.02	0.150–0.190
0.75–0.85	0.01	0.160–0.180
0.85–0.95	0.005	0.165–0.175

(Adapted from Pluta, 1988)

To increase both the microscope's resolution and system throughput, immersion liquids are used between the coverslip glass and the microscope objective, or directly between the sample and objective. An **immersion liquid** effectively increases the NA and decreases the angle of refraction at the interface between the medium and the microscope objective. Common immersion liquids include oil ($n = 1.515$), water ($n = 1.34$), and glycerin ($n = 1.48$).



Water, which is more common, or glycerin immersion objectives are mainly used for biological samples, such as living cells or a tissue culture. They provide a slightly lower NA than oil objectives but are free of the toxicity associated with immersion oils. Water immersion is usually applied without a cover slip. For fluorescent applications it is also critical to use non-fluorescent oil.

Common Light Sources for Microscopy

Common light sources for microscopy include **incandescent lamps**, such as tungsten-argon and tungsten (e.g., quartz halogen) lamps. A **tungsten-argon lamp** is primarily used for bright-field, phase-contrast, and some polarization imaging. **Halogen lamps** are inexpensive and a convenient choice for a variety of applications that require a continuous and bright spectrum.

Arc lamps are usually brighter than incandescent lamps. The most common examples include xenon (XBO) and mercury (HBO) arc lamps. Arc lamps provide high-quality monochromatic illumination if combined with the appropriate filter. Arc lamps are more difficult to align, are more expensive, and have a shorter lifetime. Their spectral range starts in the UV range and continuously extends through visible to the infrared. About 20% of the output is in the visible spectrum, while the majority is in the UV and IR. The usual lifetime is 100–200 hours.

Common Mercury Lines	
Wavelength [nm]	Color
254	Far UV
366	Near UV
405	Violet
435	Deep Blue
546	Yellow-green
578	Yellow doublet

Another light source is the **gas-arc discharge lamp**, which includes mercury, xenon, and halide lamps. The **mercury lamp** has several strong lines, which might be 100 times brighter than the average output. About 50% is located in the UV range, and should be used with protective glasses. For imaging biological samples, the proper selection of filters is necessary to protect living cell samples and micro-organisms (e.g., UV-blocking filters/cold mirrors). The xenon arc lamp has a uniform spectrum, can provide an output power greater than 100 W, and is often used for fluorescence imaging. However, over 50% of its power falls into the IR; therefore, IR-blocking filters (hot mirrors) are necessary to prevent the overheating of samples.

Metal halide lamps were recently introduced as high-power sources (over 150 W) with lifetimes several times longer than arc lamps. While in general the metal-halide lamp has a spectral output similar to that of a mercury arc lamp, it extends further into longer wavelengths.

LED Light Sources

Light-emitting diodes (LEDs) are a new, alternative light source for microscopy applications. The LED is a semiconductor diode that emits photons when in forward-biased mode. Electrons pass through the depletion region of a p-n junction and lose an amount of energy equivalent to the bandgap of the semiconductor. The characteristic features of LEDs include a long lifetime, a compact design, and high efficiency. They also emit narrowband light with relatively high energy.

Wavelengths [nm] of High-power LEDs Commonly Used in Microscopy		Total Beam Power [mW] (approximate)
455	Royal Blue	225–450
470	Blue	200–400
505	Cyan	150–250
530	Green	100–175
590	Amber	15–25
633	Red	25–50
435–675	White Light	200–300

An important feature of LEDs is the ability to combine them into arrays and custom geometries. Also, LEDs operate at lower temperatures than arc lamps, and due to their compact design they can be cooled easily with simple heat sinks and fans.

The radiance of currently available LEDs is still significantly lower than that possible with arc lamps; however, LEDs can produce an acceptable fluorescent signal in bright microscopy applications. Also, the pulsed mode can be used to increase the radiance by 20 times or more.

LED Spectral Range [nm]	Semiconductor
350–400	GaN
400–550	In _{1-x} Ga _x N
550–650	Al _{1-x} In _y Ga _x P
650–750	Al _{1-x} Ga _x As
750–1000	GaAs _{1-x} P _x

Filters

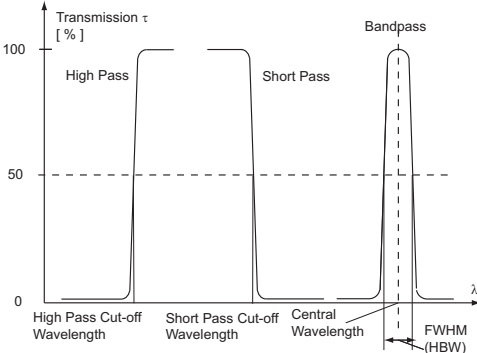
Neutral density (ND) filters are neutral (wavelength wise) gray filters scaled in units of **optical density** (OD):

$$OD = \log_{10} \left(\frac{1}{\tau} \right),$$

where τ is the transmittance.

ND filters can be combined to provide OD as a sum of the ODs of the individual filters. ND filters are used to change light intensity without tuning the light

source, which can result in a spectral shift.



Color **absorption filters** and **interference filters** (also see *Multiple Wave Interference* on page 16) isolate the desired range of wavelengths: e.g. bandpass and edge filters.

Edge filters include short-pass and long-pass filters. Short-pass filters allow short wavelengths to pass and stop long wavelengths, and long-pass filters allow long wavelengths to pass while stopping short wavelengths. Edge filters are defined for wavelengths with a 50% drop in transmission.

Bandpass filters allow only a selected spectral bandwidth to pass and are characterized with a central wavelength and full-width-half-maximum (FWHM) defining the spectral range for transmission of at least 50%.

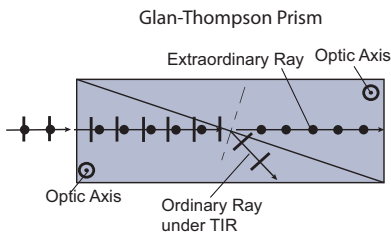
Color absorption glass filters usually serve as broad bandpass filters. They are less costly and less susceptible to damage than interference filters.

Interference filters are based on multiple beam interference in thin films. They combine between three to over 20 dielectric layers of $\lambda/2$ and $\lambda/4$, separated by metallic coatings. They can provide a sharp bandpass transmission down to the sub-nm range and full-width-half-maximum of 10–20 nm.

Polarizers and Polarization Prisms

Polarizers are built with birefringent crystals using polarization at multiple reflections, selective absorption (dichroism), form birefringance, or scattering.

For example, polarizers built with birefringent crystals (Glan-Thompson prisms) use the principle of total internal reflection to eliminate ordinary or extraordinary components (for positive or negative crystals).



Birefringent prisms are crucial components for numerous microscopy techniques, e.g., differential interference contrast. The most common birefringent prism is a **Wollaston prism**. It splits light into two beams with orthogonal polarization and propagates under different angles.

The angle between propagating beams is

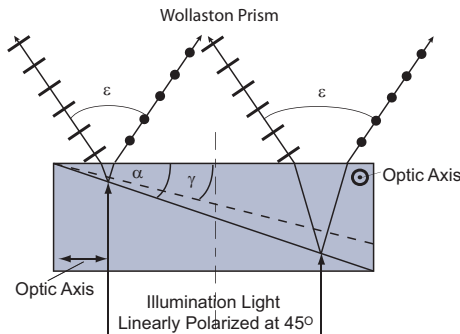
$$\varepsilon = 2|n_e - n_o|\tan\alpha .$$

Both beams produce interference with fringe period b :

$$b = \frac{\lambda}{\varepsilon} = \frac{\lambda}{2|n_e - n_o|\tan\alpha} .$$

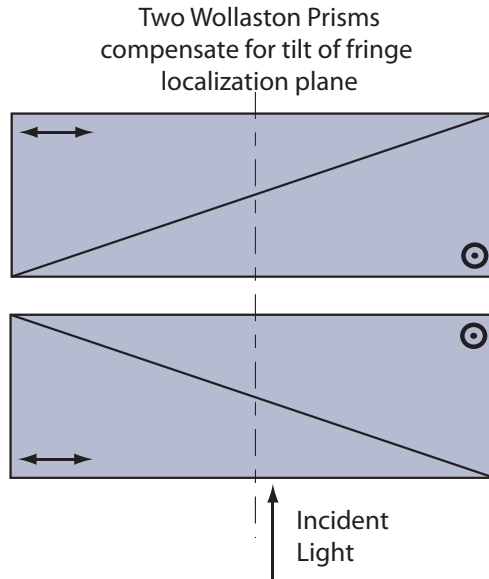
The localization plane of fringes is

$$\gamma = \frac{1}{2} \left(\frac{1}{n_e} + \frac{1}{n_o} \right) \alpha .$$

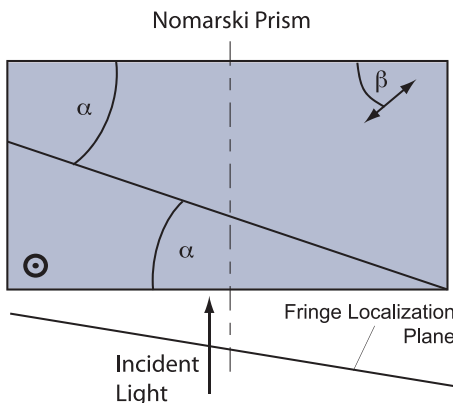


Polarizers and Polarization Prisms (cont.)

The fringe localization plane tilt can be compensated by using two symmetrical Wollaston prisms.



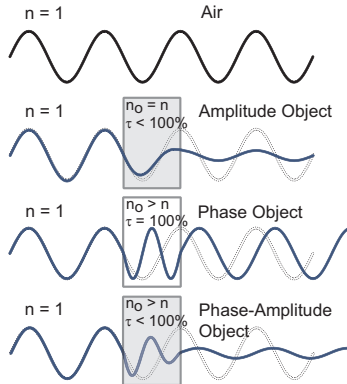
Wollaston prisms have a fringe localization plane inside the prism. One example of a modified Wollaston prism is the **Nomarski prism**, which simplifies the DIC microscope setup by shifting the plane outside the prism, i.e., the prism does not need to be physically located at the condenser front focal plane or the objective's back focal plane.



Amplitude and Phase Objects

The major object types encountered on the microscope are **amplitude** and **phase** objects. The type of object often determines the microscopy technique selected for imaging.

The amplitude object is defined as one that changes the amplitude and therefore the intensity of transmitted or reflected light. Such objects are usually imaged with bright-field microscopes. A stained tissue slice is a common amplitude object.



Phase objects do not affect the optical intensity; instead, they generate a phase shift in the transmitted or reflected light. This phase shift usually arises from an inhomogeneous refractive index distribution throughout the sample, causing differences in optical path length (OPL). Mixed amplitude-phase objects are also possible (e.g., biological media), which affect the amplitude and phase of illumination in different proportions.

Classifying objects as **self-luminous** and **non-self-luminous** is another way to categorize samples. Self-luminous objects generally do not directly relate their amplitude and phase to the illuminating light. This means that while the observed intensity may be proportional to the illumination intensity, its amplitude and phase are described by a statistical distribution (e.g., fluorescent samples). In such cases, one can treat discrete object points as secondary light sources, each with their own amplitude, phase, coherence, and wavelength properties.

Non-self-luminous objects are those that affect the illuminated beam in such a manner that discrete object points cannot be considered as entirely independent. In such cases, the wavelength and temporal coherence of the illuminating source needs to be considered in imaging. A diffusive or absorptive sample is an example of such an object.

The Selection of a Microscopy Technique

Microscopy provides several imaging principles. Below is a list of the most common techniques and object types:

Technique	Type of sample
Bright-field	Amplitude specimens, reflecting specimens, diffuse objects
Dark-field	Light-scattering objects
Phase contrast	Phase objects, light-scattering objects, light-refracting objects, reflective specimens
Differential interference contrast (DIC)	Phase objects, light-scattering objects, light-refracting objects, reflective specimens
Polarization microscopy	Birefringent specimens
Fluorescence microscopy	Fluorescent specimens
Laser scanning, Confocal microscopy, and Multi-photon microscopy	3D samples requiring optical sectioning, fluorescent and scattering samples
Super-resolution microscopy (RESOLFT, 4Pi, F_M, SI, STORM, PALM , and others)	Imaging at the molecular level; imaging primarily focuses on fluorescent samples where the sample is a part of an imaging system
Raman microscopy, CARS	Contrast-free chemical imaging
Array microscopy	Imaging of large FOVs
SPIM	Imaging of large 3D samples
Interference Microscopy	Topography, refractive index measurements, 3D coherence imaging

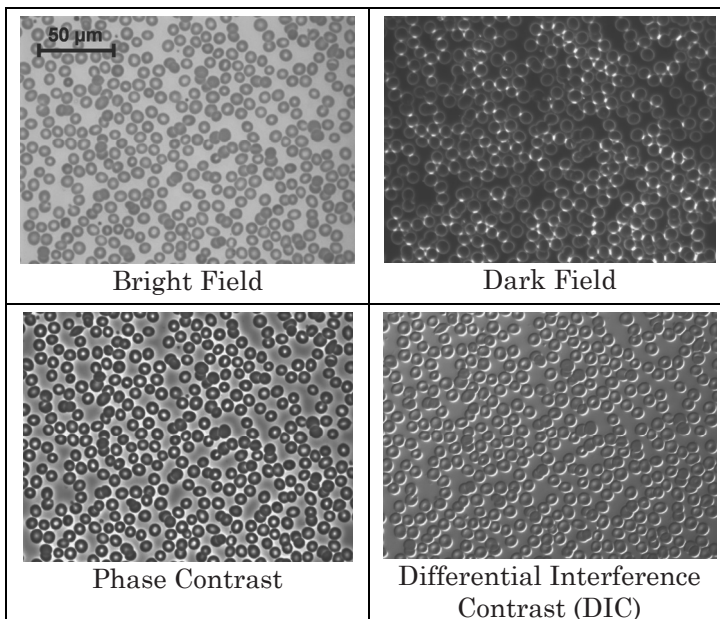
All of these techniques can be considered for transmitted or reflected light. Below are examples of different sample types:

Sample type	Sample Example
Amplitude specimens	Naturally colored specimens, stained tissue
Specular specimens	Mirrors, thin films, metallurgical samples, integrated circuits
Diffuse objects	Diatoms, fibers, hairs, micro-organisms, minerals, insects
Phase objects	Bacteria, cells, fibers, mites, protozoa
Light-refracting samples	Colloidal suspensions, minerals, powders
Birefringent specimens	Mineral sections, crystallized chemicals, liquid crystals, fibers, single crystals
Fluorescent specimens	Cells in tissue culture, fluorochrome-stained sections, smears and spreads

(Adapted from www.microscopyu.com)

Image Comparison

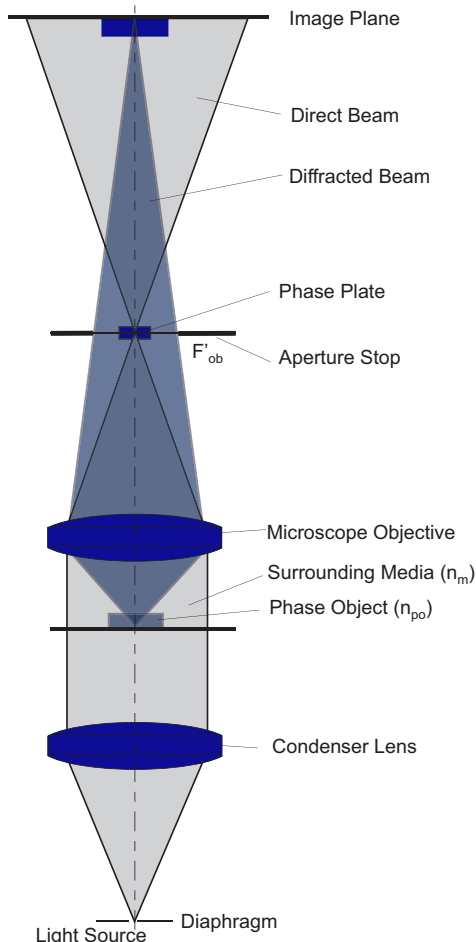
The images below display four important microscope modalities: **bright field**, **dark field**, **phase contrast**, and **differential interference contrast**. They also demonstrate the characteristic features of these methods. The images are of a blood specimen viewed with the Zeiss upright Axiovert Observer Z1 microscope. The microscope was set with an objective at $40\times$, NA = 0.6, Ph2, LD Plan Neofluor, and a cover slip glass of 0.17 mm. The pictures were taken with a monochromatic CCD camera.



The bright-field image relies on absorption and shows the sample features with decreasing amounts of passing light. The dark-field image only shows the scattering sample components. Both the phase contrast and the differential interference contrast demonstrate the optical thickness of the sample. The characteristic halo effect is visible in the phase-contrast image. The 3D effect of the DIC image arises from the differential character of images; they are formed as a derivative of the phase changes in the beam as it passes through the sample.

Phase Contrast

Phase contrast is a technique used to visualize phase objects by phase and amplitude modifications between the direct beam propagating through the microscope and the beam diffracted at the phase object. An object is illuminated with monochromatic light, and a phase-delaying (or advancing) element in the aperture stop of the objective introduces a phase shift, which provides interference contrast. Changing the amplitude ratio of the diffracted and non-diffracted light can also increase the contrast of the object features.



Phase Contrast (cont.)

Phase contrast is primarily used for imaging living biological samples (immersed in a solution), unstained samples (e.g., cells), thin film samples, and mild phase changes from mineral objects. In that regard, it provides qualitative information about the optical thickness of the sample. Phase contrast can also be used for some quantitative measurements, like an estimation of the refractive index or the thickness of thin layers. Its phase detection limit is similar to the **differential interference contrast** and is approximately $\lambda/100$. On the other hand, phase contrast (contrary to DIC) is limited to thin specimens, and phase delay should not exceed the depth of field of an objective. Other drawbacks compared to DIC involve its limited optical sectioning ability and undesired effects like halos or shading-off. (See also *Characteristic Features of Phase Contrast Microscopy* on page 71).

The most important advantages of phase contrast (over DIC) include its ability to image birefringent samples and its simple and inexpensive implementation into standard microscopy systems.

Presented below is a mathematical description of the phase contrast technique based on a vector approach. The phase shift in the figure (See page 68) is represented by the orientation of the vector. The length of the vector is proportional to amplitude of the beam. When using standard imaging on a transparent sample, the length of the light vectors passing through sample PO and surrounding media SM is the same, which makes the sample invisible. Additionally, vector PO can be considered as a sum of the vectors passing through surrounding media SM and diffracted at the object DP .

$$PO = SM + DP$$

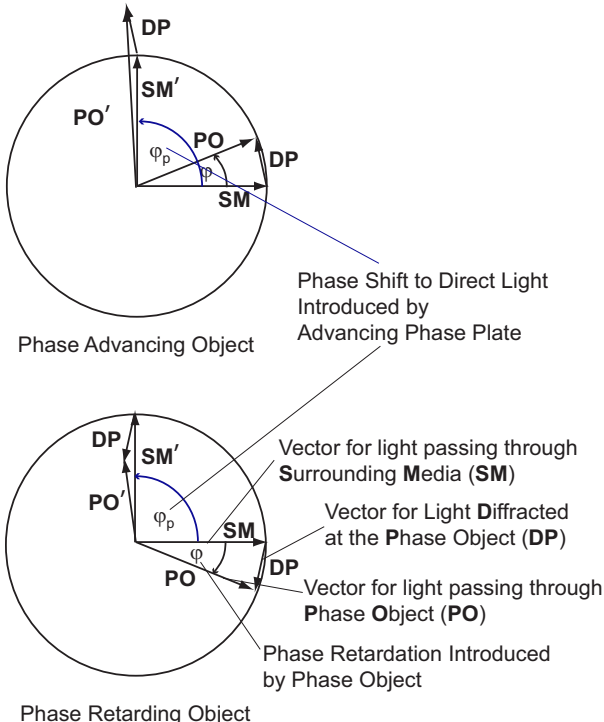
If the wavefront propagating through the surrounding media can be the subject of an exclusive phase change (diffracted light DP is not affected), the vector SM is rotated by an angle corresponding to the phase change. This exclusive phase shift is obtained with a small circular or ring phase plate located in the plane of the aperture stop of a microscope.

Phase Contrast (cont.)

Consequently, vector PO , which represents light passing through a phase sample, will change its value to PO' and provide contrast in the image:

$$PO' = SM' + DP,$$

where SM' represents the rotated vector SM .



Phase samples are considered to be **phase retarding objects** or **phase advancing objects** when their refractive index is greater or less than the refractive index of the surrounding media, respectively.

Phase plate	Object Type	Object Appearance
$\varphi_p = +\pi/2 (+90^\circ)$	phase-retarding	brighter
$\varphi_p = +\pi/2 (+90^\circ)$	phase-advancing	darker
$\varphi_p = -\pi/2 (-90^\circ)$	phase-retarding	darker
$\varphi_p = -\pi/2 (-90^\circ)$	phase-advancing	brighter

Visibility in Phase Contrast

Visibility of features in **phase contrast** can be expressed as

$$C_{\text{ph}} = \frac{I_{\text{media}} - I_{\text{object}}}{I_{\text{media}}} = \frac{|SM'|^2 - |PO'|^2}{|SM'|^2}.$$

This equation defines the phase object's visibility as a ratio between the intensity change due to phase features and the intensity of surrounding media $|SM'|^2$. It defines the negative and positive contrast for an object appearing brighter or darker than the media, respectively. Depending on the introduced phase shift (positive or negative), the same object feature may appear with a **negative** or **positive contrast**. Note that C_{ph} relates to classical contrast C as

$$C = \frac{I_{\max} - I_{\min}}{I_{\max} + I_{\min}} = \left| C_{\text{ph}} \right| \frac{|SM'|^2}{|SM'|^2 + |PO'|^2}.$$

Contrast	Phase Plate
-2ϕ	$\phi_p = +\pi/2 (+90^\circ)$
$+2\phi$	$\phi_p = -\pi/2 (-90^\circ)$

For phase changes in the $0-2\pi$ range, intensity in the image can be found using vector relations; small phase changes in the object $\phi \ll 90$ deg can be approximated as $\pm 2\phi$.

To increase the contrast of images, the intensity in the direct beam is additionally changed with beam attenuation τ in the phase ring. τ is defined as a transmittance, $\tau = 1/N$, where N is a dividing coefficient of intensity in a direct beam (intensity is decreased N times). The contrast in this case is

$$C_{\text{ph}} = -2\phi / \sqrt{\tau} = -2\phi\sqrt{N}$$

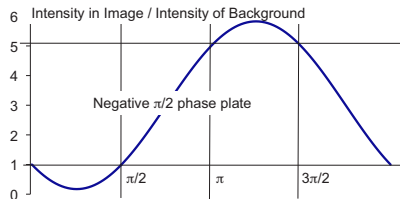
for a $+\pi/2$ phase plate, and

$$C_{\text{ph}} = +2\phi / \sqrt{\tau} = +2\phi\sqrt{N}$$

for $-\pi/2$ phase plate. The minimum perceived phase difference with phase contrast is

$$\Delta\phi_{\min} = \frac{C_{\text{ph-min}}\lambda}{4\pi\sqrt{N}}.$$

$C_{\text{ph-min}}$ is usually accepted at the contrast value of 0.02.



The Phase Contrast Microscope

The common phase-contrast system is similar to the bright-field microscope but with two modifications:

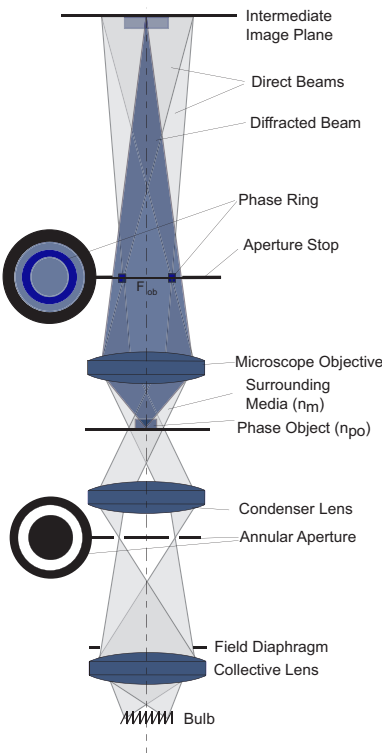
1. The condenser diaphragm is replaced with an annular aperture diaphragm.
2. A ring-shaped phase plate is introduced at the back focal plane of the microscope objective. The ring may include metallic coatings, typically providing 75% to 90% attenuation of the direct beam.

Both components are in conjugate planes and are aligned such that the image of the annular condenser diaphragm overlaps with the objective phase ring. While there is no direct access to the objective phase ring, the annular aperture in front of the condenser is easily accessible.

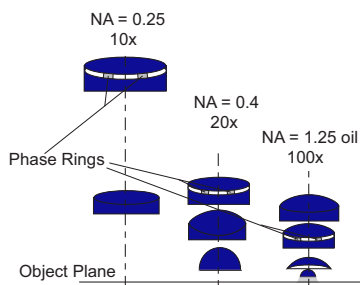
The phase shift introduced by the ring is given by

$$\phi_p = 2\pi \frac{OPD}{\lambda} = \frac{2\pi}{\lambda} (n_m - n_r) t,$$

where n_m and n_r are refractive indices of the media surrounding the phase ring and the ring itself, respectively. t is the physical thickness of the phase ring.

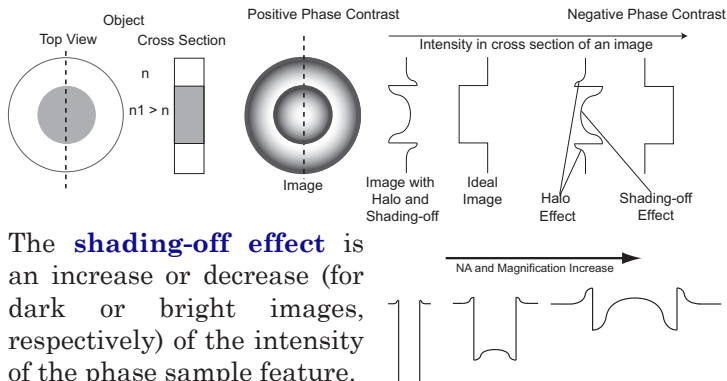
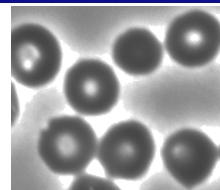


Phase Contrast Objectives



Characteristic Features of Phase Contrast

Images in phase contrast are dark or bright features on a background (positive and negative contrast, respectively). They contain undesired image effects called halo and shading-off, which are a result of the incomplete separation of direct and diffracted light. The **halo effect** is a phase contrast feature that increases light intensity around sharp changes in the phase gradient.



The **shading-off effect** is an increase or decrease (for dark or bright images, respectively) of the intensity of the phase sample feature.

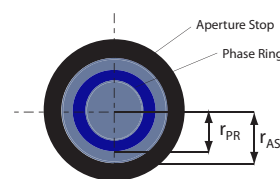
Both effects strongly increase with an increase in numerical aperture and magnification. They can be reduced by surrounding the sides of a phase ring with ND filters.

Lateral resolution of the phase contrast technique is affected by the annular aperture (the radius of phase ring r_{PR}) and the aperture stop of the objective (the radius of aperture stop is r_{AS}). It is

$$d = f'_{\text{objective}} \frac{\lambda}{(r_{AS} + r_{PR})},$$

compared to the resolution limit for a standard microscope:

$$d = f'_{\text{objective}} \frac{\lambda}{r_{AS}}.$$

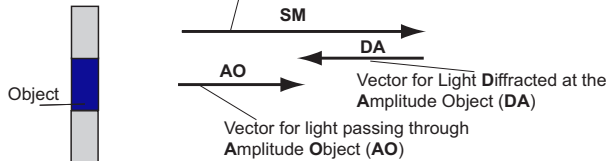
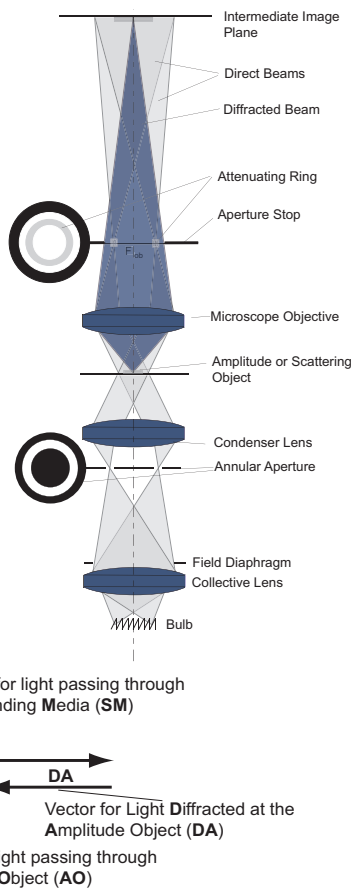


Amplitude Contrast

Amplitude contrast

changes the contrast in the images of absorbing samples. It has a layout similar to phase contrast; however, there is no phase change introduced by the object. In fact, in many cases a phase-contrast microscope can increase contrast based on the principle of amplitude contrast. The visibility of images is modified by changing the intensity ratio between the direct and diffracted beams.

A vector schematic of the technique is as follows:



Similar to visibility in phase contrast, image contrast can be described as a ratio of the intensity change due to amplitude features surrounding the media's intensity:

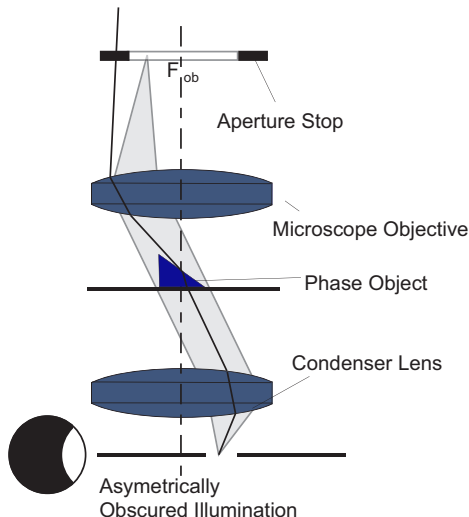
$$C_{ac} = \frac{I_{\text{media}} - I_{\text{object}}}{I_{\text{media}}} = \frac{2|SM||DA| - |DA|^2}{|SM|^2}.$$

Since the intensity of diffraction for amplitude objects is usually small, the contrast equation can be approximated with $C_{ac} = 2|DA|/|SM|$. If a direct beam is further attenuated, contrast C_{ac} will increase by factor of $N^{-1} = 1/\tau^{-1}$.

Oblique Illumination

Oblique illumination (also called **anaxial illumination**) is used to visualize phase objects. It creates pseudo-profile images of transparent samples. These reliefs, however, do not directly correspond to the actual surface profile.

The principle of oblique illumination can be explained by using either refraction or diffraction and is based on the fact that sample features of various spatial frequencies will have different intensities in the image due to a nonsymmetrical system layout and the filtration of spatial frequencies.



In practice, oblique illumination can be achieved by obscuring light exiting a condenser; translating the sub-stage diaphragm of the condenser lens does this easily.

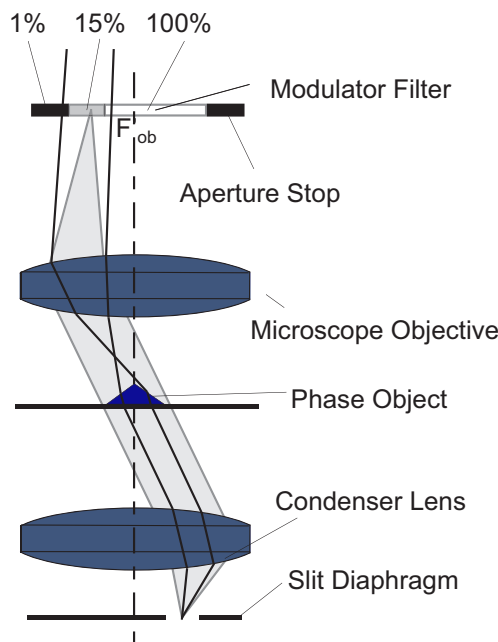
The advantage of oblique illumination is that it improves spatial resolution over Köhler illumination (up to two times). This is based on the fact that there is a larger angle possible between the 0th and 1st orders diffracted at the sample for oblique illumination. In Köhler illumination, due to symmetry, the 0th and -1st orders at one edge of the stop will overlap with the 0th and +1st order on the other side. However, the gain in resolution is only for one sample direction; to examine the object features in two directions, a sample stage should be rotated.

Modulation Contrast

Modulation contrast microscopy (MCM) is based on the fact that phase changes in the object can be visualized with the application of multilevel gray filters.

The intensities of light refracted at the object are displayed with different values since they pass through different zones of the filter located in the stop of the microscope. MCM is often configured for oblique illumination since it already provides some intensity variations for phase objects. Therefore, the resolution of the MCM changes between normal and oblique illumination.

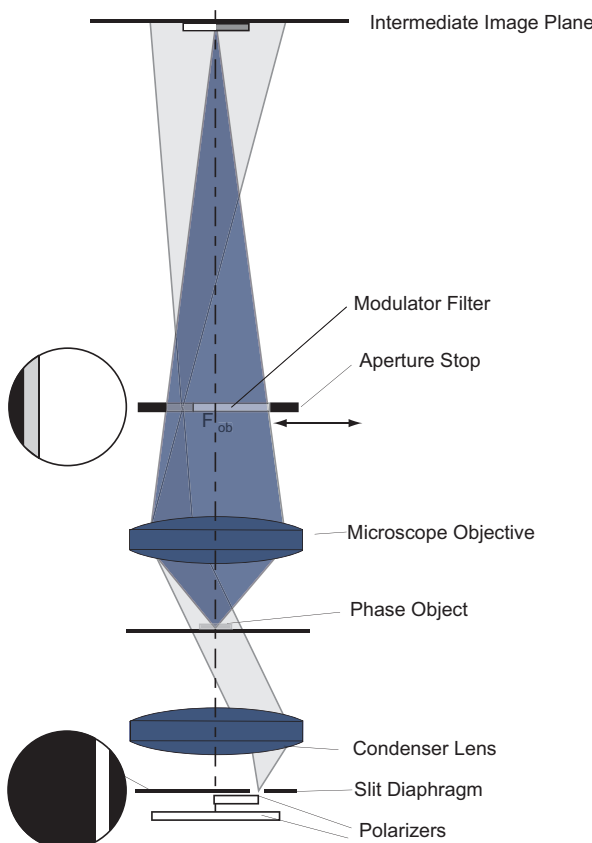
MCM can be obtained through a simple modification of a bright-field microscope by adding a slit diaphragm in front of the condenser and amplitude filter (also called the modulator) in the aperture stop of the microscope objective. The modulator filter consists of three areas: 100% (bright), 15% (gray), and 1% (dark). This filter acts in a similar way to the knife-edge in the Schlieren imaging techniques.



Hoffman Contrast

A specific implementation of MCM is **Hoffman modulation contrast**, which uses two additional polarizers located in front of the slit aperture. One polarizer is attached to the slit and obscures 50% of its width. A second can be rotated, which provides two intensity zones in the slit (for crossed polarizers, half of the slit is dark and half is bright; the entire slit is bright for the parallel position).

The major advantages of this technique include imaging at a full spatial resolution and a minimum depth of field, which allows optical sectioning. The method is inexpensive and easy to implement. The main drawback is that the images deliver a pseudo-relief image, which cannot be directly correlated with the object's form.

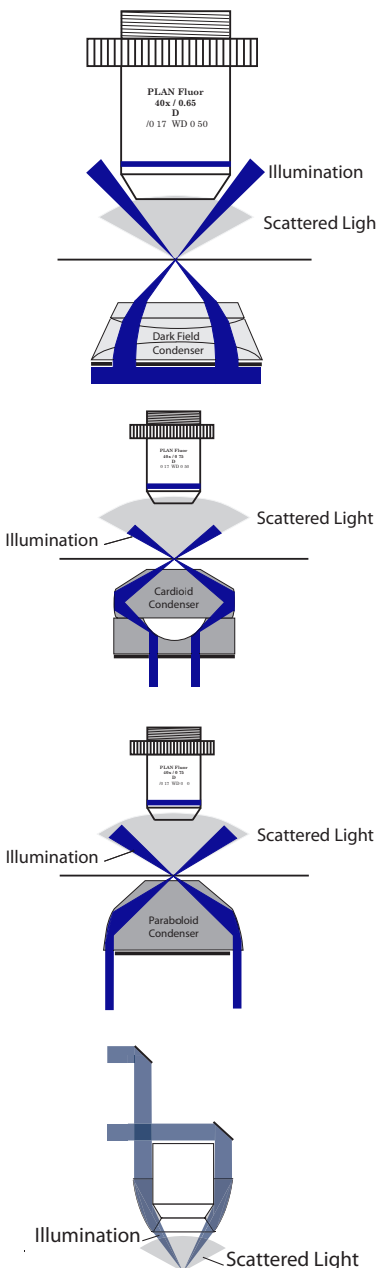


Dark Field Microscopy

In **dark-field microscopy**, the specimen is illuminated at such angles that direct light is not collected by the microscope objective. Only diffracted and scattered light are used to form the image.

The key component of the dark-field system is the condenser. The simplest approach uses an annular condenser stop and a microscope objective with an NA below that of the illumination cone. This approach can be used for objectives with $\text{NA} < 0.65$. Higher-NA objectives may incorporate an adjustable iris to reduce their NA below 0.65 for dark-field imaging. To image at a higher NA, specialized reflective dark-field condensers are necessary. Examples of such condensers include the **cardioid** and **paraboloid** designs, which enable dark-field imaging at an NA up to 0.9–1.0 (with oil immersion).

For dark-field imaging in epi-illumination, objective designs consist of external illumination, and internal imaging paths are used.



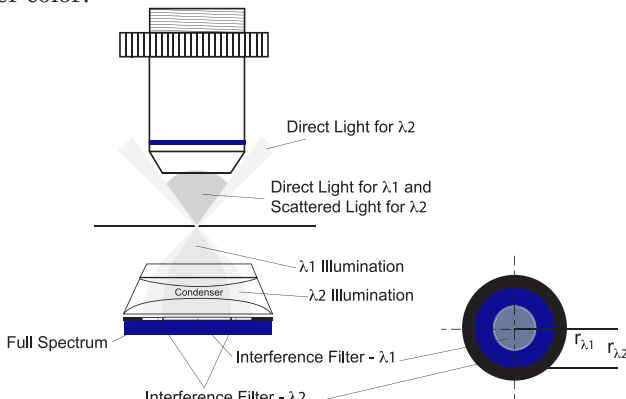
Optical Staining: Rheinberg Illumination

Optical staining is a class of techniques that uses optical methods to provide color differentiation between different areas of a sample.

Rheinberg illumination is a modification of dark-field illumination. Instead of an annular aperture, it uses two-zone color filters located in the front focal plane of the condenser. The overall diameter of the outer annular color filter is slightly greater than that corresponding to the NA of the system:

$$2r_{\lambda,2} > 2NAf'_{\text{condenser}}$$

To provide good contrast between scattered and direct light, the inner filter is darker. Rheinberg illumination provides images that are a combination of two colors. Scattering features in one color are visible on the background of the other color.



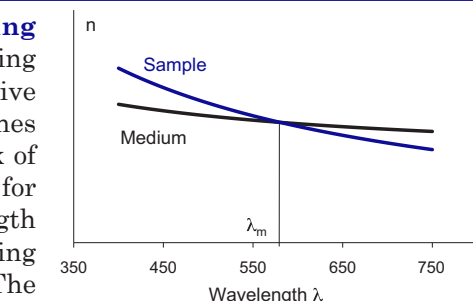
Color-stained images can also be obtained in a simplified setup where only one (inner) filter is used. For such an arrangement, images will present white-light scattering features on the colored background. Other deviations from the above technique include double illumination where transmittance and reflectance are separated into two different colors.

Optical Staining: Dispersion Staining

Dispersion staining is based on using highly dispersive media that matches the refractive index of the phase sample for a single wavelength λ_m (the matching wavelength). The system is configured

in a setup similar to dark-field or oblique illumination. Wavelengths close to the matching wavelength will miss the microscope objective, while the other will refract at the object and create a colored dark-field image. Various configurations include illumination with a dark-field condenser and an annular aperture or central stop at the back focal plane of the microscope objective.

The annular-stop technique uses low-magnification (10 \times) objectives with a stop built

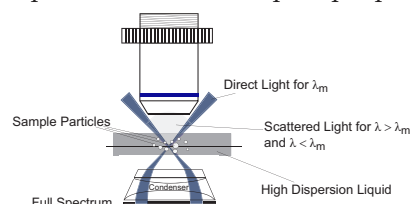


Color	λ Range [nm]	λ Mean [nm]
Violet	400–450	440
Blue	450–480	470
Blue-Green	480–510	495
Green	510–550	530
Green-Yellow	550–570	560
Yellow	570–590	580
Orange	590–630	605
Red	630–700	650

(Adapted from Pluta, 1989)

as an opaque screen with a central opening, and is used for bright-field dispersion staining. The annular stop absorbs red and blue wavelengths and allows yellow through the system. A sample appears as white with yellow borders. The image background is also white.

The central-stop system absorbs unrefracted yellow light and direct white light. Sample features show up as purple (a mixture of red and blue) borders on a dark background. Different media and sample types will modify the color's appearance.



Shearing Interferometry: The Basis for DIC

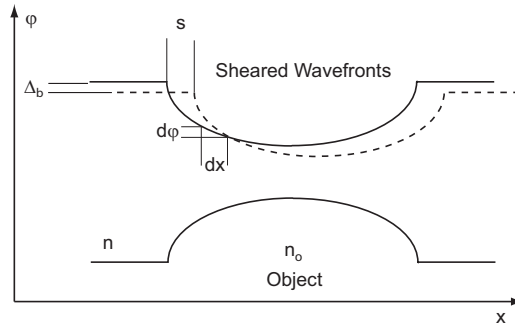
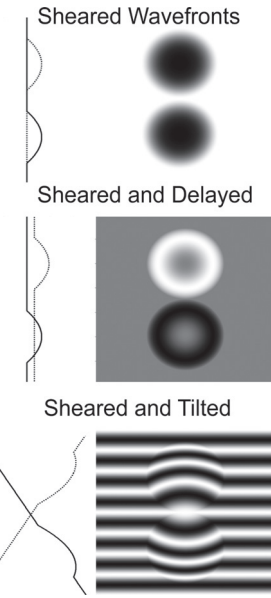
Differential interference contrast (DIC) microscopy is based on the principles of shearing interferometry. Two wavefronts propagating through an optical system containing identical phase distributions (introduced by the sample) are slightly shifted to create an interference pattern. The phase of the resulting fringes is directly proportional to the derivative of the phase distribution in the object, hence the name “differential.” Specifically, the intensity of the fringes relates to the derivative of the phase delay through the object ($\Delta\phi_o$) and the local delay between wavefronts (Δ_b):

$$I \propto I_{\max} \cos^2(\Delta_b \pm \Delta\phi_o)$$

or

$$I \propto I_{\max} \cos^2\left(\Delta_b \pm s \frac{d\phi_o}{dx}\right),$$

where s denotes the shear between wavefronts, and Δ_b is the axial delay.



Wavefront shear is commonly introduced in DIC microscopy by incorporating a Mach-Zehnder interferometer into the system (e.g., Zeiss) or by the use of birefringent prisms. The appearance of DIC images depends on the sample orientation with respect to the shear direction.

DIC Microscope Design

The most common **differential interference contrast (Nomarski DIC)** design uses two **Wollaston** or **Nomarski birefringent prisms**. The first prism splits the wavefront into ordinary and extraordinary components to produce interference between these beams. Fringe localization planes for both prisms are in conjugate planes. Additionally, the system uses a crossed polarizer and analyzer. The polarizer is located in front of prism I, and the analyzer is behind prism II. The polarizer is rotated by 45 deg with regard to the shear axes of the prisms.

If prism II is centrally located, the intensity in the image is

$$I \propto \sin^2 \left(\frac{\pi s \frac{d\phi_o}{dx}}{\lambda} \right).$$

For a translated prism, phase **bias** Δ_b is introduced, and the intensity is proportional to

$$I \propto \sin^2 \left(\Delta_b \pm s \frac{d\phi_o}{dx} \right).$$

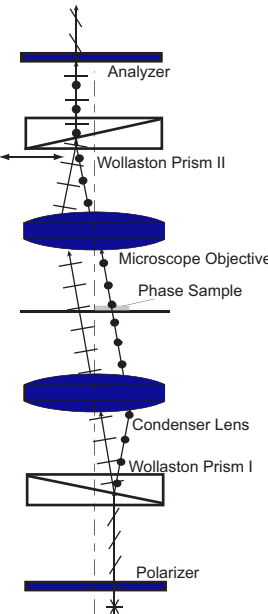
The sign in the equation depends on the direction of the shift. Shear s is

$$s = \frac{s'}{M_{\text{objective}}} = \varepsilon \frac{OTL}{M_{\text{objective}}},$$

where ε is the angular shear provided by the birefringent prisms, s' is the shear in the image space, and OTL is the optical tube length. The high spatial coherence of the source is obtained by the slit located in front of the condenser and oriented perpendicularly to the shear direction. To assure good interference contrast, the width of the slit w should be

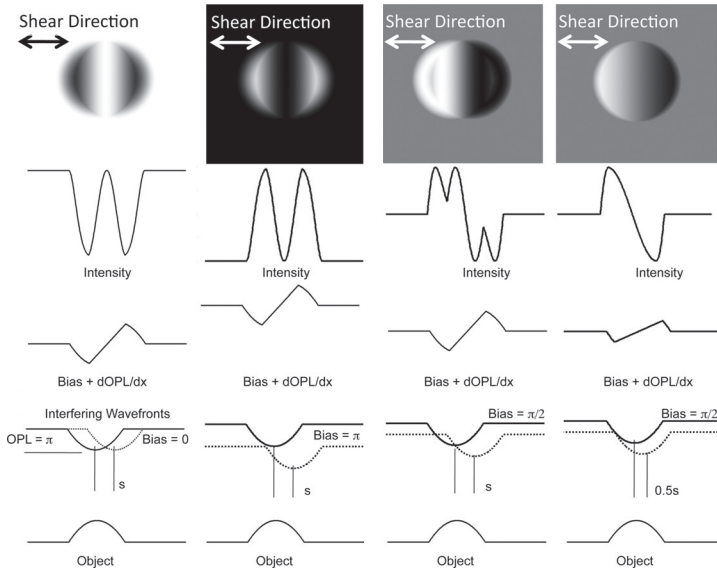
$$w = \frac{\lambda f'_{\text{condenser}}}{4s}.$$

Low-strain (low-birefringence) objectives are crucial for high-quality DIC.

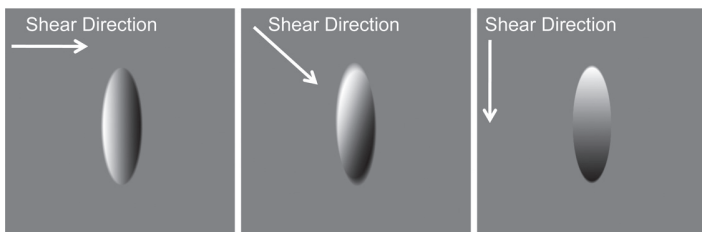


Appearance of DIC Images

In practice, shear between wavefronts in **differential interference contrast** is small and accounts for a fraction of a fringe period. This provides the differential character of the phase difference between interfering beams introduced to the interference equation.



Increased shear makes the edges of the object less sharp, while increased bias introduces some background intensity. Shear direction determines the appearance of the object.



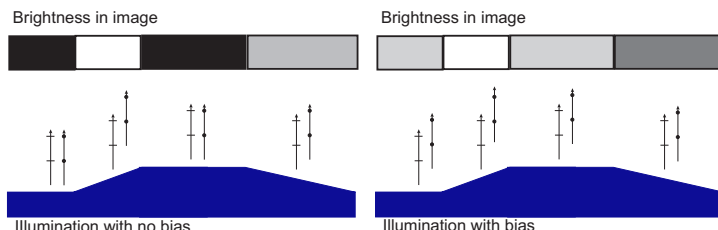
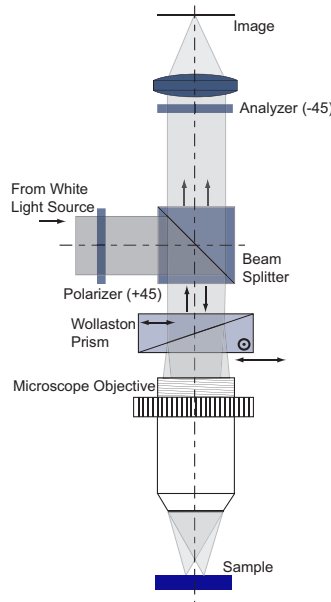
Compared to phase contrast, DIC allows for larger phase differences throughout the object and operates in full resolution of the microscope (i.e., it uses the entire aperture). The depth of field is minimized, so DIC allows optical sectioning.

Reflectance DIC

A **Nomarski interference microscope** (also called a polarization interference contrast microscope) is a reflectance DIC system developed to evaluate roughness and the surface profile of specular samples. Its applications include metallography, microelectronics, biology, and medical imaging. It uses one Wollaston or Nomarski prism, a polarizer, and an analyzer. The information about the sample is obtained for one direction parallel to the gradient in the object. To acquire information for all directions, the sample should be rotated.

If white light is used, different colors in the image correspond to different sample slopes. It is possible to adjust the color by rotating the polarizer.

Phase delay (**bias**) can be introduced by translating the birefringent prism. For imaging under monochromatic illumination, the brightness in the image corresponds to the slope in the sample. Images with no bias will appear as bright features on a dark background; with bias they will have an average background level, and slopes will vary between dark and bright. This way, it is possible to interpret the direction of the slope. Similar analysis can be performed for the colors from white-light illumination.



Polarization Microscopy

Polarization microscopy provides images containing information about the properties of anisotropic samples. A polarization microscope is a modified compound microscope with three unique components: the **polarizer**, **analyzer**, and **compensator**. A linear polarizer is located between the light source and the specimen, close to the condenser's diaphragm. The analyzer is a linear polarizer with its transmission axis perpendicular to the polarizer. It is placed between the sample and the eye/camera, at or near the microscope objective's aperture stop. If no sample is present, the image should appear uniformly dark. The compensator (a type of retarder) is a birefringent plate of known parameters used for quantitative sample analysis and contrast adjustment.

Quantitative information can be obtained by introducing known retardation. Rotation of the analyzer correlates the analyzer's angular position with the retardation required to minimize the light intensity for object features at selected wavelengths. **Retardation** introduced by the compensator plate can be described as

$$\Gamma = (n_e - n_o)t,$$

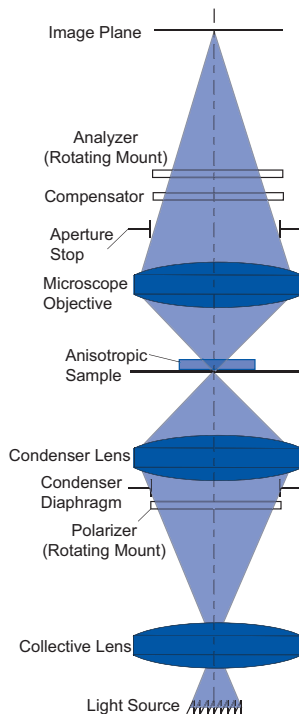
where t is the sample thickness, and subscripts e and o denote the extraordinary and ordinary beams. Retardation in concept is similar to the optical path difference for beams propagating through two different materials:

$$OPD = (n_1 - n_2)t = (n_e - n_o)t.$$

The phase delay caused by sample birefringence is therefore

$$\delta = \frac{2\pi OPD}{\lambda} = \frac{2\pi \Gamma}{\lambda}.$$

A polarization microscope can also be used to determine the orientation of the optic axis.



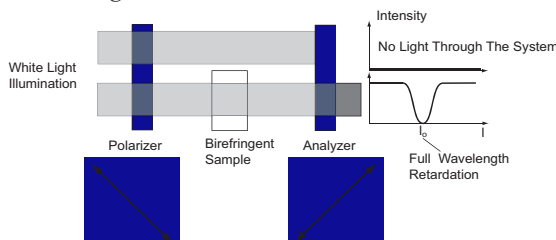
Images Obtained with Polarization Microscopes

Anisotropic samples observed under a **polarization microscope** contain dark and bright features and will strongly depend on the geometry of the sample. Objects can have characteristic elongated, linear, or circular structures:

- linear structures appear as dark or bright, depending on the orientation of the analyzer.
- circular structures have a “Maltese Cross” pattern with four quadrants of different intensities.

While polarization microscopy uses monochromatic light, it can also use white-light illumination. For broadband light, different wavelengths will be subject to different retardation; as a result, samples can provide different output colors. In practical terms, this means that color encodes information about retardation introduced by the object. The specific retardation is related to the image color. Therefore, the color allows for determination of sample thickness (for known retardation) or its retardation (for known sample thickness). If the polarizer and the analyzer are crossed, the color visible through the microscope is a complementary color to that having full wavelength retardation (a multiple of 2π , and the intensity is minimized for this color). Note that the two complementary colors combine into white light. If the analyzer could be rotated to be parallel to the analyzer, the two complementary colors will be switched (the one previously displayed will be minimized, while the other color will be maximized).

Polarization microscopy can provide quantitative information about the sample with the application of compensators (with known retardation). Estimating retardation might be performed visually or by integrating with an image acquisition system and CCD. This latter method requires one to obtain a series of images for different retarder orientations and calculate sample parameters based on saved images.



Compensators

Compensators are components that can be used to provide quantitative data about a sample's retardation. They introduce known retardation for a specific wavelength and can act as nulling devices to eliminate any phase delay introduced by the specimen. Compensators can also be used to control the background intensity level.

A **wave plate compensator** (also called a first-order red or red-I plate) is oriented at a 45-deg angle with respect to the analyzer and polarizer. It provides retardation equal to an even number of waves for 551 nm (green), which is the wavelength eliminated after passing the analyzer. All other wavelengths are retarded with a fraction of the wavelength and can partially pass the analyzer and appear as a bright red magenta. The sample provides additional retardation and shifts the colors towards blue and yellow. Color tables determine the retardation introduced by the object.

The **de Sénarmont compensator** is a quarter-wave plate (for 546 nm or 589 nm). It is used with monochromatic light for samples with retardation in the range of $\lambda/20$ to λ . A quarter-wave plate is placed between the analyzer and the polarizer with its slow ellipsoid axis parallel to the transmission axis of the analyzer. Retardation of the sample is measured in a two-step process. First, the sample is rotated until the maximum brightness is obtained. Next, the analyzer is rotated until the intensity maximally drops (the extinction position). The analyzer's rotation angle θ finds the phase delay related to retardation: $\Gamma_{\text{sample}} = 2\theta$.

A **Brace Köhler rotating compensator** is used for small retardations and monochromatic illumination. It is a thin birefringent plate with an optic axis in its plane. The analyzer and polarizer remain fixed while the compensator is rotated between the maximum and minimum intensities in the sample's image. Zero position (the maximum intensity) is determined for a slow axis being parallel to the transmission axis of the analyzer, and retardation is

$$\Gamma_{\text{sample}} = \Gamma_{\text{compensator}} \sin 2\theta .$$

Confocal Microscopy

Confocal microscopy is a scanning technique that employs pinholes at the illumination and detection planes so that only in-focus light reaches the detector. This means that the intensity for each sample point must be obtained in sequence through scanning in the x and y directions. An illumination pinhole is used in conjunction with the imaged sample plane and only illuminates the point of interest. The detection pinhole rejects the majority of out-of-focus light.

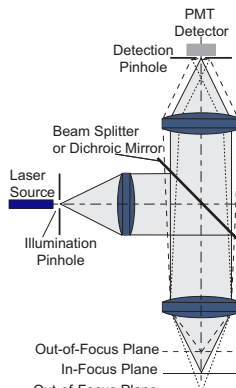
Confocal microscopy has the advantage of lowering the background light from out-of-focus layers, increasing spatial resolution, and providing the capability of imaging thick 3D samples, if combined with z scanning. Due to detection of only the in-focus light, confocal microscopy can provide images of thin sample sections. The system usually employs a photo-multiplier tube (PMT), avalanche photodiodes (APD), or a charge-coupled device (CCD) camera as a detector. For point detectors, recorded data is processed to assemble x - y images. This makes it capable of quantitative studies of an imaged sample's properties. Systems can be built for both reflectance and fluorescence imaging.

Spatial resolution of a confocal microscope can be defined as

$$d_{xy} \approx \frac{0.4\lambda}{NA},$$

and is slightly better than wide-field (bright-field) microscopy resolution. For pinholes larger than an Airy disk, the spatial resolution is the same as in a wide-field microscope. The **axial resolution** of a confocal system is

$$d_z \approx \frac{1.4n\lambda}{NA^2}.$$



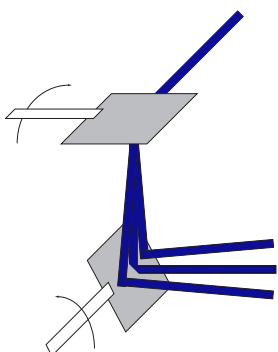
The optimum pinhole value is at the full width at half maximum (FWHM) of the Airy disk intensity. This corresponds to $\sim 75\%$ of its intensity passing through the system, minimally smaller than the Airy disk's first ring:

$$D_{\text{pinhole}} = \frac{0.5\lambda M}{NA}.$$

Scanning Approaches

A scanning approach is directly connected with the temporal resolution of confocal microscopes. The number of points in the image, scanning technique, and the frame rate are related to the signal-to-noise ratio SNR (through time dedicated to detection of a single point). To balance these parameters, three major approaches were developed: point scanning, line scanning, and disk scanning.

A **point-scanning confocal microscope** is based on point-by-point scanning using, for example, two mirror galvanometers or resonant scanners. Scanning mirrors should be located in pupil conjugates (or close to them) to avoid light fluctuations. Maximum spatial resolution and maximum background rejection are achieved with this technique.



A **line-scanning confocal microscope** uses a slit aperture that scans in a direction perpendicular to the slit. It uses a cylindrical lens to focus light onto the slit to maximize throughput. Scanning in one direction makes this technique significantly faster than a point approach. However, the drawbacks are a loss of resolution and sectioning performance for the direction parallel to the slit.

Feature	Point Scanning	Slit Slit Scanning	Disk Spinning
<i>z</i> resolution	High	Depends on slit spacing	Depends on pinhole distribution
<i>x,y</i> resolution	High	Lower for one direction	Depends on pinhole spacing
Speed	Low to moderate	High	High
Light sources	Lasers	Lasers	Laser and other
Photobleaching	High	High	Low
QE of detectors	Low (PMT) Good (APD)	Good (CCD)	Good (CCD)
Cost	High	High	Moderate

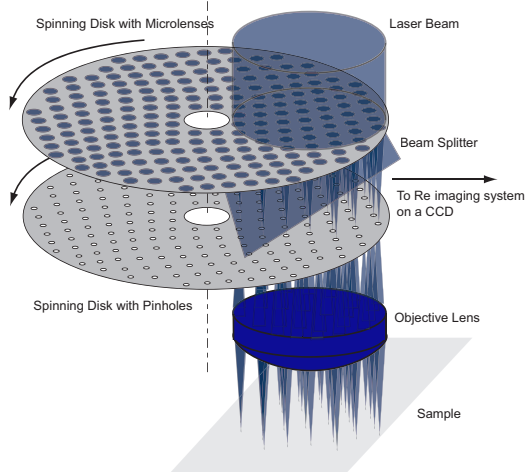
Scanning Approaches (cont.)

Spinning-disk confocal imaging is a parallel-imaging method that maximizes the scanning rate and can achieve a 100–1000 speed gain over point scanning. It uses an array of pinholes/slits (e.g., Nipkow disk, Yokogawa, Olympus DSU approach). To minimize light loss, it can be combined (e.g., with the Yokogawa approach) with an array of lenses, so each pinhole has a dedicated focusing component. Pinhole disks contain several thousand pinholes, but only a portion is illuminated at one time.

	Throughput of a confocal microscope T [%]
Array of pinholes	$T_{\text{pinhole}} = 100 \times (D / S)^2$
Multiple slits	$T_{\text{slit}} = 100 \times (D / S)$
Equations are for a uniformly illuminated mask of pinholes/slits (array of microlenses not considered). D is the pinhole's diameter or slit's width respectively, while S is the pinhole/slit separation.	

Crosstalk between pinholes and slits will reduce the background rejection. Therefore a common pinhole/slit separation S is 5–10 times larger than the pinhole's diameter or the slit's width.

Spinning-disk and slit-scanning confocal microscopes require high-sensitivity array image sensors (CCD cameras) instead of point detectors. They can use lower excitation intensity for fluorescence confocal systems; therefore, they are less susceptible to photobleaching.

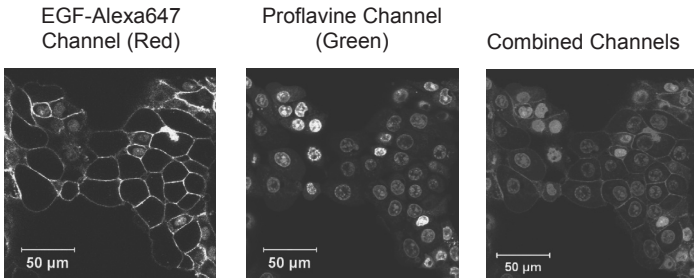
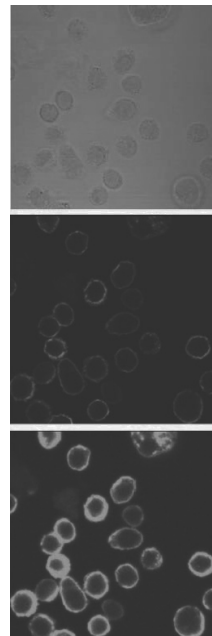


Images from a Confocal Microscope

Laser-scanning confocal microscopy rejects out-of-focus light and enables optical sectioning. It can be assembled in reflectance and fluorescent modes. A 1483 cell line, stained with membrane anti-EGFR antibodies labeled with fluorescent Alexa488 dye, is presented here. The top image shows the bright-field illumination mode. The middle image is taken by a confocal microscope with a pinhole corresponding to approximately 2.5 Airy disks. In the bottom image, the pinhole was entirely open. Clear cell boundaries are visible in the confocal image, while all out-of-focus features were removed.

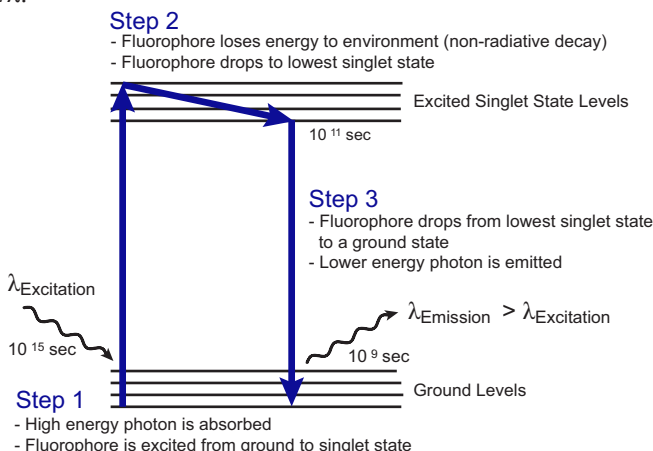
Images were taken with a Zeiss LSM 510 microscope using a $63\times$ Zeiss oil-immersion objective. Samples were excited with a 488-nm laser source.

Another example of 1483 cells labeled with EGF-Alexa647 and proflavine obtained on a Zeiss LSM 510 confocal at $63\times / 1.4$ oil is shown below. The proflavine (staining nuclei) was excited at 488 nm, with emission collected after a 505-nm long-pass filter. The EGF-Alexa647 (cell membrane) was excited at 633 nm, with emission collected after a 650–710 nm bandpass filter. The sectioning ability of a confocal system is nicely demonstrated by the channel with the membrane labeling.



Fluorescence

Specimens can absorb and re-emit light through **fluorescence**. The specific wavelength of light absorbed or emitted depends on the energy level structure of each molecule. When a molecule absorbs the energy of light, it briefly enters an excited state before releasing part of the energy as fluorescence. Since the emitted energy must be lower than the absorbed energy, fluorescent light is always at longer wavelengths than the excitation light. Absorption and emission take place between multiple sub-levels within the ground and excited states, resulting in absorption and emission spectra covering a range of wavelengths. The loss of energy during the fluorescence process causes the **Stokes shift** (a shift of wavelength peak from that of excitation to that of emission). Larger Stokes shifts make it easier to separate excitation and fluorescent light in the microscope. Note that energy quanta and wavelength are related by $E = hc/\lambda$.

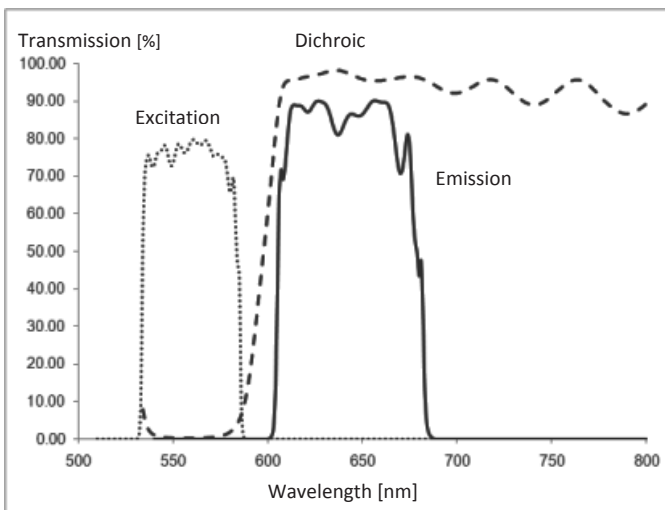
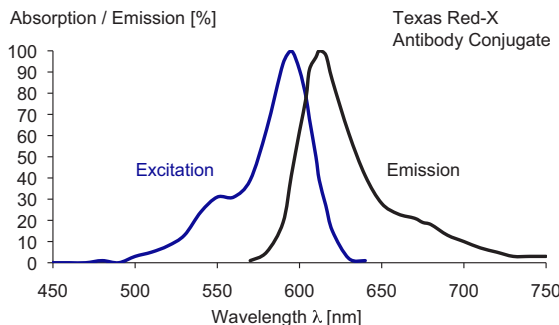


The fluorescence principle is widely used in fluorescence microscopy for both organic and inorganic substances. While it is most common for biological imaging, it is also possible to examine samples like drugs and vitamins.

Due to the application of filter sets, the fluorescence technique has a characteristically low background and provides high-quality images. It is used in combination with techniques like wide-field microscopy and scanning confocal-imaging approaches.

Configuration of a Fluorescence Microscope

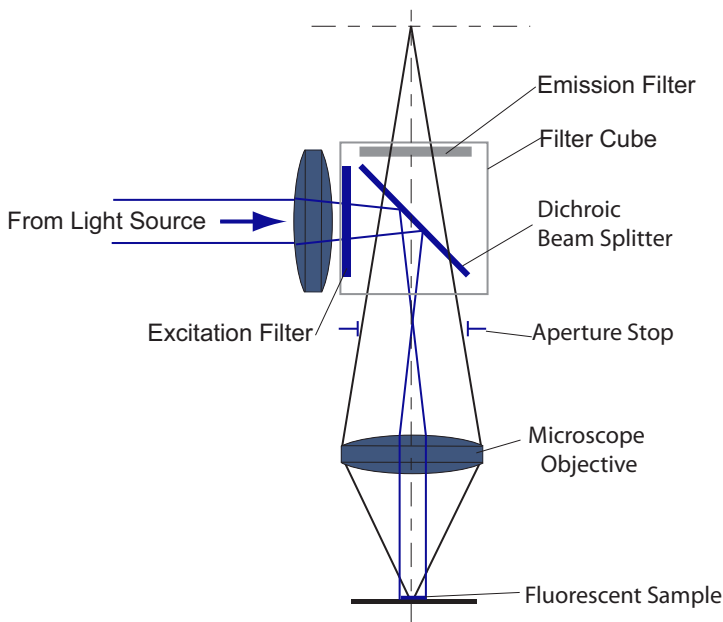
A fluorescence microscope includes a set of three **filters**: an **excitation filter**, **emission filter**, and a **dichroic mirror** (also called a **dichroic beam splitter**). These filters separate weak emission signals from strong excitation illumination. The most common fluorescence microscopes are configured in epi-illumination mode. The dichroic mirror reflects incoming light from the lamp (at short wavelengths) onto the specimen. Fluorescent light (at longer wavelengths) collected by the objective lens is transmitted through the dichroic mirror to the eyepieces or camera. The transmission and reflection properties of the dichroic mirror must be matched to the excitation and emission spectra of the fluorophore being used.



Configuration of a Fluorescence Microscope (cont.)

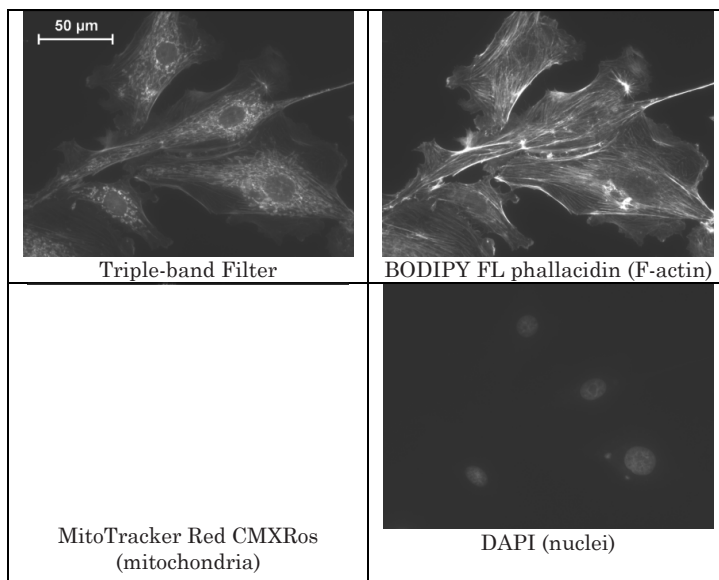
A sample must be illuminated with light at wavelengths within the excitation spectrum of the fluorescent dye. Fluorescence-emitted light must be collected at the longer wavelengths within the emission spectrum. Multiple fluorescent dyes can be used simultaneously, with each designed to localize or target a particular component in the specimen.

The **filter turret** of the microscope can hold several cubes that contain filters and dichroic mirrors for various dye types. Images are then reconstructed from CCD frames captured with each filter cube in place. Simultaneous acquisition of emission for multiple dyes requires application of multiband dichroic filters.



Images from Fluorescence Microscopy

Fluorescent images of cells labeled with three different fluorescent dyes, each targeting a different cellular component, demonstrate fluorescence microscopy's ability to target sample components and specific functions of biological systems. Such images can be obtained with individual filter sets for each fluorescent dye, or with a multiband (a triple-band in this example) filter set, which matches all dyes.



Sample: Bovine pulmonary artery epithelial cells (Invitrogen FluoCells No. 1)

Components: Plan-apochromat 40 \times /0.95, MRM Zeiss CCD (1388 \times 1040 mono)

Fluorescent labels:	Peak Excitation		
	Peak Emission		
	DAPI		461 nm
	BODIPY FL		512 nm
MitoTracker Red CMXRos	579 nm		599 nm
Filter:	Excitation	Dichroic	Emission
Triple-band	395–415	435	448–472
	480–510	510	510–550
	560–590	600	600–650
DAPI	325–375	395	420–470
GFP	450–490	495	500–550
Texas Red	530–585	600	615LP

Properties of Fluorophores

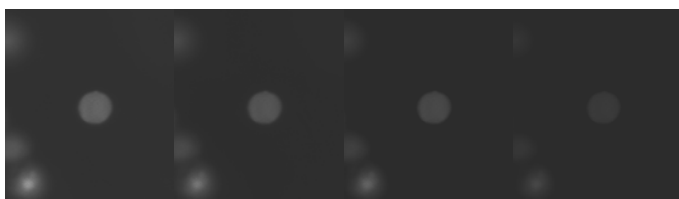
Fluorescent emission F [photons/s] depends on the intensity of excitation light I [photons/s] and fluorophore parameters like the **fluorophore quantum yield** Q and **molecular absorption cross section** σ :

$$F = \sigma Q I ,$$

where the molecular absorption cross section is the probability that illumination photons will be absorbed by fluorescent dye. The intensity of excitation light depends on the power of the light source and throughput of the optical system. The detected fluorescent emission is further reduced by the quantum efficiency of the detector.

Quenching is a partially reversible process that decreases fluorescent emission. It is a non-emissive process of electrons moving from an excited state to a ground state.

Fluorescence emission and excitation parameters are bound through a photobleaching effect that reduces the ability of fluorescent dye to fluoresce. **Photobleaching** is an irreversible phenomenon that is a result of damage caused by illuminating photons. It is most likely caused by the generation of long-living (in triplet states) molecules of singlet oxygen and oxygen free radicals generated during its decay process. There is usually a finite number of photons that can be generated for a fluorescent molecule. This number can be defined as the ratio of emission quantum efficiency to bleaching quantum efficiency, and it limits the time a sample can be imaged before entirely bleaching. Photobleaching causes problems in many imaging techniques, but it can be especially critical in time-lapse imaging. To slow down this effect, optimizing collection efficiency (together with working at lower power at the steady-state condition) is crucial.



Photobleaching effect as seen in consecutive images

Single vs Multi-Photon Excitation

Multi-photon fluorescence is based on the fact that two or more low-energy photons match the energy gap of the fluorophore to excite and generate a single high-energy photon. For example, the energy of two 700-nm photons can excite an energy transition approximately equal to that of a 350-nm photon (it is not an exact value due to thermal losses). This is contrary to traditional fluorescence, where a high-energy photon (e.g., 400 nm) generates a slightly lower-energy (longer wavelength) photon. Therefore, one big advantage of multi-photon fluorescence is that it can obtain a significant difference between excitation and emission.

Fluorescence is based on stochastic behavior, and for single-photon excitation fluorescence, it is obtained with a high probability. However, multi-photon excitation requires at least two photons delivered in a very short time, and the probability is quite low:

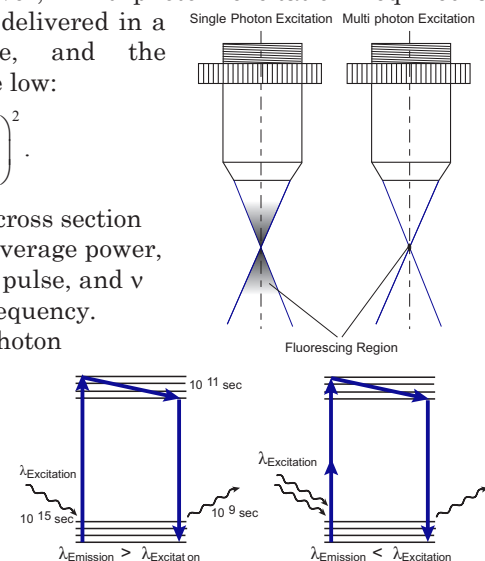
$$n_a \propto \delta \left(\frac{P_{avg}^2}{\tau v^2} \right) \left(\pi \frac{NA^2}{hc\lambda} \right)^2.$$

δ is the excitation cross section of dye, P_{avg} is the average power, τ is the length of a pulse, and v is the repetition frequency.

Therefore, multi-photon fluorescence must be used with high-power laser sources to obtain favorable probability.

Short-pulse operation will have a similar effect, as τ will be minimized.

Due to low probability, fluorescence occurs only in the focal point. Multi-photon imaging does not require scanning through a pinhole and therefore has a high signal-to-noise ratio and can provide deeper imaging. This is also because near-IR excitation light penetrates more deeply due to lower scattering, and near-IR light avoids the excitation of several autofluorescent tissue components.



Light Sources for Scanning Microscopy

Lasers are an important light source for scanning microscopy systems due to their high energy density, which can increase the detection of both reflectance and fluorescence light. For laser-scanning confocal systems, a general requirement is a single-mode TEM₀₀ laser with a short coherence length. Lasers are used primarily for point-and-slit scanning modalities. There are a great variety of laser sources, but certain features are useful depending on their specific application:

- Short-excitation wavelengths are preferred for fluorescence confocal systems because many fluorescent probes must be excited in the blue or ultraviolet range.
- Near-IR wavelengths are useful for reflectance confocal microscopy and multi-photon excitation. Longer wavelengths are less susceptible to scattering in diffused objects (like tissue) and can provide a deeper penetration depth.
- Broadband short-pulse lasers (like a Ti-Sapphire mode-locked laser) are particularly important for multi-photon generation, while shorter pulses increase the probability of excitation.

Laser Type	Wavelength [nm]
Argon-Ion	351, 364, 458, 488, 514
HeCd	325, 442
HeNe	543, 594, 633, 1152
Diode lasers	405, 408, 440, 488, 630, 635, 750, 810
DPSS (diode pumped, solid state)	430, 532, 561
Krypton-Argon	488, 568, 647
Dye	630
Ti-Sapphire*	710–920, 720–930, 750–850, 690–100, 680–1050

*High-power (1000mW or less), pulses between 1 ps and 100 fs

Non-laser sources are particularly useful for disk-scanning systems. They include arc lamps, metal-halide lamps, and high-power photo-luminescent diodes (See also pages 58 and 59).

Practical Considerations in LSM

A light source in laser-scanning microscopy must provide enough energy to obtain a sufficient number of photons to perform successful detection and a statistically significant signal. This is especially critical for non-laser sources (e.g., arc lamps) used in disk-scanning systems. While laser sources can provide enough power, they can cause fast photobleaching or photo-damage to the biological sample.

Detection conditions change with the type of sample. For example, fluorescent objects are subject to photobleaching and saturation. On the other hand, back-scattered light can be easily rejected with filter sets. In reflectance mode, out-of-focus light can cause background comparable or stronger than the signal itself. This background depends on the size of the pinhole, scattering in the sample, and overall system reflections.

Light losses in the optical system are critical for the signal level. Collection efficiency is limited by the NA of the objective; for example, a NA of 1.4 gathers approximately 30% of the fluorescent/scattered light. Other system losses will occur at all optical interfaces, mirrors, filters, and at the pinhole. For example, a pinhole matching the Airy disk allows approximately 75% of the light from the focused image point.

Quantum efficiency (QE) of a detector is another important system parameter. The most common photodetector used in scanning microscopy is the photomultiplier tube (PMT). Its quantum efficiency is often limited to the range of 10–15% (550–580 nm). In practical terms, this means that only 15% of the photons are used to produce a signal. The advantages of PMTs for laser-scanning microscopy are high speed and high signal gain. Better QE can be obtained for CCD cameras, which is 40–60% for standard designs and 90–95% for thinned, back-illuminated cameras. However, CCD image sensors operate at lower rates.

Spatial and temporal sampling of laser-scanning microscopy images imposes very important limitations on image quality. The image size and frame rate are often determined by the number of photons sufficient to form high-quality images.

Interference Microscopy

Interference microscopy

includes a broad family of techniques for quantitative sample characterization (thickness, refractive index, etc.). Systems are based on microscopic implementation of interferometers (like the Michelson and Mach-Zehnder geometries), or polarization interferometers.

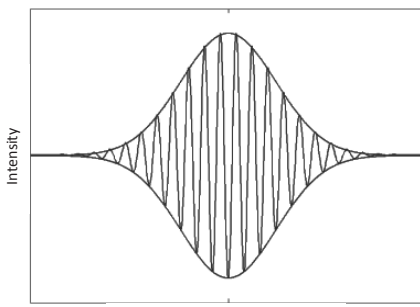
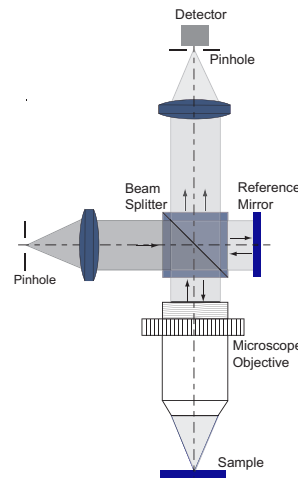
In interference microscopy, short coherence systems are particularly interesting and can be divided into two groups: **optical profilometry** and **optical coherence tomography**

(OCT) [including **optical coherence microscopy** (OCM)]. The primary goal of these techniques is to add a third (z) dimension to the acquired data.

Optical profilers use interference fringes as a primary source of object height. Two important measurement approaches include **vertical scanning interferometry** (VSI) (also called **scanning white light interferometry** or **coherence scanning interferometry**) and **phase-shifting interferometry**. Profilometry techniques are capable of achieving nanometer-level resolution in the z direction while x and y are defined by standard microscope limitations.

Profilometry is used for characterizing the sample surface (roughness, structure, microtopography, and in some cases film thickness) while OCT/OCM is dedicated to 3D imaging, primarily of biological samples.

Both types of systems are usually configured using the geometry of the Michelson or its derivatives (e.g., Mirau).



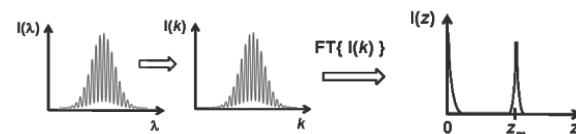
Optical Coherence Tomography/Microscopy

In early 3D coherence imaging, information about the sample was gated by the coherence length of the light source (**time-domain OCT**). This means that the maximum fringe contrast is obtained at a zero optical path difference, while the entire fringe envelope has a width related to the coherence length. In fact, this width defines the axial resolution (usually a few microns) and images are created from the magnitude of the fringe pattern envelope. **Optical coherence microscopy** is a combination of OCT and confocal microscopy. It merges the advantages of out-of-focus background rejection provided by the confocal principle and applies the coherence gating of OCT to improve optical sectioning over confocal reflectance systems.

In the mid-2000s, time-domain OCT transitioned to **Fourier-domain OCT** (FDOCT), which can acquire an entire depth profile in a single capture event. Similar to Fourier Transform Spectroscopy, the image is acquired by calculating the Fourier transform of the obtained interference pattern. The measured signal can be described as

$$I(k, z_o) = \int A_R A_S(z) \cos[k(z_m - z_o)] dz,$$

where A_R and A_S are amplitudes of the reference and sample light, respectively, and z_m is the imaged sample depth (z_o is the reference length delay, and k is the wave number).



The fringe frequency is a function of wave number k and relates to the OPD in the sample. Within the Fourier-domain techniques, two primary methods exist: **spectral-domain OCT** (SDOCT) and **swept-source OCT** (SSOCT). Both can reach detection sensitivity and signal-to-noise ratios over 150 times higher than time-domain OCT approaches. SDOCT achieves this through the use of a broadband source and spectrometer for detection. SSOCT uses a single photodetector but rapidly tunes a narrow linewidth over a broad spectral profile. Fourier-domain systems can image at hundreds of frames per second with sensitivities over 100 dB.

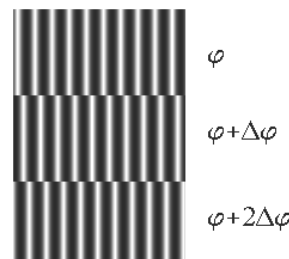
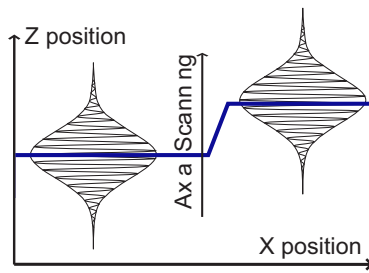
Optical Profiling Techniques

There are two primary techniques used to obtain a surface profile using white-light profilometry: **vertical scanning interferometry** (VSI) and **phase-shifting interferometry** (PSI).

VSI is based on the fact that a reference mirror is moved by a piezoelectric or other actuator, and a sequence of several images (in some cases hundreds or thousands) is acquired along the scan. During post-processing, algorithms look for a maximum fringe modulation and correlate it with the actuator's position. This position is usually determined with capacitance gauges; however, more advanced systems use optical encoders or an additional Michelson interferometer. The important advantage of VSI is its ability to ambiguously measure heights that are greater than a fringe.

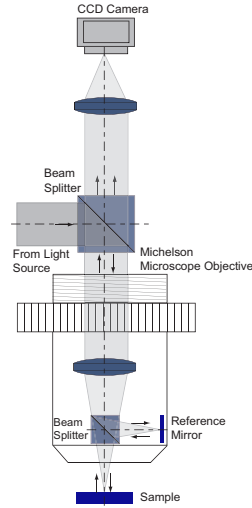
The PSI technique requires the object of interest to be within the coherence length and provides one order of magnitude or greater z resolution compared to VSI. To extend coherence length, an optical filter is introduced to limit the light source's bandwidth. With PSI, a phase-shifting component is located in one arm of the interferometer. The reference mirror can also provide the role of the phase shifter. A series of images (usually three to five) is acquired with appropriate phase differences to be used later in phase reconstruction. Introduced phase shifts change the location of the fringes. An important PSI drawback is the fact that phase maps are subject to 2π discontinuities. Phase maps are first obtained in the form of so-called phase fringes and must be unwrapped (a procedure of removing discontinuities) to obtain a continuous phase map.

Note that modern short-coherence interference microscopes combine phase information from PSI with a long range of VSI methods.



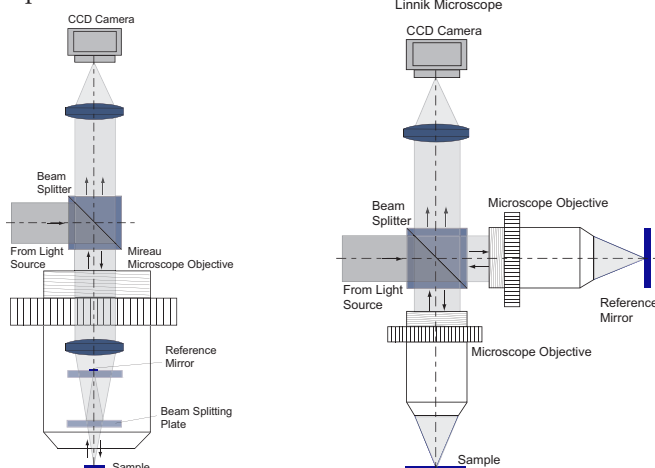
Optical Profilometry: System Design

Optical profilometry systems are based on implementing a Michelson interferometer or its derivatives into their design. There are three primary implementations: classical **Michelson** geometry, **Mireau**, and **Linnik**. The first approach incorporates a Michelson inside a microscope objective using a classical interferometer layout. Consequently, it can work only for low magnifications and short working distances. The Mireau objective uses two plates perpendicular to the optical axis inside the objective. One is a beam-splitting plate, while the other acts as a reference mirror. Such a solution extends the working distance and increases the possible magnifications.



Design	Magnification
Michelson	1× to 5×
Mireau	10× to 100×
Linnik	50× to 100×

The Linnik design utilizes two matching objectives. It does not suffer from NA limitation, but it is quite expensive and susceptible to vibrations.



Phase-Shifting Algorithms

Phase-shifting techniques find the phase distribution from interference images given by

$$I(x, y) = a(x, y) + b(x, y)\cos(\phi + n\Delta\phi),$$

where $a(x, y)$ and $b(x, y)$ correspond to background and fringe amplitude, respectively. Since this equation has three unknowns, at least three measurements (images) are required. For image acquisition with a discrete CCD camera, spatial (x, y) coordinates can be replaced by (i, j) pixel coordinates.

The most basic PSF algorithms include the **three-, four-,** and **five-image** techniques.

I denotes the intensity for a specific image (1st, 2nd, 3rd, etc.) in the selected i, j pixel of a CCD camera. The phase shift for a three-image algorithm is $\pi/2$. Four- and five-image algorithms also acquire images with $\pi/2$ phase shifts.

$$\begin{aligned}\phi &= \arctan\left(\frac{I_3 - I_2}{I_1 - I_2}\right) \\ \phi &= \arctan\left(\frac{I_4 - I_2}{I_1 - I_3}\right) \\ \phi &= \arctan\left(\frac{2[I_2 - I_4]}{I_1 - I_3 + I_5}\right)\end{aligned}$$

A reconstructed phase depends on the accuracy of the phase shifts. $\pi/2$ steps were selected to minimize the systematic errors of the above techniques. Accuracy progressively improves between the three- and five-point techniques. Note that modern PSI algorithms often use seven images or more, in some cases reaching thirteen.

After the calculations, the wrapped phase maps (modulo 2π) are obtained (arctan function). Therefore, unwrapping procedures have to be applied to provide continuous phase maps.

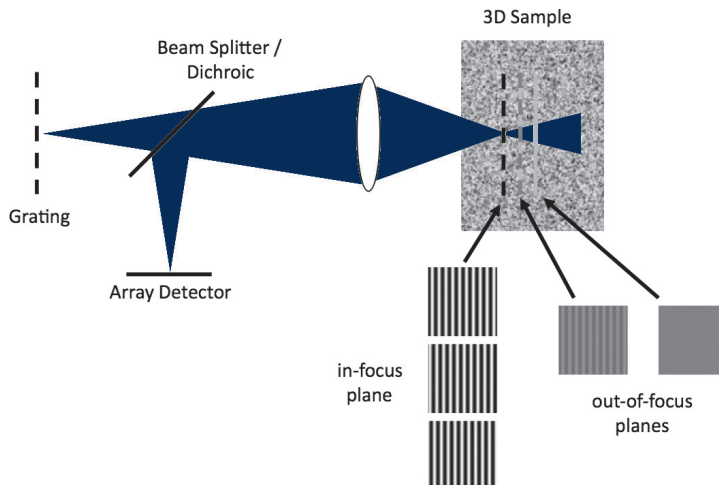
Common unwrapping methods include the line by line algorithm, least square integration, regularized phase tracking, minimum spanning tree, temporal unwrapping, frequency multiplexing, and others.

Structured Illumination: Axial Sectioning

A simple and inexpensive alternative to confocal microscopy is the **structured-illumination technique**. This method uses the principle that all but the zero (DC) spatial frequencies are attenuated with defocus. This observation provides the basis for obtaining the **optical sectioning** of images from a conventional wide-field microscope. A modified illumination system of the microscope projects a single spatial-frequency grid pattern onto the object. The microscope then faithfully images only that portion of the object where the grid pattern is in focus. The structured-illumination technique requires the acquisition of at least three images to remove the illumination structure and reconstruct an image of the layer. The reconstruction relation is described by

$$I = \sqrt{(I_0 - I_{2\pi/3})^2 + (I_0 - I_{4\pi/3})^2 + (I_{2\pi/3} - I_{4\pi/3})^2},$$

where I denotes the intensity in the reconstructed image point, while I_0 , $I_{2\pi/3}$, and $I_{4\pi/3}$ are intensities for the image point and the three consecutive positions of the sinusoidal illuminating grid (zero, 1/3 and 2/3 of the structure period).



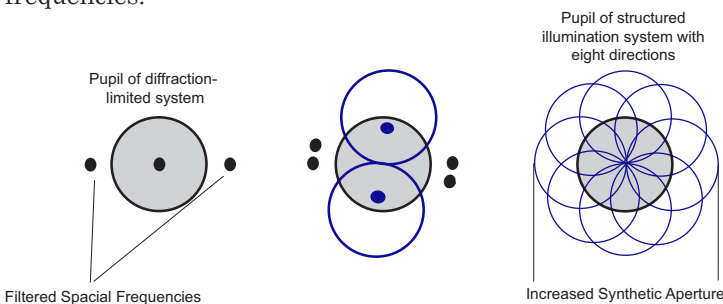
Note that the maximum sectioning is obtained for 0.5 of the objective's cut-off frequency. This sectioning ability is comparable to that obtained in confocal microscopy.

Structured Illumination: Resolution Enhancement

Structured illumination can be used to enhance the spatial resolution of a microscope. It is based on the fact that if a sample is illuminated with a periodic structure, it will create a low-frequency beating effect (Moiré fringes) with the features of the object. This new low-frequency structure will be capable of aliasing high spatial frequencies through the optical system. Therefore, the sample can be illuminated with a pattern of several orientations to accommodate the different directions of the object features. In practical terms, this means that system apertures will be doubled (in diameter), creating a new synthetic aperture.



To produce a high-frequency structure, the interference of two beams with large illumination angles can be used. Note that the blue dots in the figure represent aliased spatial frequencies.

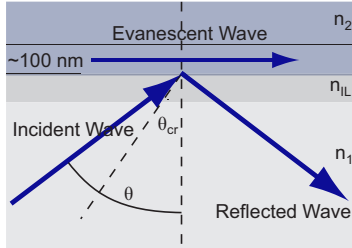


To reconstruct distribution, at least three images are required for one grid direction. In practice, obtaining a high-resolution image is possible with seven to nine images and a grid rotation, while a larger number can provide a more efficient reconstruction.

The linear-structured illumination approach is capable of obtaining two-fold resolution improvement over the diffraction limit. The application of nonlinear gain in fluorescence imaging improves resolution several times while working with higher harmonics. Sample features of 50 nm and smaller can be successfully resolved.

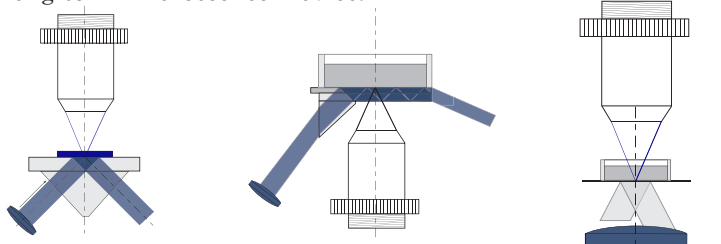
TIRF Microscopy

Total internal reflection fluorescence (TIRF) microscopy (also called evanescent wave microscopy) excites a limited width of the sample close to a solid interface. In TIRF, a thin layer of the sample is excited by a wavefront undergoing total internal reflection in the dielectric substrate, producing an **evanescent wave** propagating along the interface between the substrate and object.



The thickness of the excited section is limited to less than 100–200 nm. Very low background fluorescence is an important feature of this technique, since only a very limited volume of the sample in contact with the evanescent wave is excited.

This technique can be used for imaging cells, cytoplasmic filament structures, single molecules, proteins at cell membranes, micro-morphological structures in living cells, the adsorption of liquids at interfaces, or Brownian motion at the surfaces. It is also a suitable technique for recording long-term fluorescence movies.

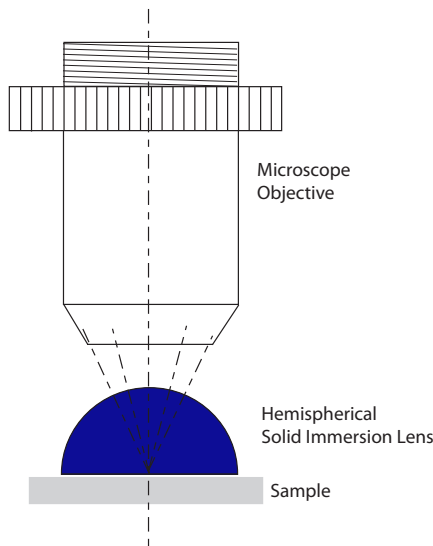


While an evanescent wave can be created without any layers between the dielectric substrate and sample, it appears that a thin layer (e.g., metal) improves image quality. For example, it can quench fluorescence in the first 10 nm and therefore provide selective fluorescence for the 10–200 nm region. TIRF can be easily combined with other modalities like optical trapping, multi-photon excitation, or interference. The most common configurations include oblique illumination through a high-NA objective or TIRF with a prism.

Solid Immersion

Optical resolution can be enhanced using **solid immersion** imaging. In the classical definition, the diffraction limit depends on the NA of the optical system and the wavelength of light. It can be improved by increasing the refractive index of the media between the sample and optical system or by decreasing the light's wavelength. The solid immersion principle is based on improving the first parameter by applying **solid immersion lenses** (SILs). To maximize performance, SILs are made with a high refractive index glass (usually greater than 2). The most basic setup for a SIL application involves a hemispherical lens. The sample is placed at the center of the hemisphere so the rays propagating through the system are not refracted (they intersect the SIL surface direction) and enter the microscope objective. The SIL is practically in contact with the object, but has a small sub-wavelength gap (<100 nm) between the sample and optical system; therefore, an object is always in an evanescent field and can be imaged with high resolution. Therefore, the technique is confined to a very thin sample volume (up to 100 nm) and can provide optical sectioning. Systems based on solid immersion can reach sub-100-nm lateral resolutions.

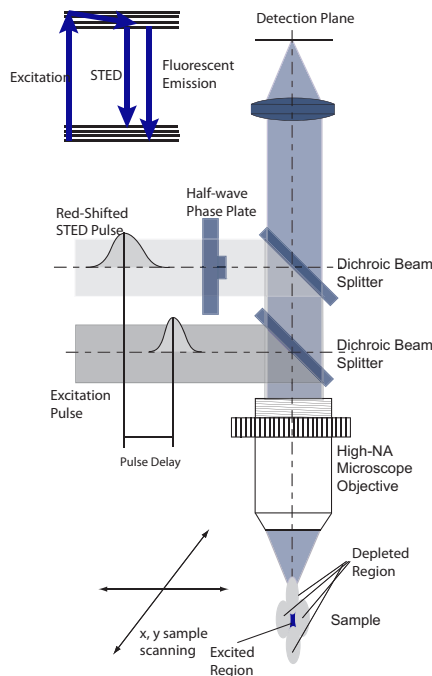
The most common solid-immersion applications are in microscopy, including fluorescence, optical data storage, and lithography. Compared to classical oil-immersion techniques, this technique is dedicated to imaging thin samples only (sub-100 nm), but provides much better resolution depending on the configuration and refractive index of the SIL.



Stimulated Emission Depletion

Stimulated emission depletion (STED) microscopy is a fluorescence super-resolution technique that allows imaging with a spatial resolution at the molecular level. The technique has shown an improvement 5–10 times beyond the possible diffraction-resolution limit.

The STED technique is based on the fact that the area around the excited object point can be treated with a pulse (depletion pulse or STED pulse) that depletes high-energy states and brings fluorescent dye to the ground state. Consequently, an actual excitation pulse excites only the small sub-diffraction resolved area. The depletion pulse must have high intensity and be significantly shorter than the lifetime of the excited states. The pulse must be shaped, for example, with a half-wave phase plate and imaging optics to create a 3D doughnut-like structure around the point of interest. The STED pulse is shifted toward red with regard to the fluorescence excitation pulse and follows it by a few picoseconds. To obtain the complete image, the system scans in the x , y , and z directions.

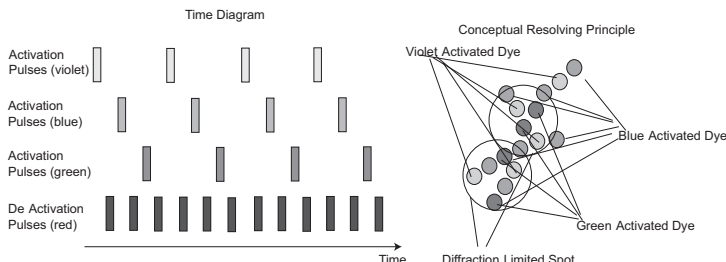


STORM

Stochastic optical reconstruction microscopy (STORM) is based on the application of multiple photo-switchable fluorescent probes that can be easily distinguished in the spectral domain. The system is configured in **TIRF** geometry. Multiple fluorophores label a sample, and each is built as a dye pair where one component acts as a fluorescence activator. The activator can be switched on or deactivated using a different illumination laser (a longer wavelength is used for deactivation—usually red). In the case of applying several dual-pair dyes, different lasers can be used for activation and only one for deactivation.

A sample can be sequentially illuminated with activation lasers, which generate fluorescent light at different wavelengths for slightly different locations on the object (each dye is sparsely distributed over the sample and activation is stochastic in nature). Activation for a different color can also be shifted in time. After performing several sequences of activation/deactivation, it is possible to acquire data for the centroid localization of various diffraction-limited spots. This localization can be performed with precision to about 1 nm. The spectral separation of dyes detects closely located object points encoded with a different color.

The STORM process requires 1000+ activation/deactivation cycles to produce high-resolution images. Therefore, final images combine the spots corresponding to individual molecules of DNA or an antibody used for labeling. STORM images can reach a lateral resolution of about 25 nm and an axial resolution of 50 nm.



4Pi Microscopy

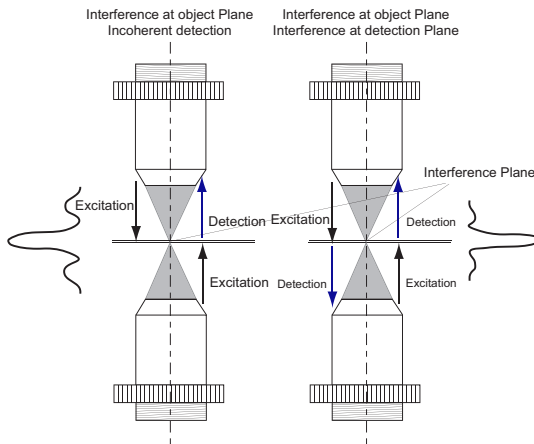
4Pi microscopy is a fluorescence technique that significantly reduces the thickness of an imaged section. The 4Pi principle is based on coherent illumination of a sample from two directions. Two constructively interfering beams improve the axial resolution by three to seven times. The possible values of z resolution using 4Pi microscopy are 50–100 nm and 30–50 nm when combined with STED.

The undesired effect of the technique is the appearance of side lobes located above and below the plane of the imaged section. They are located about $\lambda/2$ from the object. To eliminate side lobes, three primary techniques can be used:

- Combine 4Pi with confocal detection. A pinhole rejects some of the out-of-focus light.
- Detect in multi-photon mode, which quickly diminishes the excitation of fluorescence.
- Apply a modified 4Pi system, which creates interference at both the object and detection planes (two imaging systems are required).

It is also possible to remove side lobes through numerical processing, if they are smaller than 50% of the maximum intensity. However, side lobes increase with the NA of the objective; for an NA of 1.4, they are about 60–70% of the maximum intensity. Numerical correction is not effective in this case.

4Pi microscopy improves resolution only in the z direction; however, the perception of details in the thin layers is a useful benefit of the technique.



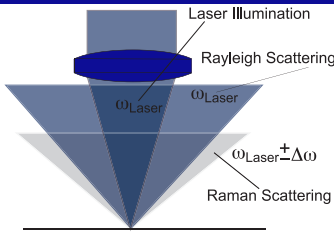
The Limits of Light Microscopy

Classical light microscopy is limited by diffraction and depends on the wavelength of light and the parameters of an optical system (NA). However, recent developments in super-resolution methods and enhancement techniques overcome these barriers and provide resolution at a molecular level. They often use a sample as a component of the optical train [resolvable saturable optical fluorescence transitions (**RESOLFT**), saturated structured-illumination microscopy (**SSIM**), photoactivated localization microscopy (**PALM**) and **STORM**] or combine near-field effects (**4Pi, TIRF, solid immersion**) with far-field imaging. The table below summarizes these methods.

		Demonstrated Values	
Method	Principles	Lateral	Axial
Bright field	Diffraction	200 nm	500 nm
Confocal	Diffraction (slightly better than bright field)	200 nm	500 nm
Solid immersion	Diffraction / evanescent field decay	< 100 nm	< 100 nm
TIRF	Diffraction / evanescent field decay	200 nm	< 100 nm
4Pi / I5	Diffraction/ interference	200 nm	50 nm
RESOLFT (e.g.,STED)	Depletion, molecular structure of sample–fluorescent probes	20 nm	20 nm
Structured illumination (SSIM)	Aliasing, nonlinear gain in fluorescent probes (molecular structure)	25–50 nm	50–100 nm
Stochastic techniques (PALM, STORM)	Fluorescent probes (molecular structure), centroid localization, time-dependant fluorophore activation	25 nm	50 nm

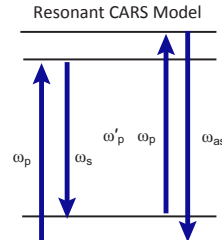
Raman and CARS Microscopy

Raman microscopy (also called chemical imaging) is a technique based on inelastic **Raman scattering** and evaluates the vibrational properties of samples (minerals, polymers, and biological objects).



Raman microscopy uses a laser beam focused on a solid object. Most of the illuminating light is scattered, reflected, and transmitted, and preserves the parameters of the illumination beam (the frequency is the same as the illumination). However, a small portion of the light is subject to a shift in frequency: $\omega_{\text{Raman}} = \omega_{\text{Laser}} \pm \Delta\omega$. This frequency shift between illumination and scattering bears information about the molecular composition of the sample. Raman scattering is weak and requires high-power sources and sensitive detectors. It is examined with spectroscopy techniques.

Coherent Anti-Stokes Raman Scattering (CARS) overcomes the problem of weak signals associated with Raman imaging. It uses a pump laser and a tunable Stokes laser to stimulate a sample with a four-wave mixing process. The fields of both lasers [pump field $E(\omega_p)$, Stokes field $E(\omega_s)$, and probe field $E'(\omega_p')$] interact with the sample and produce an anti-Stokes field [$E(\omega_{\text{as}})$] with frequency ω_{as} , so $\omega_{\text{as}} = 2\omega_p - \omega_s$.



CARS works as a resonant process, only providing a signal if the vibrational structure of the sample specifically matches $\omega_p - \omega_s$. It also must assure phase matching so that l_c (the coherence length) is greater than $\pi/\Delta k = \pi / |\mathbf{k}_{\text{as}} - (2\mathbf{k}_p - \mathbf{k}_s)|$, where Δk is a phase mismatch. CARS is orders of magnitude stronger than Raman scattering, does not require any exogenous contrast, provides good sectioning ability, and can be set up in both transmission and reflectance modes.

SPIM

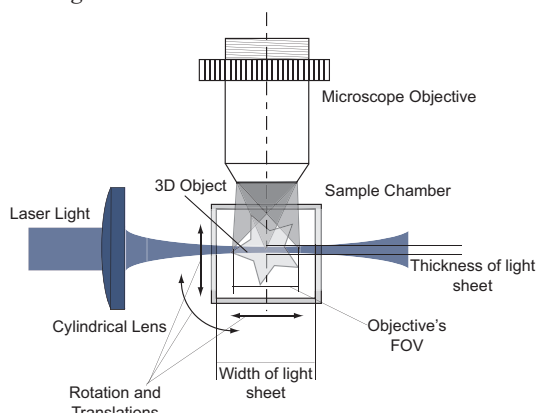
Selective plane illumination microscopy (SPIM) is dedicated to the high-resolution imaging of large 3D samples. It is based on three principles:

- The sample is illuminated with a **light sheet**, which is obtained with cylindrical optics. The light sheet is a beam focused in one direction and collimated in another. This way, the thin and wide light sheet can pass through the object of interest (see figure).
- The sample is imaged in the direction perpendicular to the illumination.
- The sample is rotated around its axis of gravity and linearly translated into axial and lateral directions.

Data is recorded by a CCD camera for multiple object orientations and can be reconstructed into a single 3D distribution. Both scattered and fluorescent light can be used for imaging.

The maximum resolution of the technique is limited by the longitudinal resolution of the optical system (for a high numerical aperture, objectives can obtain micron-level values). The maximum volume imaged is limited by the working distance of a microscope and can be as small as tens of microns or exceed several millimeters. The object is placed in an air, oil, or water chamber.

The technique is primarily used for bio-imaging, ranging from small organisms to individual cells.



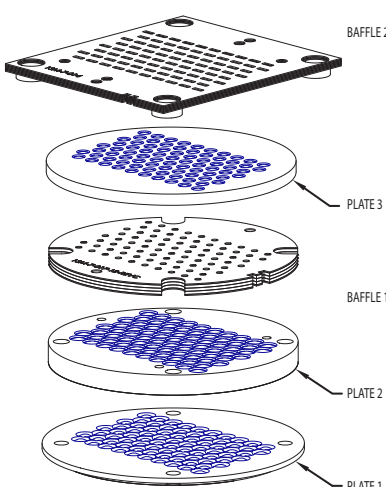
Array Microscopy

An **array microscope** is a solution to the trade-off between field of view and lateral resolution. In the array microscope, a miniature microscope objective is replicated tens of times. The result is an imaging system with a field of view that can be increased in steps of an individual objective's field of view, independent of numerical aperture and resolution. An array microscope is useful for applications that require fast imaging of large areas at a high level of detail. Compared to conventional microscope optics for the same purpose, an array microscope can complete the same task several times faster due to its parallel imaging format.

An example implementation of the array-microscope optics is shown. This array microscope is used for imaging glass slides containing tissue (histology) or cells (cytology). For this case, there are a total of 80 identical miniature $7\times/0.6$ microscope objectives. The summed field of view measures 18 mm. Each objective consists of three lens elements. The lens surfaces are patterned on three plates that are stacked to form the final array of microscopes. The plates measure 25 mm in diameter. Plate 1 is near the object at a working distance of 400 μm . Between plates 2 and 3 is a baffle plate. A second baffle is located between the third lens and the image plane. The purpose of the baffles is to eliminate cross talk and image overlap between objectives in the array.

The small size of each microscope objective and the need to avoid image overlap jointly dictate a low magnification. Therefore, the array microscope works best in combination with an image sensor divided into small pixels (e.g., 3.3 μm).

Focusing the array microscope is achieved by an up/down translation and two rotations: a pitch and a roll.



Digital Microscopy

Digital microscopy emerged with the development of electronic array image sensors and replaced the microphotography techniques previously used in microscopy. It can also work with point detectors when images are recombined in post or real-time processing. Digital microscopy is based on acquiring, storing, and processing images taken with various microscopy techniques. It supports applications that require:

- Combining data sets acquired for one object with different microscopy modalities or different imaging conditions. Data can be used for further analysis and processing in techniques like hyperspectral and polarization imaging.
- Image correction (e.g., distortion, white balance correction, or background subtraction). Digital microscopy is used in deconvolution methods that perform numerical rejection of out-of-focus light and iteratively reconstruct an object's estimate.
- Image acquisition with a high temporal resolution. This includes short integration times or high frame rates.
- Long time experiments and remote image recording.
- Scanning techniques where the image is reconstructed after point-by-point scanning and displayed on the monitor in real time.
- Low light, especially fluorescence. Using high-sensitivity detectors reduces both the excitation intensity and excitation time, which mitigates photobleaching effects.
- Contrast enhancement techniques and an improvement in spatial resolution. Digital microscopy can detect signal changes smaller than possible with visual observation.
- Super-resolution techniques that may require the acquisition of many images under different conditions.
- High throughput scanning techniques (e.g., imaging large sample areas).
- UV and IR applications not possible with visual observation.

The primary detector used for digital microscopy is a CCD camera. For scanning techniques, a photomultiplier or photodiodes are used.

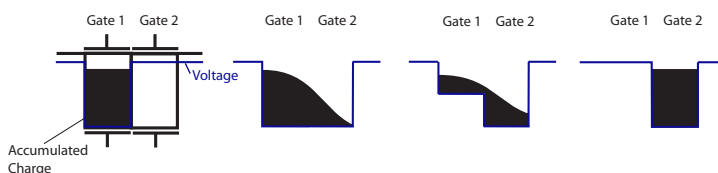
Principles of CCD Operation

Charge-coupled device (CCD) sensors are a collection of individual photodiodes arranged in a 2D grid pattern. Incident photons produce electron-hole pairs in each pixel in proportion to the amount of light on each pixel. By collecting the signal from each pixel, an image corresponding to the incident light intensity can be reconstructed.

Here are the step-by-step processes in a CCD:

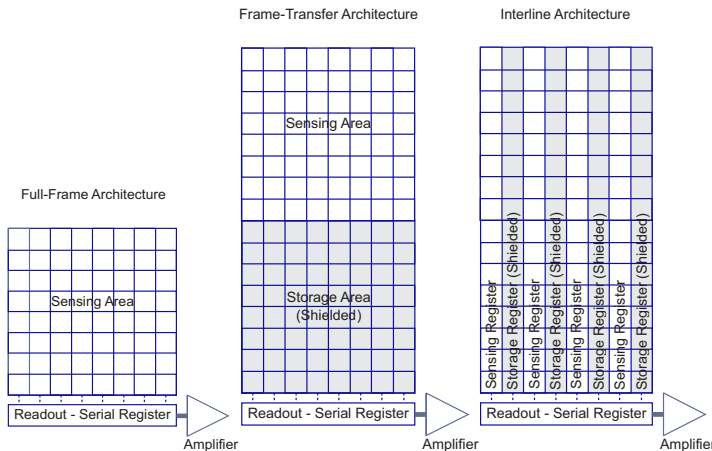
1. The CCD array is illuminated for integration time τ .
2. Incident photons produce mobile charge carriers.
3. Charge carriers are collected within the p-n structure.
4. The illumination is blocked after time τ (full-frame only).
5. The collected charge is transferred from each pixel to an amplifier at the edge of the array.
6. The amplifier converts the charge signal into voltage.
7. The analog voltage is converted to a digital level for computer processing and image display.

Each pixel (**photodiode**) is reverse biased, causing photoelectrons to move towards the positively charged electrode. Voltages applied to the electrodes produce a potential well within the semiconductor structure. During the integration time, electrons accumulate in the potential well, up to the full-well capacity. The full-well capacity is reached when the repulsive force between electrons exceeds the attractive force of the well. At the end of the exposure time, each pixel has stored a number of electrons in proportion to the amount of light received. These charge packets must be transferred from the sensor, from each pixel to a single amplifier without loss. This is accomplished by a series of parallel and serial shift registers. The charge stored by each pixel is transferred across the array by sequences of gating voltages applied to the electrodes. The packet of electrons follows the positive clocking waveform voltage from pixel-to-pixel or row-to-row. A potential barrier is always maintained between adjacent pixel charge packets.



CCD Architectures

In a **full-frame architecture**, individual pixel charge packets are transferred by a parallel row shift to the serial register, then one-by-one to the amplifier. The advantage of this approach is a 100% photosensitive area, while the disadvantage is that a shutter must block the sensor area during readout, and consequently limits the frame rate.

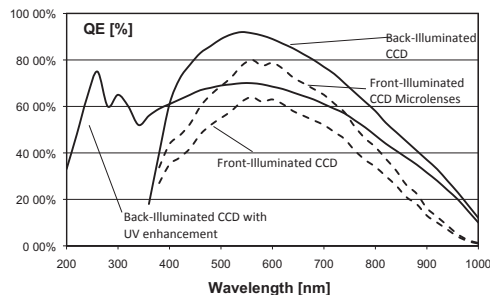


The **frame-transfer architecture** has the advantage of not needing to block an imaging area during readout. It is faster than full-frame, since readout can take place during the integration time. The significant drawback is that only 50% of the sensor area is used for imaging.

The **interline transfer architecture** uses columns with exposed imaging pixels interleaved with columns of masked storage pixels. A charge is transferred into an adjacent storage column for readout. The advantage of such an approach is a high frame rate due to a rapid transfer time (< 1 ms), while again the disadvantage is that 50% of the sensor area is used for light collection. However, recent interleaved CCDs have an increased fill factor due to the application of microlens arrays.

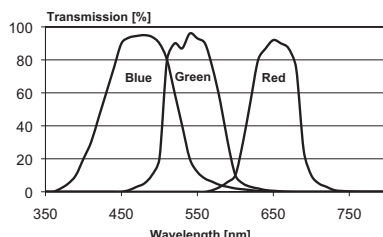
CCD Architectures (cont.)

Quantum efficiency (QE) is the percentage of incident photons at each wavelength that produce an electron in a photodiode.

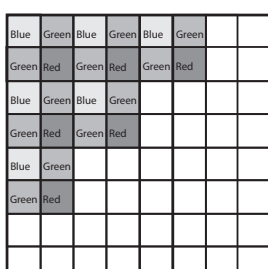


CCDs have a lower QE than individual silicon photodiodes due to the charge-transfer channels on the sensor surface, which reduces the effective light-collection area. A typical CCD QE is 40–60%. This can be improved for back-thinned CCDs, which are illuminated from behind; this avoids the surface electrode channels and improves QE to approximately 90–95%.

Recently, **electron-multiplying CCDs** (EM-CCD), primarily used for biological imaging, have become more common. They are equipped with a gain register placed between the shift register and output amplifier. A multi-stage gain register allows high gains. As a result, single electrons can generate thousands of output electrons. While the read noise is usually low, it is therefore negligible in the context of thousands of signal electrons.



CCD pixels are not color sensitive, but use color filters to separately measure red, green, and blue light intensity. The most common method is to cover the sensor with an array of **RGB** (red, green, blue) filters, which combine four individual pixels to generate a single color pixel. The **Bayer mask** uses two green pixels for every red and blue pixel, which simulates human visual sensitivity.



CCD Noise

The three main types of noise that affect CCD imaging are **dark noise**, **read noise**, and **photon noise**.

Dark noise arises from random variations in the number of thermally generated electrons in each photodiode. More electrons can reach the conduction band as the temperature increases, but this number follows a statistical distribution. These random fluctuations in the number of conduction band electrons results in a **dark current** that is not due to light. To reduce the influence of dark current for long time exposures, CCD cameras are cooled (which is crucial for the exposure of weak signals, like fluorescence, with times of a few seconds and more).

Read noise describes the random fluctuation in electrons contributing to measurement, due to electronic processes on the CCD sensor. This noise arises during the charge transfer, the charge-to-voltage conversion, and the analog-to-digital conversion. Every pixel on the sensor is subject to the same level of read noise, most of which is added by the amplifier.

Dark noise and read noise are due to the properties of the CCD sensor itself.

Photon noise (or **shot noise**) is inherent in any measurement of light, due to the fact that photons arrive at the detector randomly in time. This process is described by **Poisson statistics**. The probability P of measuring k events, given an expected value N is

$$P(k, N) = \frac{N^k e^{-N}}{k!}.$$

The standard deviation of the Poisson distribution is $N^{1/2}$. Therefore, if the average number of photons arriving at the detector is N , then the noise is $N^{1/2}$. Since the average number of photons is proportional to incident power, shot noise increases with $P^{1/2}$.

Signal-to-Noise Ratio and the Digitization of CCD

Total **noise** as a function of the number of electrons from all three contributing noises is given by

$$\text{Noise} [N_{\text{electrons}}] = \sqrt{\sigma_{\text{Photon}}^2 + \sigma_{\text{Dark}}^2 + \sigma_{\text{Read}}^2},$$

where

$\sigma_{\text{Photon}} = \sqrt{\varphi\eta\tau}$, $\sigma_{\text{Dark}} = \sqrt{I_{\text{Dark}}\tau}$, and $\sigma_{\text{Read}} = N_{\text{R}}$, I_{Dark} is dark current (electrons per second), and N_{R} is read noise (electrons, rms).

The quality of an image is determined by the **signal-to-noise ratio** (SNR). The signal can be defined as

$$\text{Signal} [N_{\text{electrons}}] = \varphi\eta\tau,$$

where φ is the incident photon flux at the CCD (photons per second), η is the quantum efficiency of the CCD (electrons per photon), and τ is the integration time (in seconds). Therefore, SNR can be defined as:

$$\text{SNR} = \frac{\varphi\eta\tau}{\sqrt{\varphi\eta\tau + I_{\text{dark}}\tau + N_{\text{R}}^2}}.$$

It is best to use a CCD under photon-noise-limited conditions. If possible, it would be optimal to increase the integration time to increase the SNR and work in photon-noise-limited conditions. However, an increase in integration time is possible until reaching full-well capacity (saturation level):

$$\text{SNR} = \frac{\varphi\eta\tau}{\sqrt{\varphi\eta\tau}} = \sqrt{\varphi\eta\tau}.$$

The **dynamic range** can be derived as a ratio of full-well capacity and read noise. Digitization of the CCD output should be performed to maintain the dynamic range of the camera. Therefore, an analog-to-digital converter should support (at least) the same number of gray levels calculated by the CCD's dynamic range. Note that a high bit depth extends readout time, which is especially critical for large-format cameras.

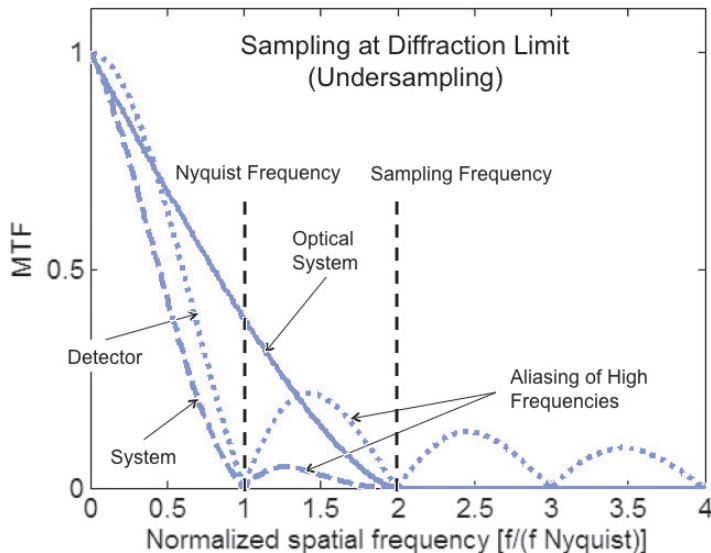
CCD Sampling

The maximum spatial frequency passed by the CCD is one half of the sampling frequency—the **Nyquist frequency**. Any frequency higher than Nyquist will be aliased at lower frequencies.

Undersampling refers to a frequency where the sampling rate is not sufficient for the application. To assure maximum resolution of the microscope, the system should be optics limited, and the CCD should provide sampling that reaches the diffraction resolution limit. In practice, this means that at least two pixels should be dedicated to a distance of the resolution. Therefore, the maximum pixel spacing that provides the diffraction limit can be estimated as

$$d_{\text{pix}} = M \frac{0.61\lambda}{2NA},$$

where M is the magnification between the object and the CCD's plane. A graph representing how sampling influences the MTF of the system, including the CCD, is presented below.



CCD Sampling (cont.)

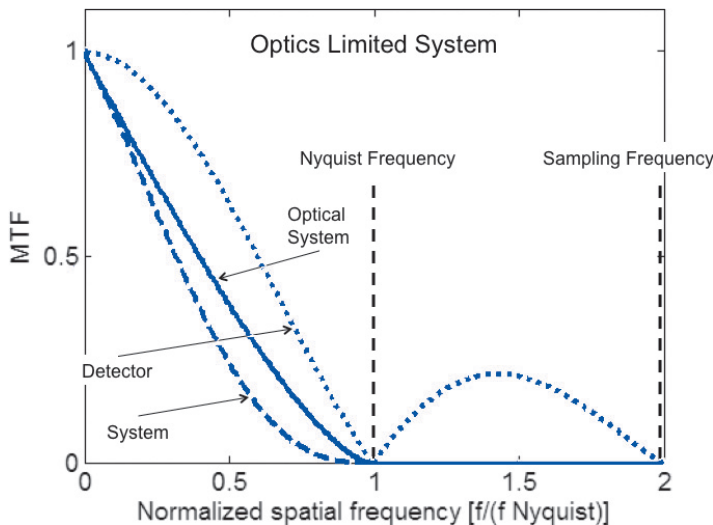
Oversampling means that more than the minimum number of pixels, according to the Nyquist criteria, are available for detection, which does not imply excessive sampling of the image. However, excessive sampling decreases the available field of view of a microscope. The relation between the extent of field D , the number of pixels in the x and y directions (N_x and N_y , respectively), and the pixel spacing d_{pix} can be calculated from

$$D_x = \frac{N_x d_{\text{pix}-x}}{M}$$

and

$$D_y = \frac{N_y d_{\text{pix}-y}}{M}.$$

This assumes that the object area imaged by the microscope is equal to or larger than D . Therefore, the size of the microscope's field of view and the size of the CCD chip should be matched.



Equation Summary

Quantized Energy:

$$E = h\nu = hc / \lambda$$

Propagation of an electric field and wave vector:

$$E = A \sin(\omega t - kz + \varphi_0) = A \exp[-i(\omega t - kz + \varphi_0)]$$

$$\omega = \frac{2\pi}{T} = \frac{2\pi V_m}{\lambda} \quad E(z, t) = E_x + E_y$$

$$E_x = A_x \exp[-i(\omega t - kz + \varphi_x)] \quad E_y = A_y \exp[-i(\omega t - kz + \varphi_y)]$$

Refractive index:

$$n = \frac{c}{V_m}$$

Optical path length:

$$\text{OPL} = nL$$

$$\text{OPL} = \int_{P1}^{P2} n ds$$

$$ds^2 = dx^2 + dy^2 + dz^2$$

Optical path difference and phase difference:

$$\text{OPD} = n_1 L_1 - n_2 L_2$$

$$\Delta\varphi = 2\pi \frac{\text{OPD}}{\lambda}$$

TIR:

$$\theta_{\text{cr}} = \arcsin\left(\frac{n_1}{n_2}\right)$$

$$I = I_0 \exp(-y/d)$$

$$d = \frac{\lambda}{4\pi n_1} \cdot \frac{1}{\sqrt{\sin^2 \theta - \sin^2 \theta_c}}$$

Coherence length:

$$l_c = \frac{\lambda^2}{\Delta\lambda}$$

Equation Summary (cont'd)

Two-beam interference:

$$I = EE^*$$

$$I = I_1 + I_2 + 2\sqrt{I_1 I_2} \cos(\Delta\phi)$$

$$\Delta\phi = \phi_2 - \phi_1.$$

Contrast:

$$C = \frac{I_{\max} - I_{\min}}{I_{\max} + I_{\min}}$$

Diffraction grating equation:

$$m\lambda = d(\sin \beta \pm \sin \alpha)$$

Resolving power of diffraction grating:

$$\frac{\lambda}{\Delta\lambda} = mN$$

Free spectral range:

$$\Delta\lambda = \frac{m+1}{m}\lambda_1 - \lambda_1 = \frac{\lambda_1}{m}.$$

Newtonian equation:

$$xx' = ff'$$

$$xx' = -f'^2$$

Gaussian imaging equation:

$$\frac{n'}{z'} = \frac{n}{z} + \frac{1}{f_e}$$

$$\frac{1}{z'} = \frac{1}{z} + \frac{1}{f_e}$$

$$f_e = \frac{1}{\varphi} = -\frac{f}{n} = \frac{f'}{n'}$$

Transverse magnification:

$$M = \frac{h'}{h} = -\frac{x'}{f'} = -\frac{f}{x} = \frac{z'}{z} = \frac{-f}{z-f} = \frac{-(z'-f')}{f'}$$

Longitudinal magnification:

$$\frac{\Delta z'}{\Delta z} = \left(-\frac{f'}{f} \right) M_1 M_2$$

Equation Summary (cont'd)

Optical transfer function:

$$\text{OTF}(\rho) = \text{MTF}(\rho) \exp[i\phi(\rho)]$$

Modulation transfer function:

$$\text{MTF}(\rho) = \frac{C(\rho)_{\text{image}}}{C(\rho)_{\text{object}}}$$

Field of view of microscope:

$$\text{FOV} = \frac{\text{FieldNumber}}{M_{\text{objective}}} [\text{mm}]$$

Magnifying power:

$$\text{MP} = \frac{u'}{u} = \frac{d_o(f - z')}{f(z' - l)}$$

$$MP \approx \frac{250 \text{ mm}}{f}$$

Magnification of the microscope objective:

$$M_{\text{objective}} = \frac{\text{OTL}}{f_{\text{objective}}}$$

Magnifying power of the microscope:

$$\text{MP}_{\text{microscope}} = M_{\text{objective}} \text{MP}_{\text{eyepiece}} = -\frac{\text{OTL}}{f_{\text{objective}}} \frac{250 \text{ mm}}{f_{\text{eyepiece}}}$$

Numerical aperture:

$$NA = n \sin u$$

$$NA = NA' M_{\text{objective}}$$

Airy disk:

$$d = \frac{1.22\lambda}{n \sin u} = \frac{1.22\lambda}{NA}$$

Rayleigh resolution limit:

$$d = \frac{0.61\lambda}{n \sin u} = \frac{0.61\lambda}{NA}$$

Sparrow resolution limit:

$$d = 0.5\lambda/NA$$

Equation Summary (cont'd)

Abbe resolution limit:

$$d = \frac{\lambda}{NA_{\text{objective}} + NA_{\text{condenser}}}$$

Resolving power of the microscope:

$$d_{\text{mic}} = \frac{d_{\text{eye}}}{M_{\min}} = \frac{d_{\text{eye}}}{M_{\text{obj}} M_{\text{eyepiece}}}$$

Depth of focus and depth of field:

$$DOF = 2\Delta z' = \frac{n'\lambda}{NA'^2}$$

$$2\Delta z' = M_{\text{objective}}^2 2\Delta z \frac{n'}{n}$$

Depth perception of stereoscopic microscope:

$$\delta z = \frac{250\alpha_s}{M_{\text{microscope}} \tan \gamma} [\text{mm}]$$

Minimum perceived phase in phase contrast:

$$\Delta\phi_{\min} = \frac{C_{\text{ph-min}}\lambda}{4\pi\sqrt{N}}$$

Lateral resolution of the phase contrast:

$$d = f'_{\text{objective}} \frac{\lambda}{(r_{\text{AS}} + r_{\text{PR}})}$$

Intensity in DIC:

$$I \propto \sin^2 \left(\frac{\pi s \frac{d\phi_o}{dx}}{\lambda} \right)$$

$$I \propto \sin^2 \frac{\pi \left(\Delta_b \pm s \frac{d\phi_o}{dx} \right)}{\lambda}$$

Retardation:

$$\Gamma = (n_e - n_o)t$$

Equation Summary (cont'd)

Birefringence:

$$\delta = \frac{2\pi OPD}{\lambda} = \frac{2\pi\Gamma}{\lambda}$$

Resolution of a confocal microscope:

$$d_{xy} \approx \frac{0.4\lambda}{NA},$$

$$d_z \approx \frac{1.4n\lambda}{NA^2}$$

Confocal pinhole width:

$$D_{\text{pinhole}} = \frac{0.5\lambda M}{NA}$$

Fluorescent emission:

$$F = \sigma QI$$

Probability of two-photon excitation:

$$n_a \propto \delta \left(\frac{P_{\text{avg}}^2}{\tau V^2} \right) \left(\pi \frac{NA^2}{hc\lambda} \right)^2$$

Intensity in FD-OCT:

$$I(k, z_o) = \int A_R A_S(z) \cos[k(z_m - z_o)] dz$$

Phase-shifting equation:

$$I(x, y) = a(x, y) + b(x, y) \cos(\varphi + n\Delta\varphi)$$

Three-image algorithm ($\pi/2$ shifts):

$$\varphi = \arctan \left(\frac{I_3 - I_2}{I_1 - I_2} \right)$$

Four-image algorithm:

$$\varphi = \arctan \left(\frac{I_4 - I_2}{I_1 - I_3} \right)$$

Five-image algorithm:

$$\varphi = \arctan \left(\frac{2[I_2 - I_4]}{I_1 - I_3 + I_5} \right)$$

Equation Summary (cont'd)

Image reconstruction structure illumination (sectioning):

$$I = \sqrt{(I_0 - I_{2\pi/3})^2 + (I_0 - I_{4\pi/3})^2 + (I_{2\pi/3} - I_{4\pi/3})^2}$$

Poisson statistics:

$$P(k, N) = \frac{N^k e^{-N}}{k!}$$

Noise:

$$\begin{aligned} \text{Noise}[N_{\text{electrons}}] &= \sqrt{\sigma_{\text{Photon}}^2 + \sigma_{\text{Dark}}^2 + \sigma_{\text{Read}}^2} \\ \sigma_{\text{Photon}} &= \sqrt{\phi \eta \tau}, \quad \sigma_{\text{Dark}} = \sqrt{I_{\text{Dark}} \tau}, \quad \sigma_{\text{Read}} = N_{\text{R}}, \quad I_{\text{Dark}} \end{aligned}$$

Signal-to-noise ratio (SNR):

$$\text{Signal}[N_{\text{electrons}}] = \phi \eta \tau$$

$$\text{SNR} = \frac{\phi \eta \tau}{\sqrt{\phi \eta \tau + I_{\text{dark}} \tau + N_{\text{R}}^2}}$$

$$\text{SNR} = \frac{\phi \eta \tau}{\sqrt{\phi \eta \tau}} = \sqrt{\phi \eta \tau}$$

Bibliography

- M. Bates, B. Huang, G.T. Dempsey, and X. Zhuang, “Multicolor Super-Resolution Imaging with Photo-Switchable Fluorescent Probes.” *Science* **317**, 1749 (2007).
- J. R. Benford, Microscope objectives, Chapter 4 (p. 178), in *Applied Optics and Optical Engineering, Vol. III*, R. Kingslake, ed., Academic Press, New York, NY (1965).
- M. Born and E. Wolf, *Principles of Optics*, Sixth Edition, Cambridge University Press, Cambridge, UK (1997).
- S. Bradbury and P. J. Evennett, *Contrast Techniques in Light Microscopy*, BIOS Scientific Publishers, Oxford, UK (1996).
- T. Chen, T. Milster, S. K. Park, B. McCarthy, D. Sarid, C. Poweleit, and J. Menendez, “Near-field solid immersion lens microscope with advanced compact mechanical design.” *Optical Engineering* **45**(10), 103002 (2006).
- T. Chen, T. D. Milster, S. H. Yang, and D. Hansen, “Evanescent imaging with induced polarization by using a solid immersion lens.” *Optics Letters* **32**(2), 124–126 (2007).
- J.-X. Cheng and X. S. Xie, “Coherent anti-stokes raman scattering microscopy: instrumentation, theory, and applications.” *J. Phys. Chem. B* **108**, 827-840 (2004).
- M. A. Choma, M. V. Sarunic, C. Yang, and J. A. Izatt, “Sensitivity advantage of swept source and Fourier domain optical coherence tomography.” *Opt. Express* **11**, 2183–2189 (2003).
- J. F. de Boer, B. Cense, B. H. Park, M.C. Pierce, G. J. Tearney, and B. E. Bouma, “Improved signal-to-noise ratio in spectral-domain compared with time-domain optical coherence tomography.” *Opt Lett* **28**, 2067–2069 (2003).
- E. Dereniqak, materials for SPIE Short Course on Imaging Spectrometers, SPIE, Bellingham, WA (2005).
- E. Dereniqak, *Geometrical Optics*, Cambridge University Press, Cambridge, UK (2008).
- M. Descour, materials for OPTI 412, “Optical Instrumentation,” University of Arizona (2000).

Bibliography

- D. Goldstein, *Polarized Light*, Second Edition, Marcel Dekker, New York, NY (1993).
- D. S. Goodman, Basic optical instruments, Chapter 4, in *Geometrical and Instrumental Optics*, D. Malacara, ed., Academic Press, New York, NY (1988).
- J. Goodman, *Introduction to Fourier Optics*, 3rd Edition, Roberts and Company Publishers, Greenwood Village, CO (2004).
- E. P. Goodwin and J. C. Wyant, *Field Guide to Interferometric Optical Testing*, SPIE Press, Bellingham, WA (2006).
- J. E. Greivenkamp, *Field Guide to Geometrical Optics*, SPIE Press, Bellingham, WA (2004).
- H. Gross, F. Blechinger, and B. Achtner, *Handbook of Optical Systems, Vol. 4: Survey of Optical Instruments*, Wiley-VCH, Germany (2008).
- M. G. L. Gustafsson, “Nonlinear structured-illumination microscopy: Wide-field fluorescence imaging with theoretically unlimited resolution.” *PNAS*, **102**(37) 13081–13086 (2005).
- M. G. L. Gustafsson, “Surpassing the lateral resolution limit by a factor of two using structured illumination microscopy.” *Journal of Microscopy*, **198**(2), 82–87 (2000).
- Gerd Häusler and Michael Walter Lindner, ““Coherence Radar” and “Spectral Radar”—New tools for dermatological diagnosis.” *Journal of Biomedical Optics* **3**(1), 21–31 (1998).
- E. Hecht, *Optics*, Fourth Edition, Addison-Wesley, Upper Saddle River, New Jersey (2002).
- S. W. Hell, “Far-field optical nanoscopy.” *Science* **316**, 1153 (2007).
- B. Herman and J. Lemasters, *Optical Microscopy: Emerging Methods and Applications*, Academic Press, New York, NY (1993).
- P. Hobbs, *Building Electro-Optical Systems: Making It All Work*, Wiley and Sons, New York, NY (2000).

Bibliography

- G. Holst and T. Lomheim, *CMOS/CCD Sensors and Camera Systems*, JCD Publishing, Winter Park, FL (2007).
- B. Huang, W. Wang, M. Bates, and X. Zhuang, “Three-dimensional super-resolution imaging by stochastic optical reconstruction microscopy.” *Science* **319**, 810 (2008).
- R. Huber, M. Wojtkowski, and J. G. Fujimoto, “Fourier domain mode locking (FDML): A new laser operating regime and applications for optical coherence tomography.” *Opt. Express* **14**, 3225–3237 (2006).
- Invitrogen, <http://www.invitrogen.com>
- R. Jozwicki, *Teoria Odwzorowania Optycznego* (in Polish), PWN (1988).
- R. Jozwicki, *Optyka Instrumentalna* (in Polish), WNT (1970).
- R. Leitgeb, C. K. Hitzenberger, and A. F. Fercher, “Performance of Fourier-domain versus time-domain optical coherence tomography.” *Opt. Express* **11**, 889–894 (2003).
- D. Malacara and B. Thompson, Eds., *Handbook of Optical Engineering*, Marcel Dekker, New York, NY (2001).
- D. Malacara and Z. Malacara, *Handbook of Optical Design*, Marcel Dekker, New York, NY (1994).
- D. Malacara, M. Servin, and Z. Malacara, *Interferogram Analysis for Optical Testing*, Marcel Dekker, New York, NY (1998).
- D. Murphy, *Fundamentals of Light Microscopy and Electronic Imaging*, Wiley-Liss, Wilmington, DE (2001).
- P. Mouroulis and J. Macdonald, *Geometrical Optics and Optical Design*, Oxford University Press, New York, NY (1997).
- M. A. A. Neil, R. Juškaitis, and T. Wilson, “Method of obtaining optical sectioning by using structured light in a conventional microscope.” *Optics Letters*, **22**(24), 1905–1907 (1997).
- Nikon Microscopy U, <http://www.microscopyu.com/>
-

Bibliography

- C. Palmer (Erwin Loewen, First Edition), *Diffraction Grating Handbook*, Newport Corp. (2005).
- K. Patorski, *Handbook of the Moiré Fringe Technique*, Elsevier, Oxford, UK(1993).
- J. Pawley, Ed., *Biological Confocal Microscopy*, Third Edition, Springer, New York, NY (2006).
- M. C. Pierce, D. J. Javier and R. Richards-Kortum, “Optical contrast agents and imaging systems for detection and diagnosis of cancer.” *Int. J. Cancer* **123**, 1979–1990 (2008).
- M. Pluta, *Advanced Light Microscopy, Volume One: Principle and Basic Properties*, PWN and Elsevier, New York, NY (1988).
- M. Pluta, *Advanced Light Microscopy Volume Two: Specialized Methods*, PWN and Elsevier, New York, NY (1989).
- M. Pluta, *Advanced Light Microscopy, Volume Three: Measuring Techniques*, PWN, Warsaw, Poland; and North Holland, Amsterdam, Holland (1993).
- E. O. Potma, C. L. Evans, and X. S. Xie, “Heterodyne coherent anti-Stokes Raman scattering (CARS) imaging.” *Optics Letters*, **31**(2), 241–243 (2006).
- D. W. Robinson, G. T. Reed,, Eds., *Interferogram Analysis*, IOP Publishing, Bristol, UK (1993).
- M. J. Rust, M. Bates, and X. Zhuang, “Sub-diffraction-limit imaging by stochastic optical reconstruction microscopy (STORM).” *Nature Methods*, **3**, 793–796 (2006).
- B. Saleh and M. C. Teich, *Fundamentals of Photonics*, Second Edition, Wiley, New York, NY (2007).
- J. Schwiegerling, *Field Guide to Visual and Ophthalmic Optics*, SPIE Press, Bellingham, WA (2004).
- W. Smith, *Modern Optical Engineering*, Third Edition, McGraw-Hill, New York, NY (2000).
- D. Spector and R. Goldman, Eds., *Basic Methods in Microscopy*, Cold Spring Harbor Laboratory Press, Woodbury, NY (2006).

Bibliography

Thorlabs website resources: <http://www.thorlabs.com/>

P. Török and F. J. Kao, Eds., *Optical Imaging and Microscopy*, Springer, New York, NY (2007).

Veeco Optical Library entry,
http://www.veeco.com/pdf/Optical_Library/Challenges_in_White_Light.pdf

R. Wayne, *Light and Video Microscopy*, Elsevier (reprinted by Academic Press), New York, NY (2009).

H. Yu, P. C. Cheng, P. C. Li, F. J. Kao, Eds., *Multi Modality Microscopy*, World Scientific, Hackensack, NJ (2006).

S. H. Yun, G. J. Tearney, B. J. Vakoc, M. Shishkov, W. Y. Oh, A. E. Desjardins, M. J. Suter, R. C. Chan, J. A. Evans, I. K. Jang, N. S. Nishioka, J. F. de Boer, and B. E. Bouma, "Comprehensive volumetric optical microscopy *in vivo*." *Nature Med* **12**, 1429–1433 (2006).

Zeiss Corporation, <http://www.zeiss.com>

Index

- 4Pi, 64, 109, 110
 4Pi microscopy, 109
- Abbe number, 25
 Abbe resolution limit, 39
 absorption filter, 60
 achromatic objectives, 51
 achromats, 51
 Airy disk, 38
 Amici lens, 55
 amplitude contrast, 72
 amplitude object, 63
 amplitude ratio, 15
 amplitude splitting, 17
 analyzer, 83
 anaxial illumination, 73
 angular frequency, 4
 angular magnification, 23
 angular resolving power, 40
 anisotropic media,
 propagation of light in, 9
 aperture stop, 24
 apochromats, 51
 arc lamp, 58
 array microscope, 113
 array microscopy, 64, 113
 astigmatism, 28
 axial chromatic
 aberration, 26
 axial resolution, 86
- bandpass filter, 60
 Bayer mask, 117
 Bertrand lens, 45, 55
 bias, 80
 Brace Köhler
 compensator, 85
 bright field, 64, 65, 76
- charge-coupled device
 (CCD), 115
- chief ray, 24
 chromatic aberration, 26
 chromatic resolving
 power, 20
 circularly polarized light, 10
 coherence length, 11
 coherence scanning
 interferometry, 98
 coherence time, 11
 coherent, 11
 coherent anti-Stokes
 Raman scattering
 (CARS), 64, 111
 coma, 27
 compensators, 83, 85
 complex amplitudes, 12
 compound microscope, 31
 condenser's diaphragm, 46
 cones, 32
 confocal microscopy, 64, 86
 contrast, 12
 contrast of fringes, 15
 cornea, 32
 cover glass, 56
 cover slip, 56
 critical angle, 7
 critical illumination, 46
 cutoff frequency, 30
- dark current, 118
 dark field, 64, 65
 dark noise, 118
 de Séarmornt
 compensator, 85
 depth of field, 41
 depth of focus, 41
 depth perception, 47
 destructive interference, 19

Index

- DIA, 44
 DIC microscope design, 80
 dichroic beam splitter, 91
 dichroic mirror, 91
 dielectric constant, 3
 differential interference contrast (DIC), 64–65, 67, 79
 diffraction, 18
 diffraction grating, 19
 diffraction orders, 19
 digital microscopy, 114
 digitization of CCD, 119
 dispersion, 25
 dispersion staining, 78
 distortion, 28
 dynamic range, 119
- edge filter, 60
 effective focal length, 22
 electric fields, 12
 electric vector, 10
 electromagnetic spectrum, 2
 electron-multiplying CCDs, 117
 emission filter, 91
 empty magnification, 40
 entrance pupil, 24
 entrance window, 24
 epi-illumination, 44
 epithelial cells, 2
 evanescent wave microscopy, 105
 excitation filter, 91
 exit pupil, 24
 exit window, 24
 extraordinary wave, 9
 eye, 32, 46
 eye point, 48
 eye relief, 48
 eye's pupil, 46
- eyepiece, 48
 Fermat's principle, 5
 field curvature, 28
 field diaphragm, 46
 field number (FN), 34, 48
 field stop, 24, 34
 filter turret, 92
 filters, 91
 finite tube length, 34
 five-image technique, 102
 fluorescence, 90
 fluorescence microscopy, 64
 fluorescent emission, 94
 fluorites, 51
 fluorophore quantum yield, 94
 focal length, 21
 focal plane, 21
 focal point, 21
 Fourier-domain OCT (FDOCT), 99
 four-image technique, 102
 fovea, 32
 frame-transfer architecture, 116
 Fraunhofer diffraction, 18
 frequency of light, 1
 Fresnel diffraction, 18
 Fresnel reflection, 6
 frustrated total internal reflection, 7
 full-frame architecture, 116
- gas-arc discharge lamp, 58
 Gaussian imaging equation, 22
 geometrical aberrations, 25

Index

- geometrical optics, 21
 - Goos-Hänchen effect, 8
 - grating equation, 19–20
 - half bandwidth (HBW), 16
 - halo effect, 65, 71
 - halogen lamp, 58
 - high-eye point, 49
 - Hoffman modulation
 - contrast, 75
 - Huygens, 48–49
 - I⁵M, 64
 - image comparison, 65
 - image formation, 22
 - image space, 21
 - immersion liquid, 57
 - incandescent lamp, 58
 - incidence, 6
 - infinity-corrected
 - objective, 35
 - infinity-corrected systems, 35
 - infrared radiation (IR), 2
 - intensity of light, 12
 - interference, 12
 - interference filter, 16, 60
 - interference microscopy, 64, 98
 - interference order, 16
 - interfering beams, 15
 - interferometers, 17
 - interline transfer
 - architecture, 116
 - intermediate image plane, 46
 - inverted microscope, 33
 - iris, 32
 - Köhler illumination, 43–45
 - laser scanning, 64
 - lasers, 96
 - laser-scanning microscopy (LSM), 97
 - lateral magnification, 23
 - lateral resolution, 71
 - laws of reflection and refraction, 6
 - lens, 32
 - light sheet, 112
 - light sources for
 - microscopy, common, 58
 - light-emitting diodes (LEDs), 59
 - limits of light microscopy, 110
 - linearly polarized light, 10
 - line-scanning confocal microscope, 87
 - Linnik, 101
 - long working distance objectives, 53
 - longitudinal
 - magnification, 23
 - low magnification objectives, 54
 - Mach-Zehnder interferometer, 17
 - macula, 32
 - magnetic permeability, 3
 - magnification, 21, 23
 - magnifier, 31
 - magnifying power (MP), 37
 - marginal ray, 24
 - Maxwell's equations, 3
 - medium permittivity, 3
 - mercury lamp, 58
 - metal halide lamp, 58
 - Michelson, 17, 53, 98, 100, 101
-

Index

- minimum focus distance, 32
 - Mirau, 53, 98, 101
 - modulation contrast
 - microscopy (MCM), 74
 - modulation transfer function (MTF), 29
 - molecular absorption cross section, 94
 - monochromatic light, 11
 - multi-photon fluorescence, 95
 - multi-photon microscopy, 64
 - multiple beam interference, 16
 - nature of light, 1
 - near point, 32
 - negative birefringence, 9
 - negative contrast, 69
 - neutral density (ND), 60
 - Newtonian equation, 22
 - Nomarski interference microscope, 82
 - Nomarski prism, 62, 80
 - non-self-luminous, 63
 - numerical aperture (NA), 38, 50
 - Nyquist frequency, 120
 - object space, 21
 - objective, 31
 - objective correction, 50
 - oblique illumination, 73
 - optic axis, 9
 - optical coherence
 - microscopy (OCM), 98
 - optical coherence tomography (OCT), 98
 - optical density (OD), 60
 - optical path difference (OPD), 5
 - optical path length (OPL), 5
 - optical power, 22
 - optical profilometry, 98, 101
 - optical rays, 21
 - optical sectioning, 103
 - optical spaces, 21
 - optical staining, 77
 - optical transfer function, 29
 - optical tube length, 34
 - ordinary wave, 9
 - oversampling, 121
 - PALM, 64, 110
 - paraxial optics, 21
 - parfocal distance, 34
 - partially coherent, 11
 - particle model, 1
 - performance metrics, 29
 - phase-advancing objects, 68
 - phase contrast
 - microscope, 70
 - phase contrast, 64, 65, 66
 - phase object, 63
 - phase of light, 4
 - phase retarding objects, 68
 - phase-shifting algorithms, 102
 - phase-shifting interferometry (PSI), 98, 100
 - photobleaching, 94
 - photodiode, 115
 - photon noise, 118
 - Planck's constant, 1
-

Index

- point spread function (PSF), 29
 point-scanning confocal microscope, 87
 Poisson statistics, 118
 polarization microscope, 84
 polarization microscopy, 64, 83
 polarization of light, 10
 polarization prisms, 61
 polarization states, 10
 polarizers, 61–62
 positive birefringence, 9
 positive contrast, 69
 pupil function, 29
 quantum efficiency (QE), 97, 117
 quasi-monochromatic, 11
 quenching, 94
 Raman microscopy, 64, 111
 Raman scattering, 111
 Ramsden eyepiece, 48
 Rayleigh resolution limit, 39
 read noise, 118
 real image, 22
 red blood cells, 2
 reflectance coefficients, 6
 reflected light, 6, 16
 reflection law, 6
 reflective grating, 20
 refracted light, 6
 refraction law, 6
 refractive index, 4
 RESOLFT, 64, 110
 resolution limit, 39
 retardation, 83
 retina, 32
 RGB filters, 117
 Rheinberg illumination, 77
 rods, 32
 Sagnac interferometer, 17
 sample conjugate, 46
 sample path, 44
 scanning approaches, 87
 scanning white light interferometry, 98
 Selective plane illumination microscopy (SPIM), 64, 112
 self-luminous, 63
 semi-apochromats, 51
 shading-off effect, 71
 shearing interferometer, 17
 shearing interferometry, 79
 shot noise, 118
 SI, 64
 sign convention, 21
 signal-to-noise ratio (SNR), 119
 Snell's law, 6
 solid immersion, 106
 solid immersion lenses (SILs), 106
 Sparrow resolution limit, 30
 spatial coherence, 11
 spatial resolution, 86
 spectral-domain OCT (SDOCT), 99
 spectrum of microscopy, 2
 spherical aberration, 27
 spinning-disc confocal imaging, 88
 stereo microscopes, 47
-

Index

- stimulated emission depletion (STED), 107
 - stochastic optical reconstruction microscopy (STORM), 64, 108, 110
 - Stokes shift, 90
 - Strehl ratio, 29, 30
 - structured illumination, 103
 - super-resolution microscopy, 64
 - swept-source OCT (SSOCT), 99
 - telecentricity, 36
 - temporal coherence, 11, 13–14
 - thin lenses, 21
 - three-image technique, 102
 - total internal reflection (TIR), 7
 - total internal reflection fluorescence (TIRF) microscopy, 105
 - transmission coefficients, 6
 - transmission grating, 20
 - transmitted light, 16
 - transverse chromatic aberration, 26
 - transverse magnification, 23
 - tube length, 34
 - tube lens, 35
 - tungsten-argon lamp, 58
 - ultraviolet radiation (UV), 2
 - undersampling, 120
 - uniaxial crystals, 9
 - upright microscope, 33
 - useful magnification, 40
 - UV objectives, 54
 - velocity of light, 1
 - vertical scanning interferometry (VSI), 98, 100
 - virtual image, 22
 - visibility, 12
 - visibility in phase contrast, 69
 - visible spectrum (VIS), 2
 - visual stereo resolving power, 47
 - water immersion objectives, 54
 - wave aberrations, 25
 - wave equations, 3
 - wave group, 11
 - wave model, 1
 - wave number, 4
 - wave plate compensator, 85
 - wavefront propagation, 4
 - wavefront splitting, 17
 - wavelength of light, 1
 - Wollaston prism, 61, 80
 - working distance (WD), 50
 - x-ray radiation, 2
-



Tomasz S. Tkaczyk is an Assistant Professor of Bioengineering and Electrical and Computer Engineering at Rice University, Houston, Texas, where he develops modern optical instrumentation for biological and medical applications. His primary research is in microscopy, including endo-microscopy, cost-effective high-performance optics for diagnostics, and multi-dimensional imaging (snapshot hyperspectral microscopy and spectro-polarimetry).

Professor Tkaczyk received his M.S. and Ph.D. from the Institute of Micromechanics and Photonics, Department of Mechatronics, Warsaw University of Technology, Poland. Beginning in 2003, after his postdoctoral training, he worked as a research professor at the College of Optical Sciences, University of Arizona. He joined Rice University in the summer of 2007.